1986

Beach Sedimentation Cycles (1962-1985) Along a Microtidal Wave-Dominated Coast: South Shore of Rhode Island

James C. Gibeaut
University of Rhode Island

BEACH SEDIMENTATION CYCLES (1962-1985) ALONG A MICROTIDAL WAVE-DOMINATED COAST: SOUTH SHORE OF RHODE ISLAND

BY

JAMES C. GIBEAUT

A THESIS SUBMITTED IN PARTIAL FULFILLMENT OF THE REQUIREMENTS FOR THE DEGREE OF

MASTER OF SCIENCE

IN

GEOLOGY

UNIVERSITY OF RHODE ISLAND

1986

ABSTRACT

Long-term beach profiling along the southwest shore of Rhode Island has resulted in the following data set: 4 locations measured 2 times per month since 1962; 4 locations measured 2 times per month starting between 1975 and 1977; and 2 locations measured 5 times per month beginning in 1977 and 1981. Currently, the 32 km stretch of barrier spit and headland shoreline from Watch Hill Point to Point Judith is covered by 10 profiles; all profiles are located on barrier spits and are not evenly spaced. The total number of profiles is now 3,500.

Computer plotting and statistical programs have been developed which allow direct comparison of the differing data sets. Eigenfunction analyses have defined modes of variances called beach-functions. Beach-functions are named according to the geomorphic area in which they are most sensitive to change. The following beach-functions have been identified: 1) shoreface-berm; 2) backberm; 3) beachface; 4) foredune; and 5) hybrid functions which are combinations of the above beach-functions.

Profile volume plots show that the beaches eroded from 1962 to 1985. Superimposed on the erosional trends are strong 10-11-year and subordinate 5-year beach-volume cycles. The importance of seasonal volume cycles varies but are always subordinate to the 10-11 year cycles and, except in one case, are subordinate to the five year cycles.

Backberm and beachface temporal functions often show 2-4 year cycles that represent backberm filling and profile shortening. The 2-4 year cycles do not involve important volume changes and are thought to be primarily caused by wave-climate cycles.

Weekly averages of hourly water levels recorded by the Newport Rhode Island tide gauge reveals an 11-to 14-year sea level cycle with an amplitude of .15 m. Sea level highs occurred in 1972 and 1983-84, and lows occurred in 1965 and 1979. Sea level highs on the 11-to 14-year scale coincide with beach volume highs. It is hypothesized that periods of dominant southeast to east swells cause a sea level set-up on the coast. These long wave length swells, in turn, may enhance onshore sediment transport from the shoreface (about 8 m depth). Previous workers discovered a shore-parallel sand bulge at 8 m depth. It is plausible that, during periods of long wave length swells, asymmetrical wave orbital velocities cause grain-wise sand transport from around 8 m depth to the beach.

Long-term (24 years) erosional trends are caused by aperiodic storms and periods of closely spaced storms. Beach erosion caused by sea level rise only becomes important on time-scales of over 25 years.

ACKNOWLEDGMENTS

A research project that spans 24 years inevitably involves many people. Since 1961, literally dozens of people have been involved in data collection for this study, as documented by the annual beach reports (McMaster 1961-present). Often, wind, rain, cold, vehicle problems, and funding made the job of going to the beach quite formidable. Of course, such a long-term project requires continuity and perseverance which was provided by Dr. R. L. McMaster. Dr. McMaster started and currently supervises the collection of beach data which I have found to be unmatched in its length and detail. The citizens of Rhode Island will benifit from Dr. McMaster's foresight for years to come. Personally, I would like to thank Dr. McMaster for making the original data available to me and explaining and discussing with me the complexities of coastal geology.

I also thank my adivisor, Dr. J. C. Boothroyd, from whom I first learned about beaches and sedimentology in general. Dr. Boothroyd has greatly influenced my geological thought and I will benefit from his teaching for the rest of my career.

Dr. J. A. Cain made many helpful comments on the manuscript and did so on short notice, for that I am grateful. I also thank Dr. K. L. Hartt for being the defense chairman.

Many of my fellow students have helped me collect beach data, and the following is a partial list: Chuck Gricus;

Mike Dacey; Caroline Szak; Dave Pickart; John Grant; and Scott Graves.

I thank the numerous people in the User Services Department of the Academic Computer Center for their help in overcoming system related problems. Dave Jones, Dr. D. P. Murray, and even Nasir Hamidzada, helped me with many microcomputer applications.

I especially thank Mike Dacey, Chuck Gricus, Caroline Szak, Tim Ling, and Sue Ponte for their friendship, advice, and help (in that order) in getting me through the Rhode Island experience.

For her many ways of support, I thank Julia.

This thesis is dedicated to Mom and Dad for all the usual stuff students say about their parents in thesis dedications but more importantly for those things my parents have given me for which words on paper are no match. Thanks!

TABLE OF CONTENTS

page

LIST OF TABLES

LIST OF FIGURES

Figures page

INTRODUCTION

The shoreline of southern Rhode Island (Fig. 1) is relatively undeveloped compared to other Atlantic and Gulf Coast states such as New Jersey, Maryland, and Florida. This is due in part to the geological effects of direct wave attack and storm-surge driven overwash during the 1938 and 1954 hurricanes (Boothroyd et al. 1986). Severe beach erosion can also occur when storms of an extratropical origin pass to the west of Rhode Island producing southeasterly onshore winds and storm waves for up to several days (Rosenberg 1985). Currently, erosion caused by storms of lesser than hurricane intensity and the alongshore variation in sediment supply influence shoreline management decisions (Boothroyd et al. 1986). It is essential to understand the relative importance of storms and longer-term processes to properly plan for the future. This study uses 5 to 24 year long beach profile time series from 10 locations to decipher beach sedimentation cycles and trends along the southern Rhode Island shoreline (Fig. 1).

Beach profiling is useful in understanding sedimentation patterns in time and space (Abele 1977, Aubrey 1979, Boothroyd et al. 1978, Davis and Fox 1972, Davis et al. 1972, Fox and Davis 1973, Hine 1979, Wright and Short 1984). Long-term beach profile analysis reveals the importance of single storms and seasonality compared to the longer-term trends. This study used eigenfunction and fourier analysis to synthesize and analyze the profile data

Fig. 1.- Southwest Rhode Island Coast and Profile Locations.

PROFILE LOCATIONS

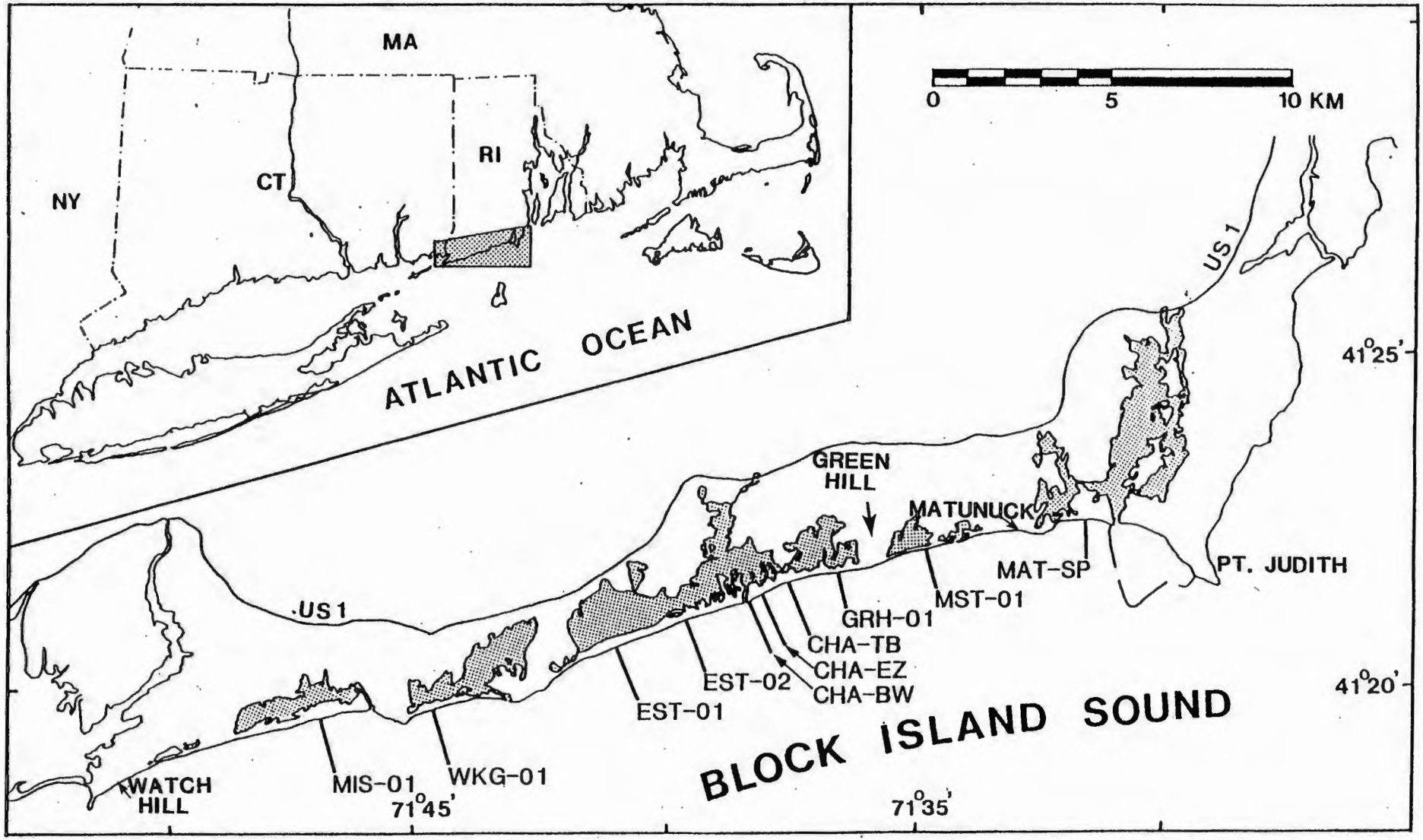

sets. Hourly water levels recorded by the Newport Rhode Island tide gauge have been analyzed to provide a first approximation of a forcing function causing the observed beach patterns. Water levels recorded at coastal stations are sensitive to astronomical, eustatic, tectonic, and meteorlogically generated changes in sea level (Komar 1976, Heaps 1985, Aubrey and Emery 1983, Aubrey and Emery 1986, Flick and Cayan 1984) all of which affect beach sedimentation (Rosenberg 1985, Lafond 1938, Bruun 1962, Flick and Cayan 1984, Clarke and Eliot 1983b). Armed with the results of this study, coastal planners can make decisions that are more geologically sound.

Most of the data for this study (Table 1) have been summarized on a yearly basis by the workers who measured the profiles (McMaster 1961-present). In addition, McMaster and Friedrich (1986) summarized and qualitatively described beach profile changes from 1961 to 1984. A rigorous long-term analysis, however, had not been done. Fisher and Simpson (1979) determined erosion and accretion rates for the Rhode Island south shore by comparing 4 sets of aerial photographs from 1939 to 1975. The results of the Fisher and Simpson study are comparable with the results of this study. The profile data sets used in this study, however, are a relatively continuous record of beach sedimentation compared to those represented on the aerial photographs. The profiles also provide elevation information perpendicular to the beach which the aerial photographs do not have. The

data set for this study is believed to be unique in its detail and longevity compared to other beach profile data sets.

PHYSICAL SETTING

General

The southwest shore of Rhode Island (Fig. 1) is a microtidal, wave dominated coastline in the classification of Hayes (1979) and Nummedal and Fischer (1978) (Fig. 2). Mean tidal range in the open ocean ranges from 0.8-1.2 m (NOAA 1986). A wave-pressure sensor recorded wave heights from April, 1974 to April, 1975 off the Charlestown Breachway (CHA-BW, Fig.1), significant wave heights were less than 0.5 m 68% of time, and greater than 1.5 m 2.2% of the time (Raytheon 1975). Breaker heights, however, have reached up to 4.0 m during storms.

The shoreline consists of low, narrow barrier spits alternating with headland bluffs composed of Pleistocene till or glaciofluvial sand and gravel. Lagoons are landward of the barriers. The barriers are 1-8 km long, 200-300 m wide, have foredunes commonly 1-4 m in elevation, and backbarrier flats dominated by overwash processes during major storms. The spits are separated by small tidal inlets both natural and maintained.

Fig. 2.- Mean Tidal Range vs. Mean Wave Height and Classification Scheme.

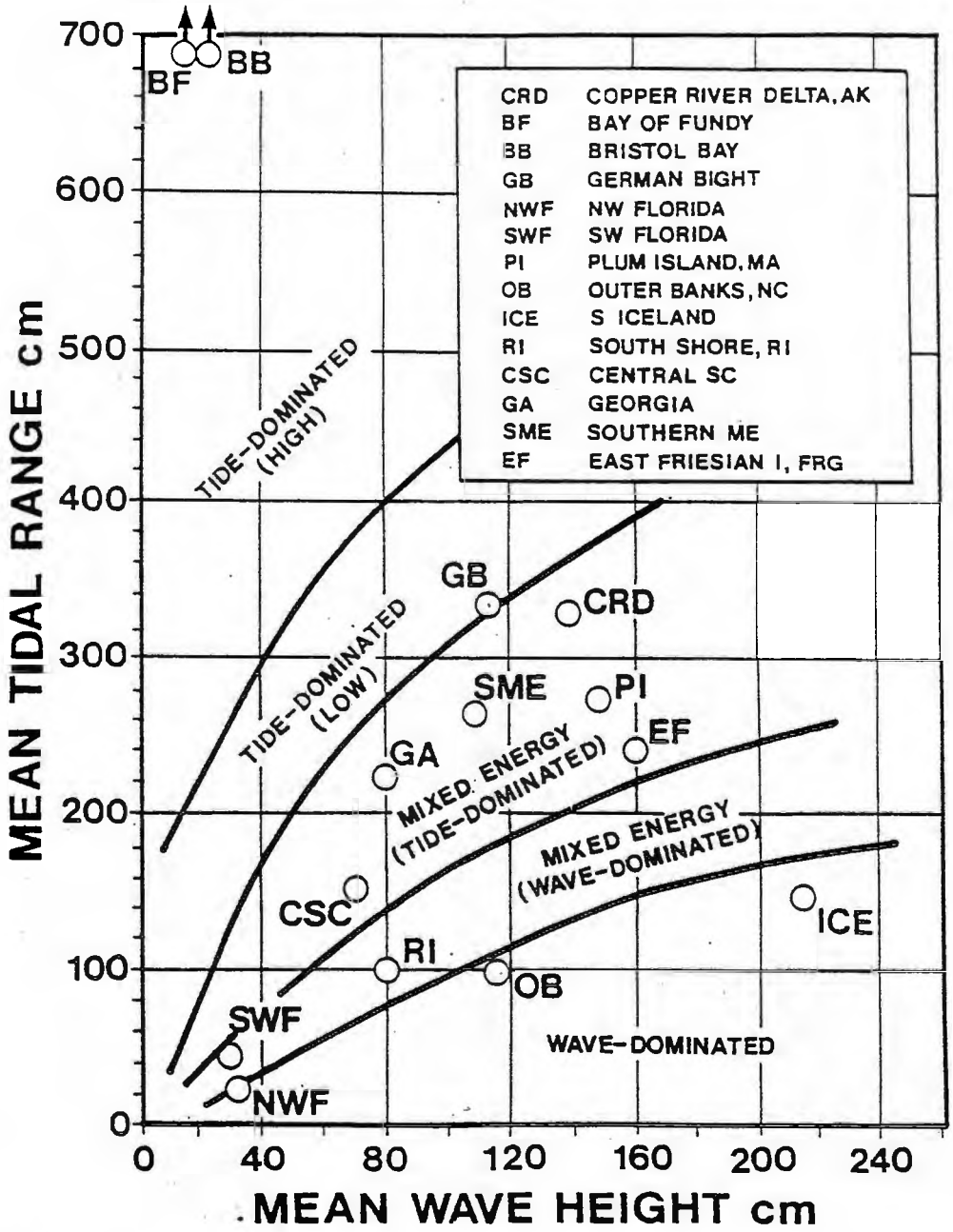
MEAN TIDAL RANGE cm
MEAN WAVE HEIGHT cm
700
600
500
400
300
200
100
0
0
40
80
120
160
200
240
CRD COPPER RIVER DELTA, AK
BF BAY OF FUNDY
BB BRISTOL BAY
GB GERMAN BIGHT
NWF NW FLORIDA
SWF SW FLORIDA
PI PLUM ISLAND, MA
OB OUTER BANKS, NC
ICE S ICELAND
RI SOUTH SHORE, RI
CSC CENTRAL SC
GA GEORGIA
SME SOUTHERN ME
EF EAST FRIESIAN I, FRG
TIDE-DOMINATED (HIGH)
TIDE-DOMINATED (LOW)
MIXED ENERGY (TIDE-DOMINATED)
MIXED ENERGY (WAVE-DOMINATED)
WAVE-DOMINATED
BF
BB
GB
CRD
SME
PI
EF
GA
CSC
RI
OB
ICE
SWF
NWF

Meteorology

Rhode Island is located in the prevailing westerlies (a belt of prevailing westerly winds between 35 and 60 degrees north). Surface winds generally blow from the southwest but polar winds are frequent and strong (Strahler and Strahler 1978). The migration of the polar front jet stream and the Bermuda High dominate the weather patterns (Havens et al. 1972). In the fall and winter, the jet stream expands and stronger north-northwest winds prevail. Storm events are more frequent and more intense. In the spring and summer, the jet stream contracts and the Bermuda High expands causing surface winds to decrease and shift to the southwest. During late summer and early fall, tropical storms or hurricanes may affect the area. Rosenberg (1985) plotted the tracks of 17 major storms from 1977 to 1982 and found 4 major tracks. These tracks were later modified by Blais (1986) (Fig. 3). The proximal tracks include the following: 1) extratropical cyclones moving southeast or east from the northwest, and 2) storms proceeding northeast along the U.S. East Coast that pass to the west of Rhode Island. The distal tracks consist of: 1) extratropical cyclones that approach from the Midwest and travel parallel to the St. Lawrence River Valley, and 2) Mid-Atlantic tropical cyclones (hurricanes) that curve to the northeast within a few hundred kilometers of New England.

Fig. 3.- Major Storm Tracks (from Blais 1986).

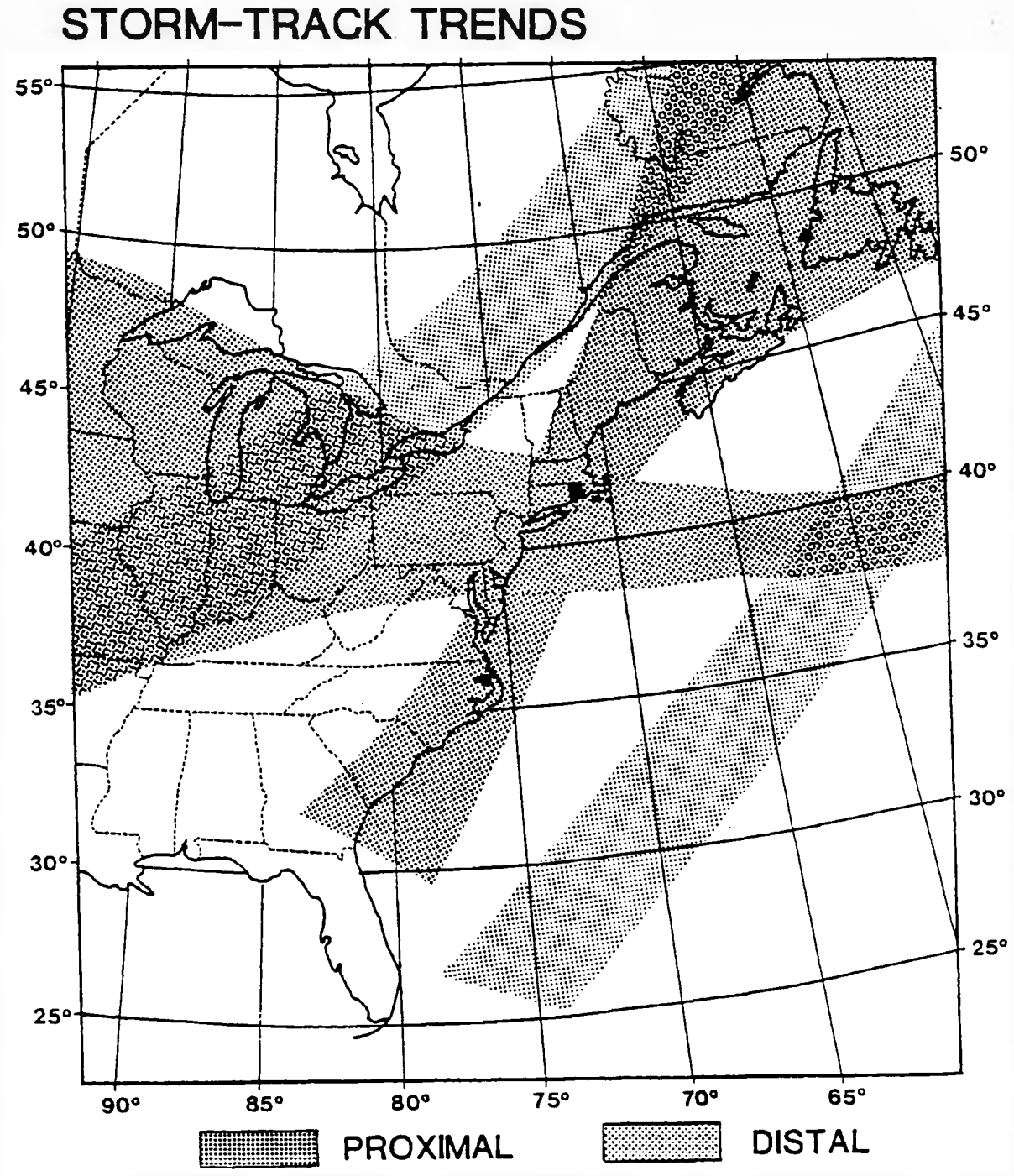
STORM-TRACK TRENDS
55°
50°
45°
40°
35°
30°
25°
50°
45°
40°
35°
30°
25°
90°
85°
80°
75°
70°
65°
PROXIMAL
DISTAL

Sedimentary Sources and Processes

The Rhode Island barrier-lagoon system is a sediment-starved transgressive shoreline. Average shoreline retreat from 1939 to 1975 was 0.7 m/yr (Fisher and Simpson 1979). The beaches on the barriers consist of fine to medium quartz sand with local concentrations of gravel usually arranged in cusps (McMaster 1961). Sediment sources for the barriers include eroding till and glaciofluvial headlands and glacial outwash sand and gravel on which the barriers are developed. No major rivers supply sediment to the coast. Flood tidal deltas, storm-surge platforms, and the shoreface are major sediment sinks.

The beaches have storm-fair weather cycles typical of other microtidal beaches (Davis et al. 1972, Owens 1977, Owens and Frobel 1977, Eliot and Clarke 1982). Major beach erosion is usually caused by southeast swells associated with northward travelling storms. Recovery is fairly rapid and normally completed within 3 to 7 days (Rosenberg 1985). Beach responses to specific storms are not always the same at all profile locations (McMaster 1961-present). Longshore sediment variation and complex offshore topography causing complicated wave refraction patterns are at least partly responsible for varying beach responses.

Fisher and Simpson (1979) used photogrammetric techniques to determine the relative importance of sedimentary processes in barrier island retreat along the Rhode Island south shore. They found flood tidal delta

sedimentation to be 1 1/3 times more effective than washover sedimentation in the landward transportation of sediment. Boothroyd et al. (1985) determined that for one major storm, the "Blizzard of 1978", 27% of eroded beach material along Charlestown Beach (Fig. 1, CHA-EZ location) was deposited as washover fans, 20% moved offshore to greater than 5 m water depths, and the remaining 53% of the sediment moved alongshore to the Ninigret tidal inlet or to another beach location. In another study, side scan sonar revealed shore-perpendicular fields of mega ripples after a storm (Morang and McMaster 1980). Morang and McMaster suggested the megaripple fields were formed by rip currents moving up to 400 m offshore to depths of 5 m. A regular spacing of 50 m was found for the megaripple fields off Misquamicut Beach after one storm, however, no rhythmic pattern occurred for the rest of the shore. DeKay (1981) discovered shore-normal lobes and troughs with 10's of centimeters of relief on the upper shoreface (less than 3 m. depth) off East Beach (EST-01 profile location). These features develop during fairweather. The troughs are a result of non-deposition and landward transport of sand until a basal gravel armor is left; the lobes exist in equilibrium with onshore and offshore sand transport. Aerial photographs show these features to occur all along the southwest shore, and their regular spacing suggests edge waves to be important in their formation.

The study that contains the longest-term alongshore sediment transport information was completed by McMaster (1961). McMaster analyzed heavy minerals in the beach sand and deduced that alongshore sediment transport converges on the Charlestown Inlet area (CHA-BW location, Fig. 1) from Watch Hill Pt. to the west and from Matunuck headland to the east.

EMPIRICAL EIGENFUNCTION ANALYSIS

This study relies heavily on the ability of eigenfunction analysis to reduce the data set and to identify different modes of variance. Plotting of the profiles in a standard format using a 5:1 vertical exaggeration has allowed visual comparison between data sets and within each time series for specific dates (Volumes 2, 3). The number of profiles, however, makes it necessary to reduce the data set to a few parameters which best describe the profiles so that the important trends may be discerned. Time series of profile volumes give a general idea of the health of the beach and sedimentation patterns along the shore. Simple profile volume plots, however, do not contain information on changes in beach configuration or sediment transport within the profile length; therefore, in addition to volume plots, empirical eigenfunction analyses have been performed on profile elevation data (Figs. 4-23).

The advantage of eigenfunction analysis lies in its ability to reduce, separate, rank, and define the number of important variables causing variation in a data set (Davis 1973). Eigenfunction analysis on time series data separates temporal and spatial dependence and defines unrelated (orthogonal) modes of variation. Aubrey (1983) gives the properties of empirical eigenfunctions as the following:

1) Empirical eigenfunctions provide the most efficient method of compressing the data; i.e., the first n terms in the expansion represent more of the data variability than the first n terms of any other orthogonal expansion.

2) Since both the spatial and temporal eigenfunctions are orthogonal sets, each corresponding set may be regarded as representing a mode of variability which is uncorrelated with any other mode.

3) The eigenfunction representation is convenient when using the method of minimum mean square error estimation. The eigenfunctions provide a useful a priori method for reducing the number of variables in this estimation theory, and also provide a means of removing the noise (or less predictable part of the data) from the data set.

When applied to beach profile data, each eigenfunction mode may describe types of variability occurring on different time scales. Fourier analysis

(Rayner 1971) has been used on the temporal dependence of the eigenfunction modes to identify cycles of the forcing functions.

There have been several studies using eigenfunction analysis on beach profile data. Aubrey (1979) identified seasonal sediment exchange patterns perpendicular to the shore at Torrey Pines Beach, California. Aubrey's profiles extended from the dune area to a depth of 8 m below mean sealevel. Bowman (1981) analyzed one year of supratidal data from seven beaches on the southern Mediterranean coast of Israel. Using spatial eigenfunction analysis, Bowman identified characteristic beach configurations and grouped the locations accordingly. Mizuguchi et al. (1982) applied eigenfunction analysis to describe three-dimensional beach transformations in a laboratory wave basin. Mizuguchi found that the second eigenfunction and eigenvalue are related, respectively, to two-dimensional beach change and alongshore transport rate. Aubrey (1983) analyzed 7 U.S. beaches exposed to varying wave climates in a study involving at least 5 years of monthly profile data. Aubrey used eigenfunction analysis as an objective and standard method of calculating profile variances between data sets that varied in spatial and temporal resolution and time period. Aubrey correlated low profile variance with low wave energy and high variance with high wave energy. Clarke and Eliot (1983) examined eighteen closely spaced profiles, extending to mean low water, obtained over five years along a beach in

New South Wales, Australia. They performed eigenfunction analysis for different elevations along the beach and also for each profile perpendicular to the beach. By grouping the spatial eigenfunctions according to similarities in shape and associated time series spectra, they identified zones of stability and instability along the beach and correlated these zones with offshore bars and rip channels, respectively. In Clarke and Eliot's study, eigenfunction analysis also revealed the variance mode describing the onshore-offshore sediment exchange to be more important for profiles backed by a reflective rock rip-rap seawall. Aubrey and Ross (1985) used the first two eigenfunctions plus the mean profile of a five year set of onshore-offshore profiles from Torrey Pines Beach, California to reconstruct profiles involved in certain geomorphic cycles. Plotting the first temporal eigenfunction against the second and using rotary component analysis, they described sequential changes in beach profile shape and identified 1 and .5 year cycles.

Some studies have combined eigenfunction and spectral analysis to detect cycles in the different modes of beach variance. Clarke and Eliot (1983) examined temporal eigenfunctions in the spectral domain to aid in grouping similar eigenfunctions of different shore-normal profiles and of different levels of the beach alongshore. They also discovered cycles of variation with 24, 12, and 6 month periods on Warilla Beach, New South Wales, Australia.

Clarke and Eliot (1984) studied Coledale Beach, Australia over a monthly lunar tidal cycle. Performing eigenfunction and spectral analyses for different elevations on the beach, they discovered patterns of change dominated by the 28-30 day lunar tidal cycle and an increasing phase shift from the bermcrest level to the mid-tidal zone, down the beachface.

There has been some success with using eigenfunction representations of profile data in predictive models of beach sedimentation. Aubrey et al. (1980), working with a 5-year data set from Torrey Pines Beach, California, used 4 different spectral representations of the wave field (energy, radiation stress, energy flux, and wave steepness) in linear statistical estimation models which involved eigenfunctions of beach profile data. Hashimoto et al. (1981) used eigenfunction analysis to predict beach profiles around breakwaters and groins in a movable bed model with wave height and direction as the input variables.

In Rhode Island, three studies involving eigenfunction analysis of beach profile data have been completed. Morton et al. (1982) used eigenfunction analysis to describe differences in seasonal variance among 7 profiles located on Misquamicut Beach (Fig. 1 near MIS-01) measured from 1962 to 1973. Profiles located near the jettied Weekapaug Inlet showed the greatest amount of seasonal and overall variability. DeKay (1981) analyzed 5 years of profile data (1975-80) from the EST-01 location (Fig. 1). DeKay deduced general shoreline retreat by examining the first temporal

eigenfunction and identified Hurricane Belle (August, 1976) as having caused significant shoreline retreat which brought the beach profile to equilibrium with the current sea level. DeKay also performed eigenfunction analysis on 4 closely spaced profiles measured for a year on East Beach (EST-01) and extending from the dune to 7 m depth. Dekay was able to separate and identify variance modes associated with onshore-offshore and alongshore sediment transport. Rosenberg (1985) analyzed 5 years of the CHA-EZ profile data (1977-82) (Fig. 1) and found variance modes involving onshore-offshore and beachface-berm top exchanges of sediment. Rosenberg proposed that the landward extent of profile variability described by the second eigenfunction (beachface-berm top variance mode) be used as an unbiased point from which construction set-back distances are measured.

DATA SET

Long-term beach profiling along the southwest shore of Rhode Island has resulted in the following data set: 4 locations measured 2 times per month since 1962, (McMaster 1961-present); 4 locations measured 2 times per month starting between 1975 and 1977 (McMaster 1961-present); and 2 locations measured 5 times per month beginning in 1977 and in 1981 (Boothroyd et al. 1986). Currently, there are 10 profiles on the 32 km stretch of shoreline from Watch Hill Point to Point Judith (see

location map, Fig. 1); all profiles, however, are located on barrier spits and are not evenly spaced. The total number of profiles is now 3,500, and they continue to be measured. All profiles extend from the backdune area to approximately mean low water. Table 1 gives the starting date and number of profiles analyzed for this study. Appendix 1 gives directions to the profiles and contains ground and aerial photographs of the profile locations.

TABLE 1.- Profile Data Sets

location (W-E)	start date	# profiles	profiler
MIS -01	Jul. 77	154	McMaster
WKG -01	Dec. 62	430	McMaster
EST -01	Dec. 62	431	McMaster
EST -02	Aug. 76	162	McMaster
CHA -BW	Jan. 77	161	McMaster
CHA -EZ	Oct. 77	479	Boothroyd
CHA -TB	Nov. 75	183	McMaster
GRH -01	Dec. 62	432	McMaster
MST -01	Dec. 62	420	McMaster
MAT -SP	Aug. 81	207	Boothroyd

METHODS

Profile Measurements (CHA-EZ, MAT-SP)

The CHA-EZ and MAT-SP profiles are measured using a modified Emery method (Emery 1961, Rosenberg 1985). Elevation measurements begin at a permanent marker of known elevation landward of the foredune crest and proceed perpendicular to the shoreline into the swash zone at a maximum interval of 2 meters. The intervals may be shorter where reference markers, obstacles, or specific geomorphic features are encountered. Profiles are measured within 2 hours of low tide. Blais (1986) determined the amount of error in this method by comparing duplicate measurements taken by two different profiling teams on several occasions. He found the average variation to be 1.7% of the total profile volume (area under the profile curve times 1 meter) with the largest amounts of error occurring in the swash zone when the profile rods were undermined. Individual stations are determined within 5 cm horizontally and within 1 cm vertically. Profiles are measured on the average of 5 times per month with surveys specially made before and after major storms.

Profile Measurements (MIS-01, WKG-01, EST-01, EST-02, CHA-BW, CHA-TB, GRH-01, MST-01)

These profiles are measured with a transit and stadia rod. At each survey site the profile begins from a fixed stake or other permanent feature in the dune area. The first elevation station is now the dune crest but in years past has been the base of the foredune scarp, or the base of the foredune ramp. Elevations are measured at points of noticeable inflection perpendicular to the shoreline down to the landward extent of the swash. Where the dune crest has been worn down by workers over the years, a side shot is taken to give the natural elevation of the crest. Profiles are usually made on the same day as close to low tide as possible, but due to travel time and vehicle problems this may vary by several hours and some locations may be missed. Individual stations are determined within 2 m horizontally and 10 cm vertically. Profiles are measured on the average of 1.5 times per month but not necessarily before and after major storms.

Profile Plotting and Volume Calculations

A Fortran program written by Roger Greenall of the University of Rhode Island Academic Computer Center was modified to create the individual profile plots in Volumes 2

and 3, and to calculate profile volumes. Profile volume is defined as the area between the profile curve and mean low water line (MLW) times a 1 m length considered to be centered on and perpendicular to the profile line. The areas are calculated by trapezoid summation with the sides of each trapezoid determined by the elevation stations. If an elevation station is measured below MLW, a point is interpolated at MLW. If the last elevation station does not reach MLW at the CHA-EZ and MAT-SP locations, a least squares regression is performed on the last 4 points and an extrapolation is drawn using the regression slope from the last point to MLW. For the other profiles only the last 2 points determine the extrapolation slope. If the extrapolation would extend beyond a reasonable distance (determined by the extrapolation slope and the elevation of the last data point), it is not made and the volume is calculated to the last data point.

The elevations of the datum stakes at CHA-EZ and MAT-SP are known and used in the profile plots. The elevations of the datum stakes for the remaining profiles, however, are determined by finding the median vertical displacement for an arbitrary starting elevation and then changing the datum stake elevation so that half of the profiles are extrapolated and half are interpolated. Datum stakes are sometimes altered vertically so the determination is made for the life of each datum stake.

Horizontal shifts in datum stake positions or poor spatial resolution in the dune areas are compensated for in the final volumes by adding or subtracting areas in the profiles. Profile volume time series plots thus show relative changes around the mean volume for each time series (Figs. 14-23). However, all volumes appear uncorrected in the profile plots (Volumes 2 and 3).

Analysis

For the eigenfunction analysis, the above MLW portion of each profile was interpolated at 1 m intervals out to 100 m from the datum stake. Where the profile did not reach 100 m an elevation value of zero was assigned. Horizontal shifts in datum stake positions are compensated for by shifting all subsequent profiles. A mean profile was determined by averaging the elevations at each horizontal position through time. This mean profile was removed and a 100 by 100 spatial covariance matrix formed. Spatial eigenfunctions were extracted and principal component scores (temporal eigenfunctions) were determined for the covariance matrix using a Statistics Analysis System routine (SAS 1985) on an IBM 360/370 mainframe computer. For an explanation of eigenfunction analysis see Davis (1973) , and for an explanation of beach profile interpretation using eigenfunction analysis see Rosenberg (1985) and Aubrey (1983).

For the spectral analysis, volume time series and temporal eigenfunctions were artificially sampled at equal time intervals by linear interpolation. The interpolation interval for MAT-SP and CHA-EZ is 2 days and for the other profiles 7 days. All time series for the spectral analyses, therefore, have about 3 times the number of original data points. Before the spectral analyses were performed, a least squares linear regression line was subtracted from the data. The time series were then embedded in zero arrays and a fast fourier transform routine invoked using Asyst Software (Asyst 1985) on an IBM XT microcomputer.

Hourly water levels from the Newport Rhode Island tide gauge were averaged weekly (every 168 hours) and plotted. If there is a gap in the data of more than 12 hours, that week is not included in the time series plot. A total of 95 weeks are missing out of the 25 years of data. The weekly averages were then averaged to yield yearly average sea levels.

RESULTS AND INTERPRETATIONS

Sediment Volume

The volume plots (Figs. 4a-13a) show different amounts of variability. The CHA-EZ and MAT-SP plots show the most variability because of special sampling after storms, and because the Emery method of measurement with its higher spatial resolution is more sensitive to subtle

Figs. 4-13.- Profile Time-series Plots.

4) Weekapaug Beach 1.
a) profile volume b) first temporal eigenfunction c) second temporal eigenfunction d) third temporal eigenfunction e) fourth temporal eigenfunction

5) East Beach 1.
a-e) same as above

6) Green Hill Beach 1.
a-e) same as above

7) Moonstome Beach 1.
a-e) same as above

8) Misquamicut Beach 1.
a-e) same as above

9) East Beach 2.
a-e) same as above

10) Charlestown Breachway Beach.
a-e) same as above

11) Charlestown EZ Beach.
a-e) same as above

12) Charlestown Town Beach.
a-e) same as above

13) Matunuck SP Beach.
a-e) same as above

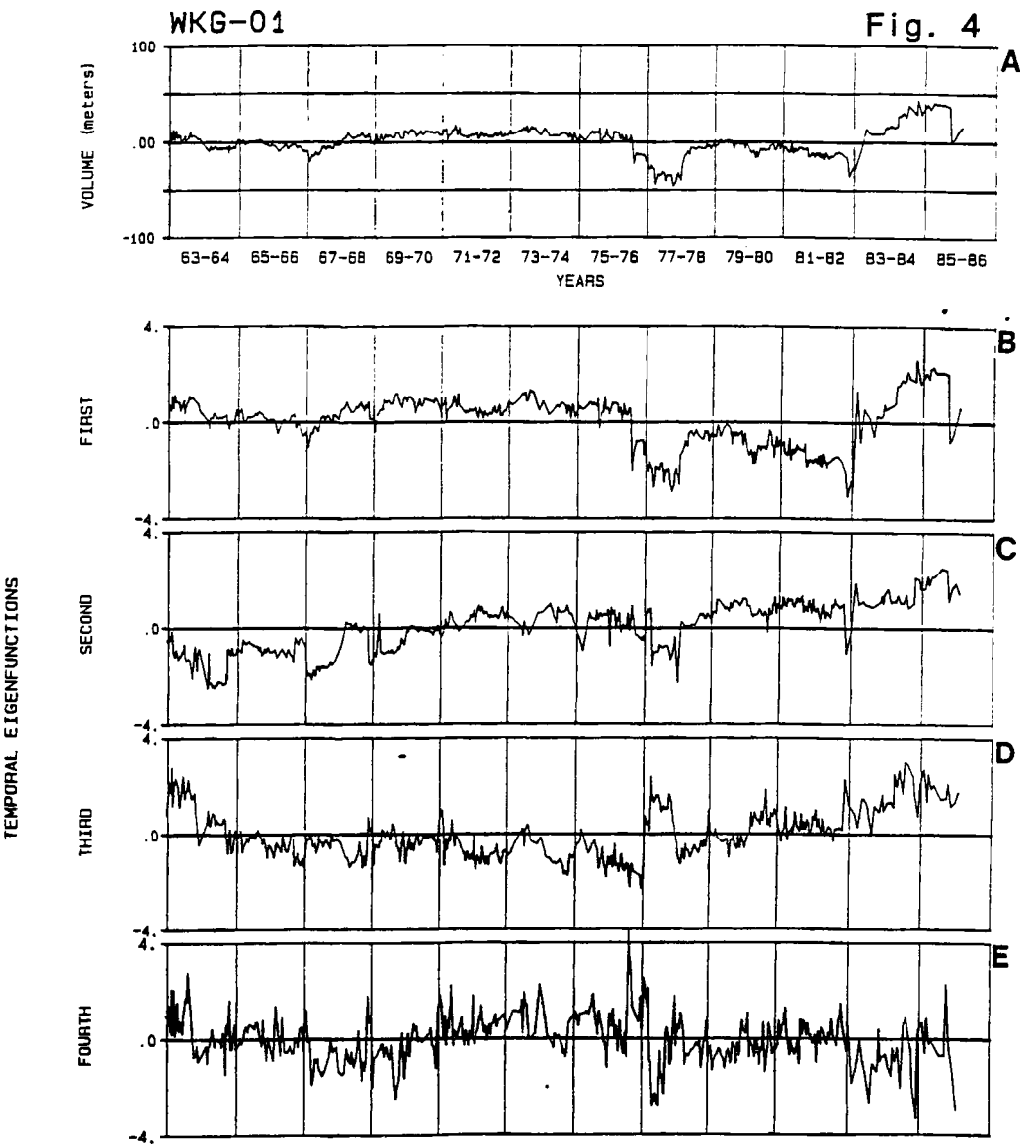
WKG-01
Fig. 4
A
VOLUME (meters)
100
.00
-100
63-64
65-66
67-68
69-70
71-72
73-74
75-76
77-78
79-80
81-82
83-84
85-86
YEARS
TEMPORAL EIGENFUNCTIONS
B
FIRST
C
SECOND
D
THIRD
E
FOURTH
4.
.0
-4.

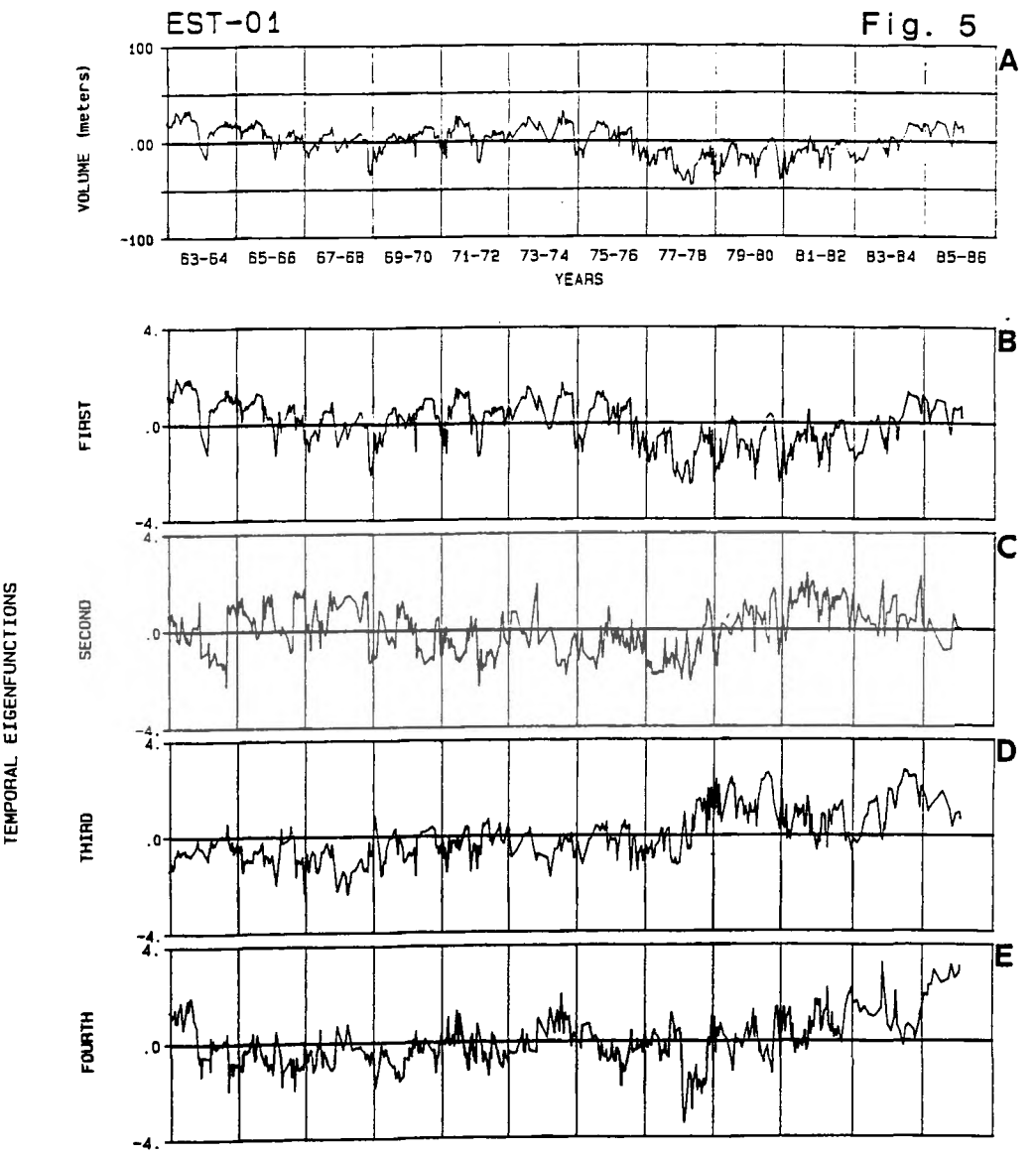
EST-01
Fig. 5
A
100
.00
-100
VOLUME (meters)
63-64 65-66 67-68 69-70 71-72 73-74 75-76 77-78 79-80 81-82 83-84 85-86
YEARS
B
4.
.0
-4.
FIRST
C
4.
.0
-4.
SECOND
D
4.
.0
-4.
THIRD
E
4.
.0
-4.
FOURTH
TEMPORAL EIGENFUNCTIONS

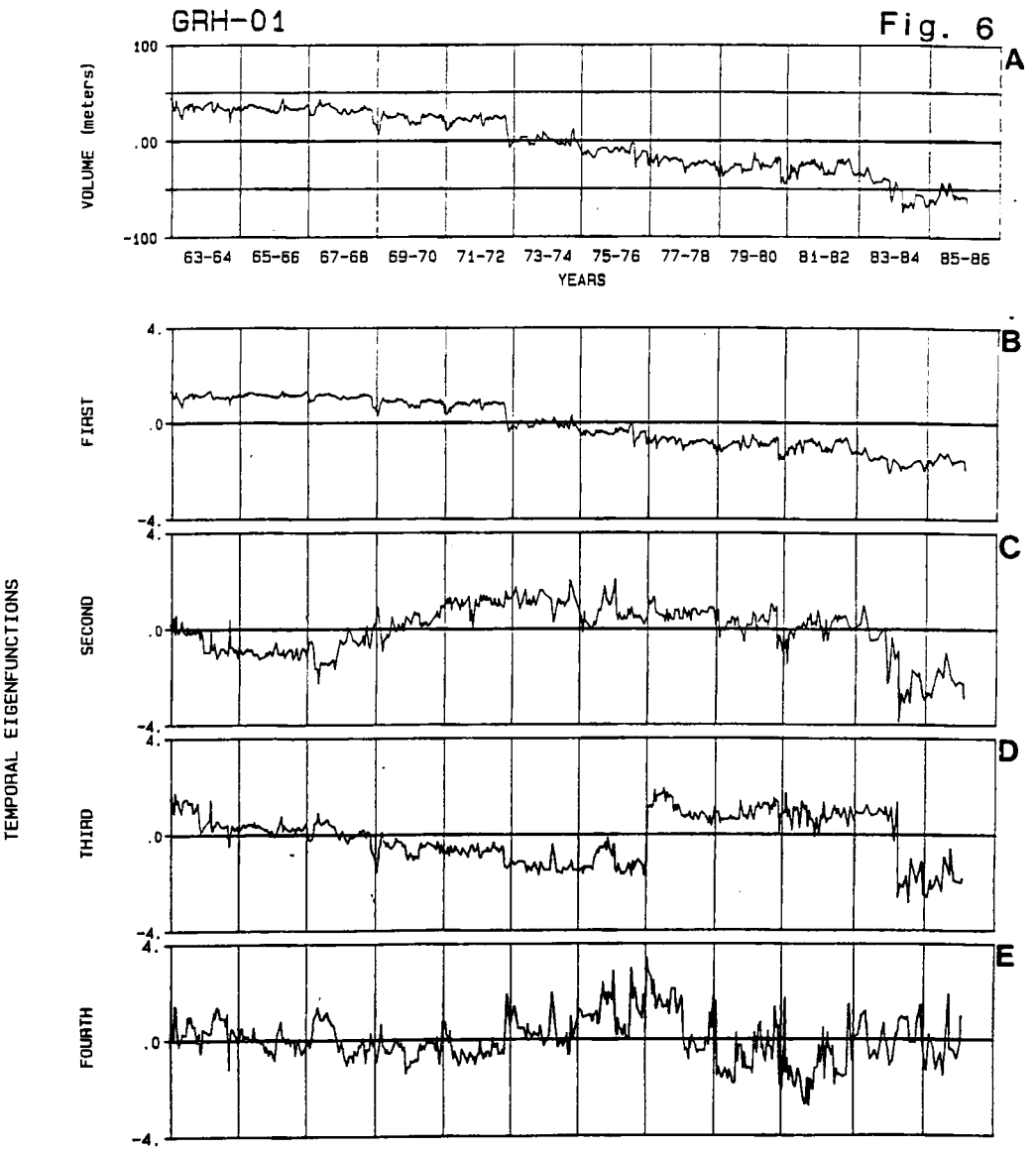
GRH-01
Fig. 6
A
100
.00
-100
VOLUME (meters)
63-64
65-66
67-68
69-70
71-72
73-74
75-76
77-78
79-80
81-82
83-84
85-86
YEARS
TEMPORAL EIGENFUNCTIONS
B
FIRST
4.
.0
-4.
C
SECOND
D
THIRD
E
FOURTH

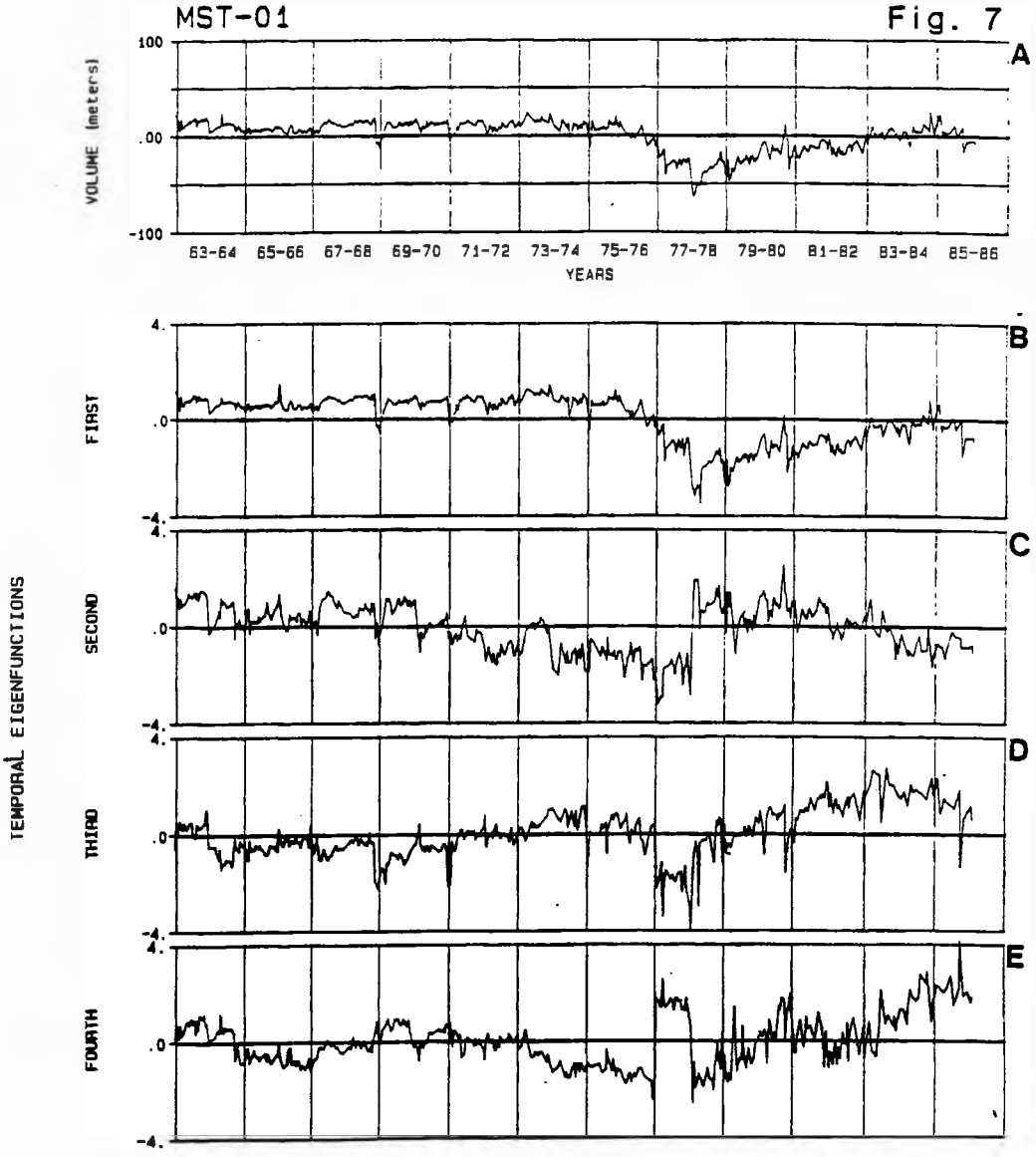
MST-01
Fig. 7
A
VOLUME (meters)
100
.00
-100
63-64
65-66
67-68
69-70
71-72
73-74
75-76
77-78
79-80
81-82
83-84
85-86
YEARS
TEMPORAL EIGENFUNCTIONS
B
FIRST
4.
.0
-4.
C
SECOND
D
THIRD
E
FOURTH

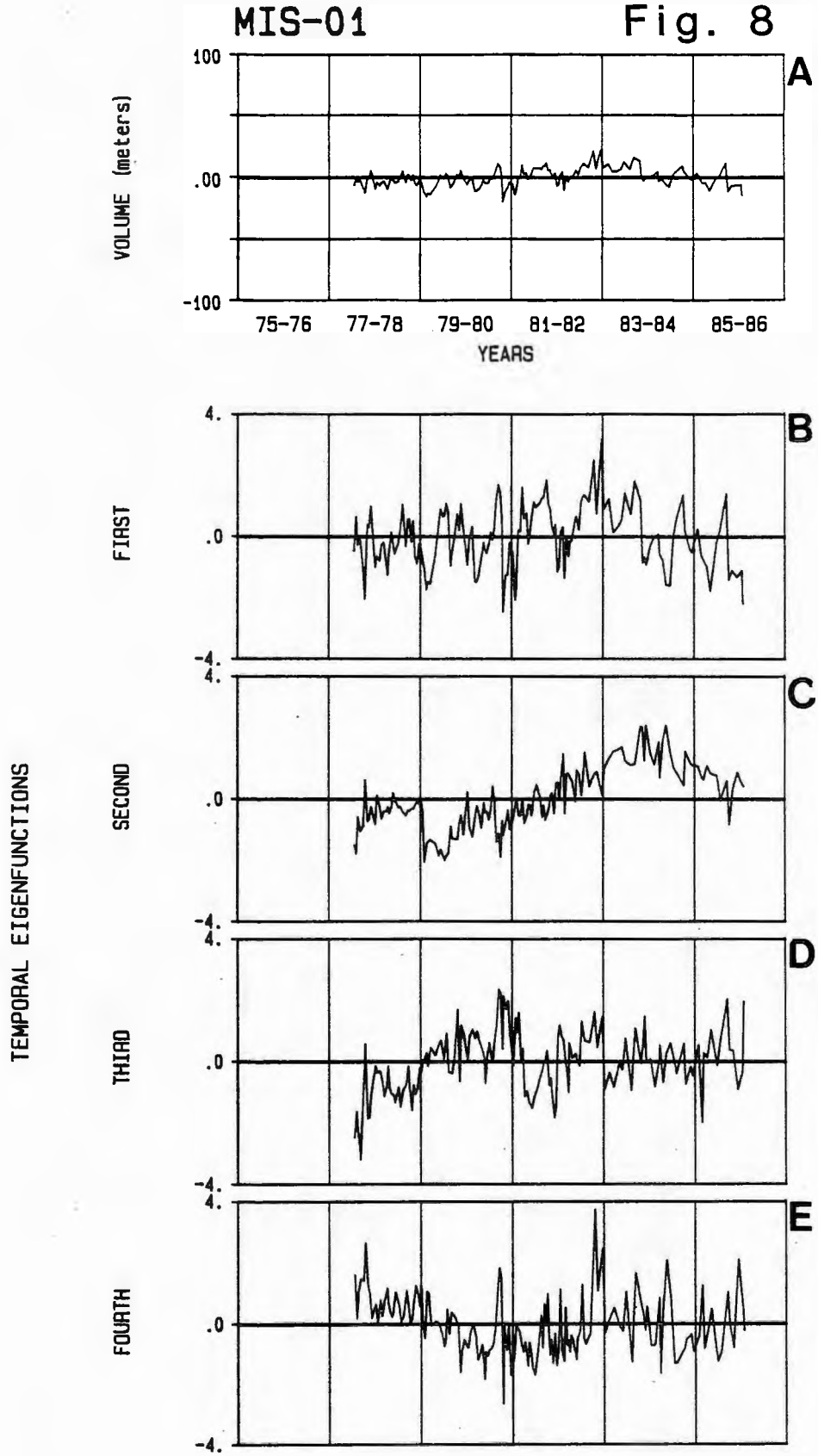
MIS-01
Fig. 8
A
100
.00
-100
VOLUME (meters)
75-76
77-78
79-80
81-82
83-84
85-86
YEARS
TEMPORAL EIGENFUNCTIONS
B
FIRST
4.
.0
-4.
C
SECOND
D
THIRD
E
FOURTH

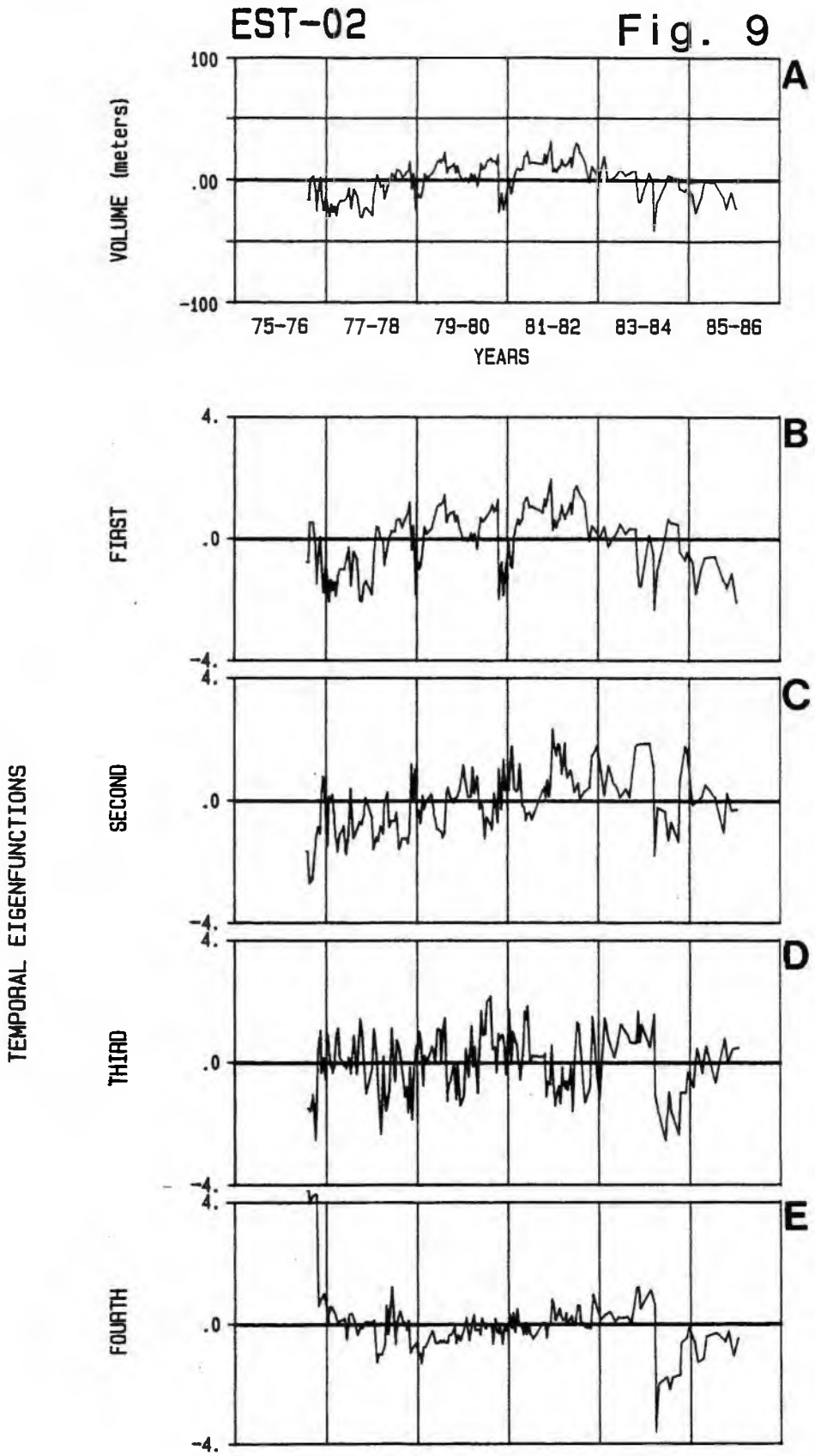
EST-02
Fig. 9
A
VOLUME (meters)
100
.00
-100
75-76
77-78
79-80
81-82
83-84
85-86
YEARS
TEMPORAL EIGENFUNCTIONS
B
FIRST
4.
.0
-4.
C
SECOND
D
THIRD
E
FOURTH

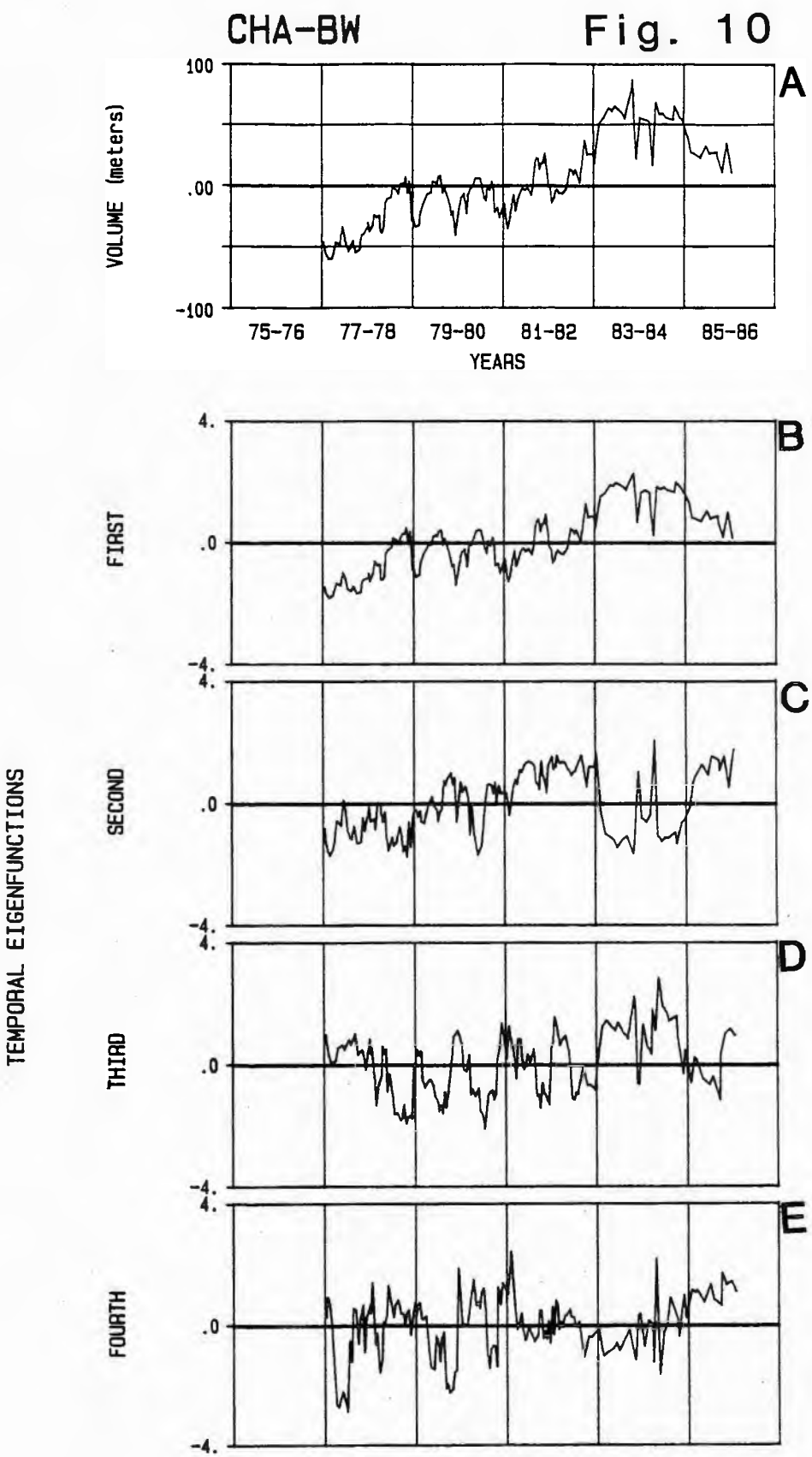
CHA-BW
Fig. 10
A
100
.00
-100
VOLUME (meters)
75-76
77-78
79-80
81-82
83-84
85-86
YEARS
TEMPORAL EIGENFUNCTIONS
B
FIRST
4.
.0
-4.
C
SECOND
D
THIRD
E
FOURTH

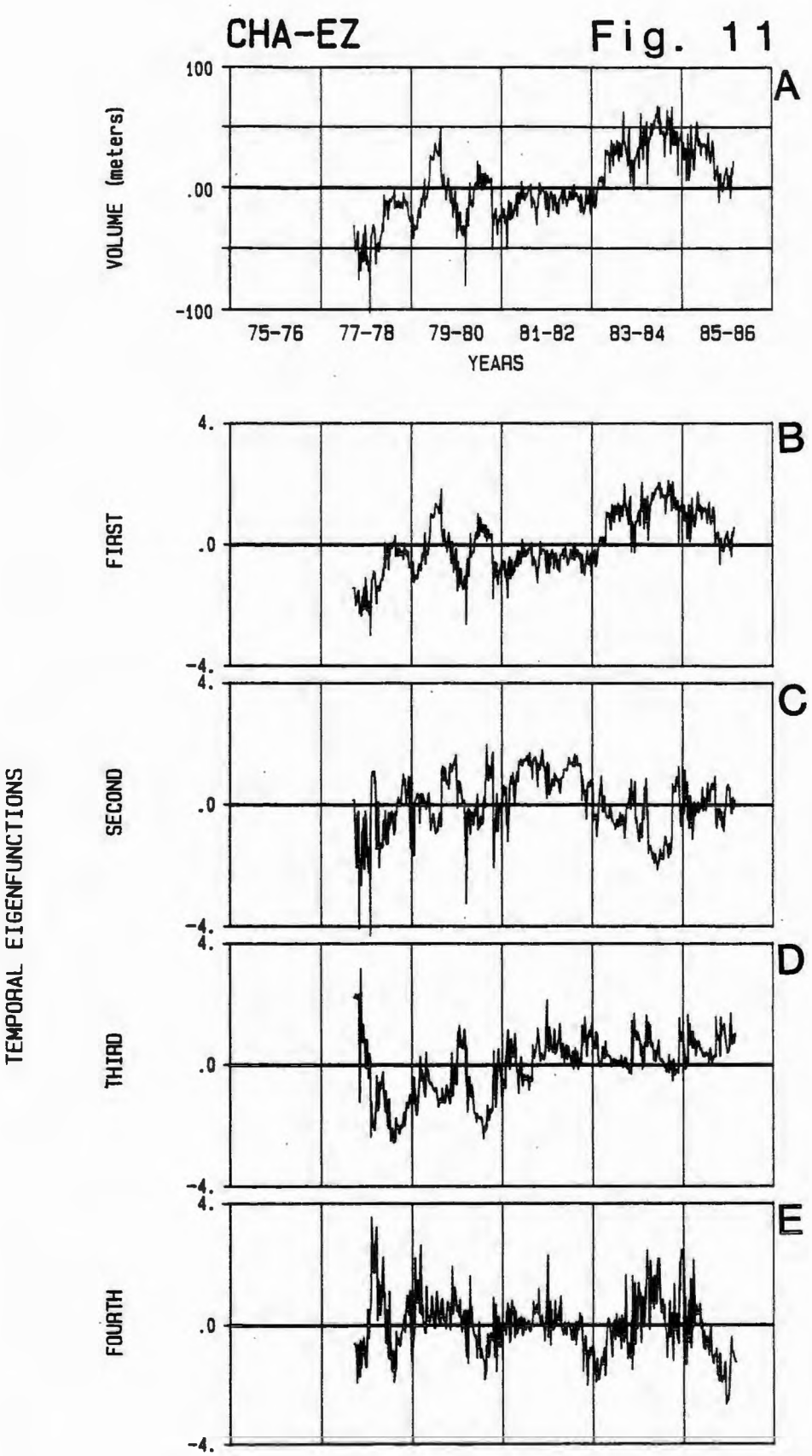
CHA-EZ
Fig. 11
A
VOLUME (meters)
100
.00
-100
75-76
77-78
79-80
81-82
83-84
85-86
YEARS
TEMPORAL EIGENFUNCTIONS
B
FIRST
4.
.0
-4.
C
SECOND
D
THIRD
E
FOURTH

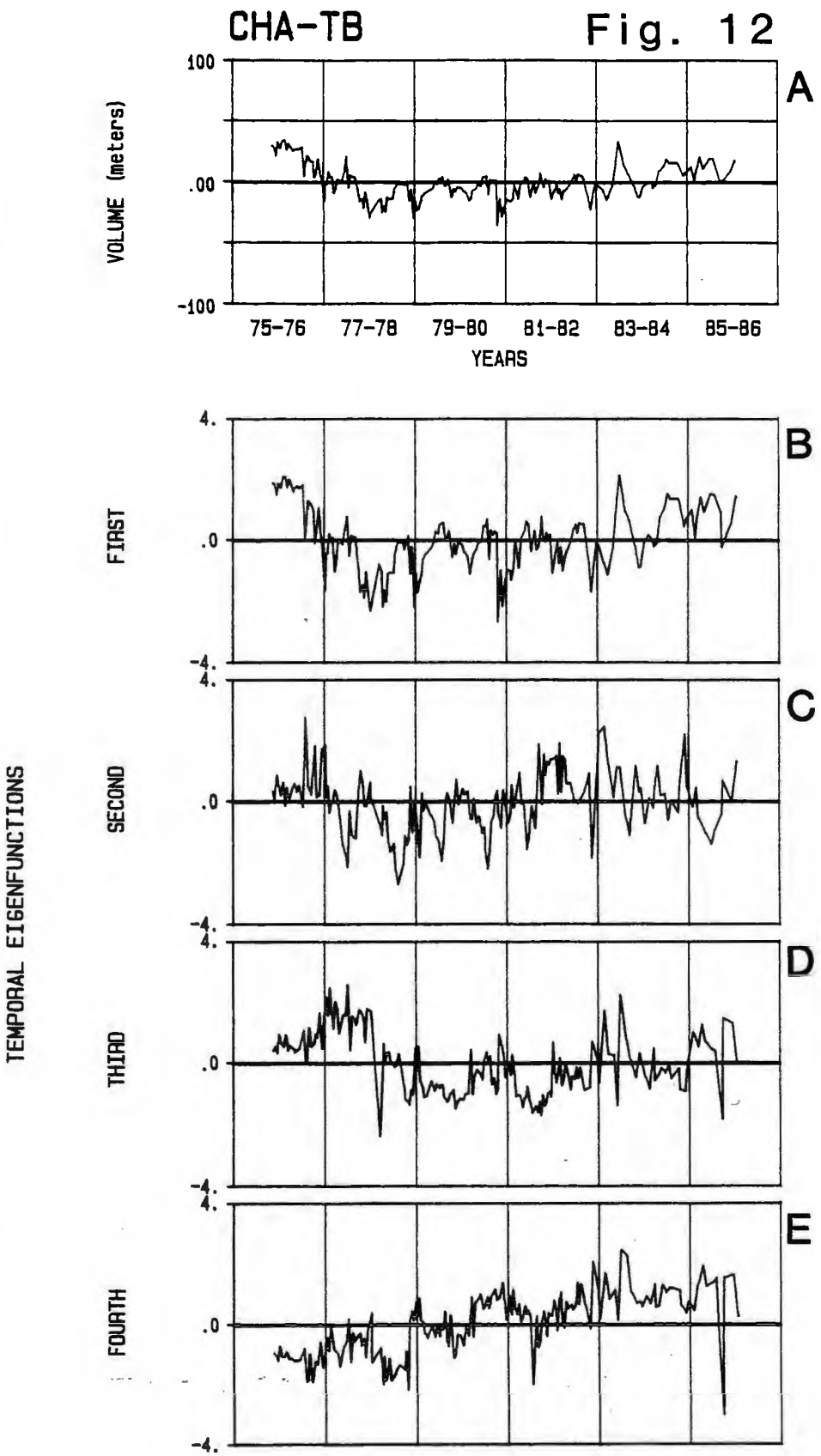
CHA-TB
Fig. 12
A
VOLUME (meters)
100
.00
-100
75-76
77-78
79-80
81-82
83-84
85-86
YEARS
TEMPORAL EIGENFUNCTIONS
B
FIRST
4.
.0
-4.
C
SECOND
D
THIRD
E
FOURTH

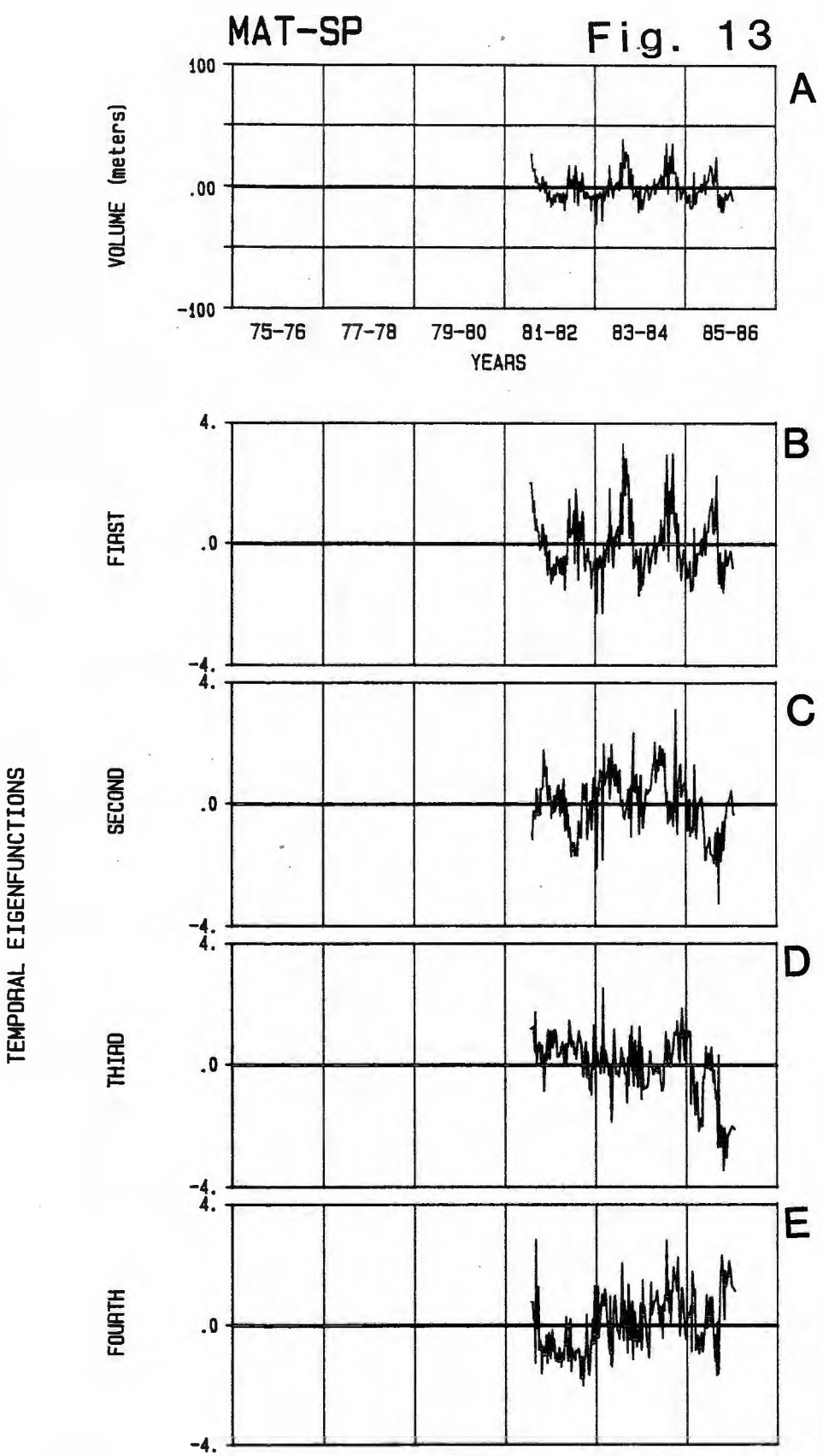
MAT-SP
Fig. 13
A
VOLUME (meters)
100
.00
-100
75-76
77-78
79-80
81-82
83-84
85-86
YEARS
TEMPORAL EIGENFUNCTIONS
B
FIRST
4.
.0
-4.
C
SECOND
4.
.0
-4.
D
THIRD
4.
.0
-4.
E
FOURTH
4.
.0
-4.

changes than the transit/stadia rod method. The CHA-EZ and CHA-BW volume plots, however, are very similar for these nearby locations, even though they have been measured differently.

A comparison of profiles taken on the same day at all locations except CHA-EZ and MAT-SP indicates that MIS-01, which is the only beach with a well-defined offshore bar system, has by far the least amount of volume variance (46 m^3). In contrast, CHA-BW located near a jettied inlet, has by far the greatest variance (838 m^3). The volume variance for the remaining profiles ranges from 121 m^3 to 306 m^3 and are given in table 2. Also shown in table 2 are the variances over the 24 year period of the four-long running profiles. From 1962 to 1986, the erosion trend of GRH-01 results in its very high variance.

Table 2 gives deposition and erosion rates derived by least squares linear regression on the volume time series. The four beaches measured since 1963 show a decrease in sediment volume. GRH-01 has the greatest erosional trend, 4.4 $m^3 \cdot yr^{-1}$ from 1963 to 1986. EST-01 and MST-01 show slight erosional trends of 1.2 and 1.4 $m^3 \cdot yr^{-1}$, respectively. WKG-01 has a very slight erosional trend (-0.1 $m^3 \cdot yr^{-1}$, but it would be greater if the unprecedented volume increase from 1983 to 1985 were subtracted out. The six shorter-term surveyed beaches all show depositional trends during their time periods. It is believed, however,

that longer-term surveys at these locations would also yield erosional trends.

TABLE 2.- Profile Erosion/Deposition Rates, and Volume Variances

Location (W-E)	Start	Erosion/Deposition From Start Date. rate ($m^3 \cdot yr^{-1}$)	Variance (m^3) (Jul 77- Jan 86)
MIS-01	Jul 77	0.8	46
WKG-01	Dec 62	-0.1	306
EST-01	Dec 62	-1.2	240
EST-02	Aug 76	0.5	205
CHA-BW	Jan 77	11.1	838
CHA-TB	Nov 75	0.1	121
GRH-01	Dec 62	-4.4	186
MST-01	Dec 62	-1.4	242
			Variance (m^3) (Dec 62-Jan 86)
WKG-01			181
EST-01			280
GRH-01			910
MST-01			287
			Variance (m^3) (Oct 77-Mar 86)
CHA-EZ	Oct 77	8.9	904
			Variance (m^3) (Aug 81-Mar 86)
MAT-SP	Aug 81	0.2	139

A significant decrease in sediment volume occurred between 1976 and 1978 at all locations except GRH-01 and MIS-01 (Gibeaut et al. 1986); MAT-SP was not measured during this time. A second period of significant volume decrease occurred during the winter of 1982-83 at WKG-01 (Plate WKG-Vol). The other locations, however, do not show

Fig. 14-23.- Spectral Plots.

14) Weekapaug Beach 1.
a) volume spectrum b) first temporal eigenfunction spectrum c) second temporal eigenfunction spectrum d) third temporal eigenfunction spectrum e) fourth temporal eigenfunction spectrum

15) East Beach 1.
a-e) same as above

16) Green Hill Beach 1.
a-e) same as above

17) Moonstome Beach 1.
a-e) same as above

18) Misquamicut Beach 1.
a-e) same as above

19) East Beach 2.
a-e) same as above

20) Charlestown Breachway Beach.
a-e) same as above

21) Charlestown EZ Beach.
a-e) same as above

22) Charlestown Town Beach.
a-e) same as above

23) Matunuck SP Beach.
a-e) same as above

Fig. 14

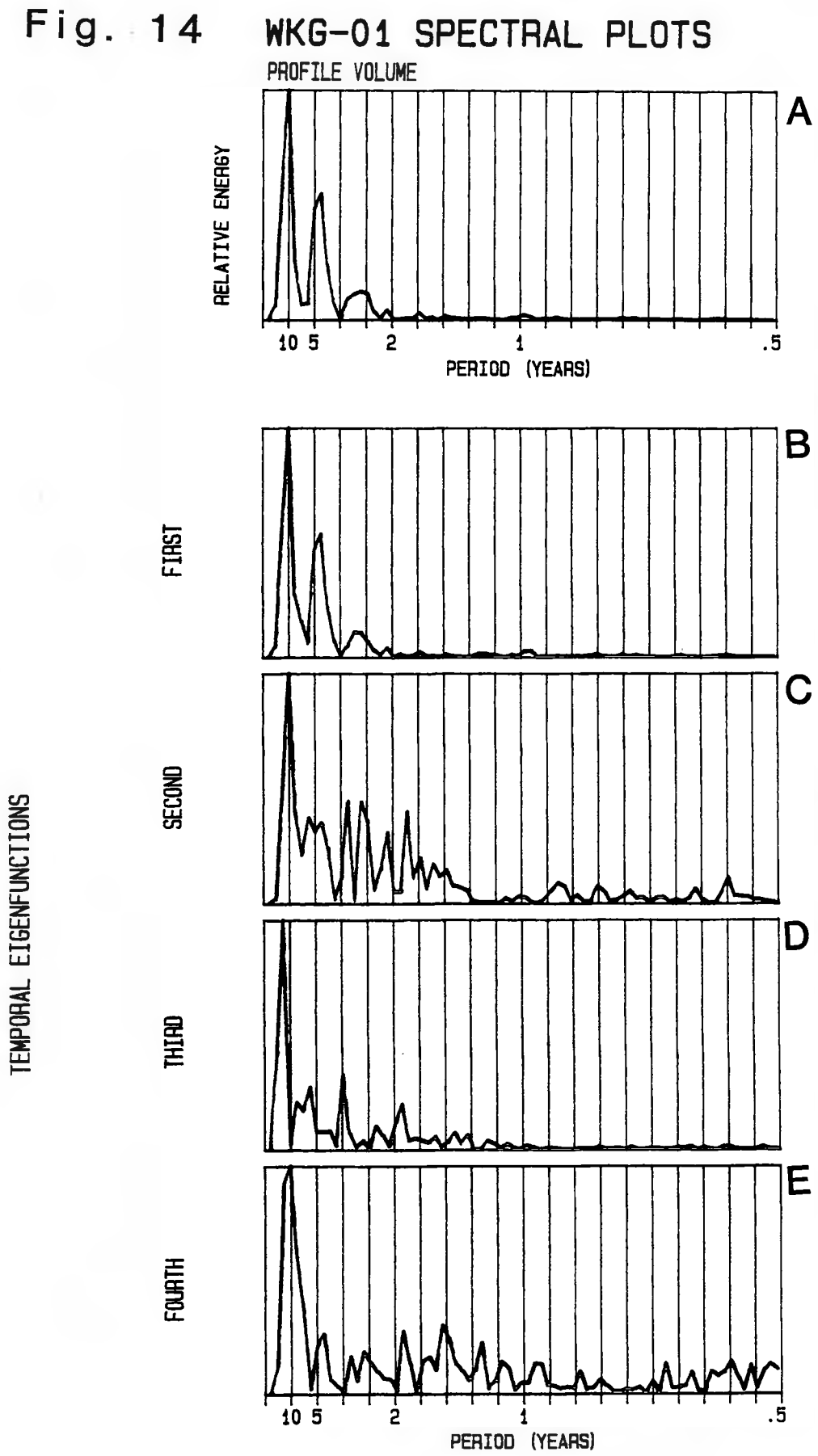
WKG-01 SPECTRAL PLOTS
PROFILE VOLUME
A
RELATIVE ENERGY
10 5
2
1
.5
PERIOD (YEARS)
TEMPORAL EIGENFUNCTIONS
FIRST
B
SECOND
C
THIRD
D
FOURTH
E
10 5
2
1
.5
PERIOD (YEARS)

Fig. 15

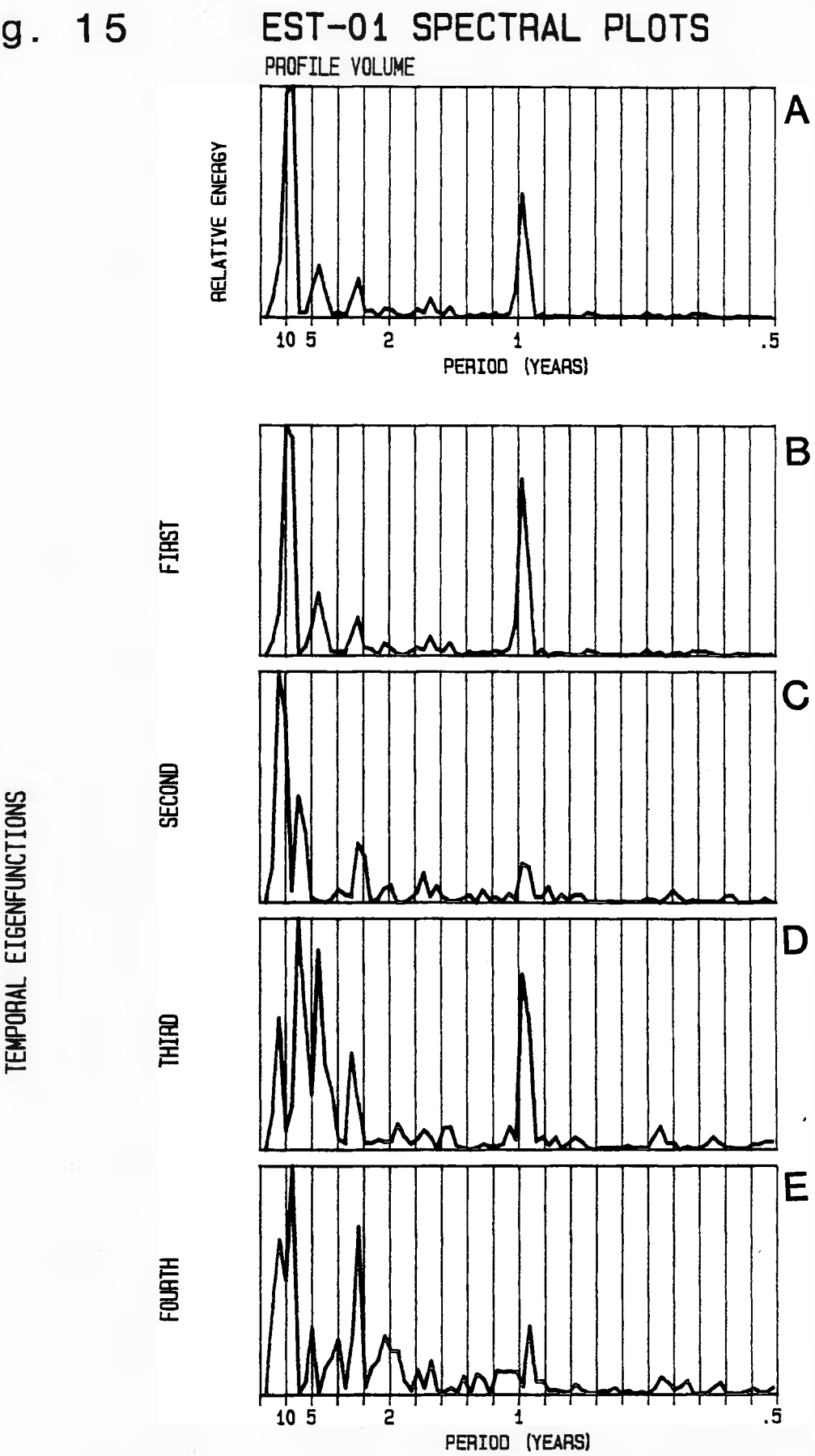
EST-01 SPECTRAL PLOTS
PROFILE VOLUME
RELATIVE ENERGY
A
10 5
2
1
.5
PERIOD (YEARS)
TEMPORAL EIGENFUNCTIONS
FIRST
B
SECOND
C
THIRD
D
FOURTH
E
10 5
2
1
.5
PERIOD (YEARS)

Fig. 16

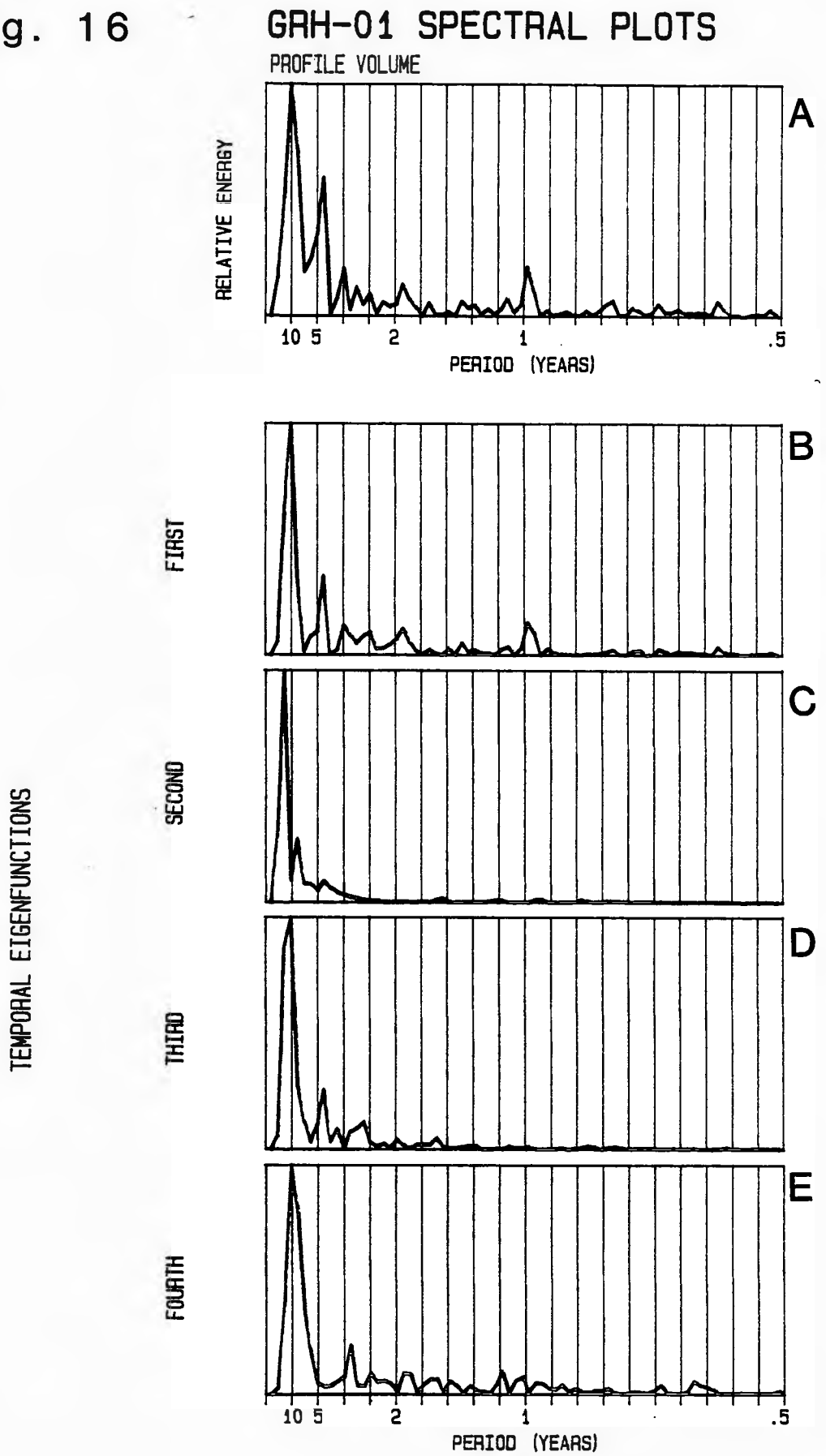
GRH-01 SPECTRAL PLOTS
PROFILE VOLUME
RELATIVE ENERGY
A
10 5 2 1 .5
PERIOD (YEARS)
TEMPORAL EIGENFUNCTIONS
FIRST
B
SECOND
C
THIRD
D
FOURTH
E
10 5 2 1 .5
PERIOD (YEARS)

Fig. 17

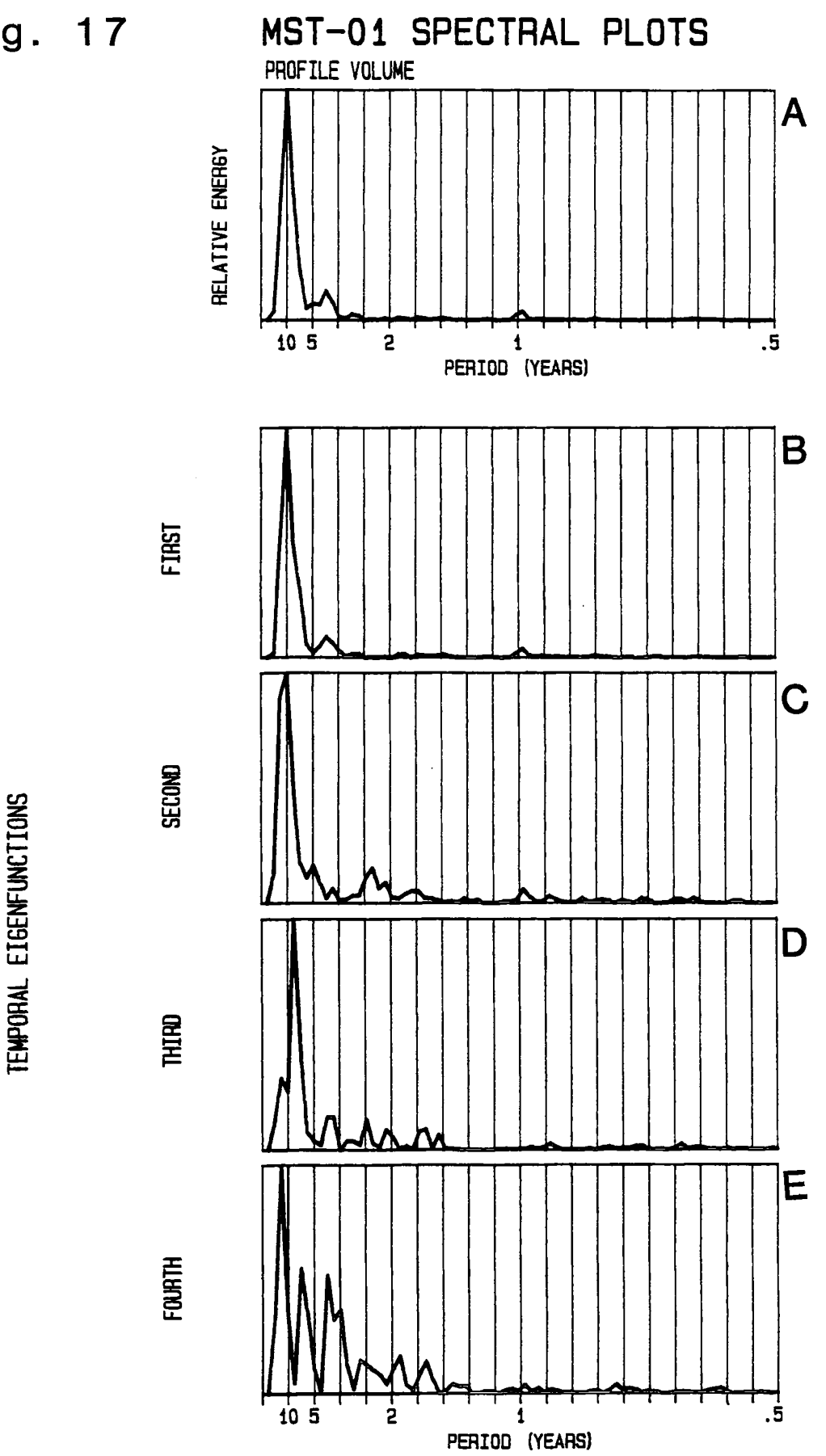
MST-01 SPECTRAL PLOTS
PROFILE VOLUME
RELATIVE ENERGY
A
10 5
2
1
.5
PERIOD (YEARS)
TEMPORAL EIGENFUNCTIONS
FIRST
B
SECOND
C
THIRD
D
FOURTH
E
10 5
2
1
.5
PERIOD (YEARS)

Fig. 18

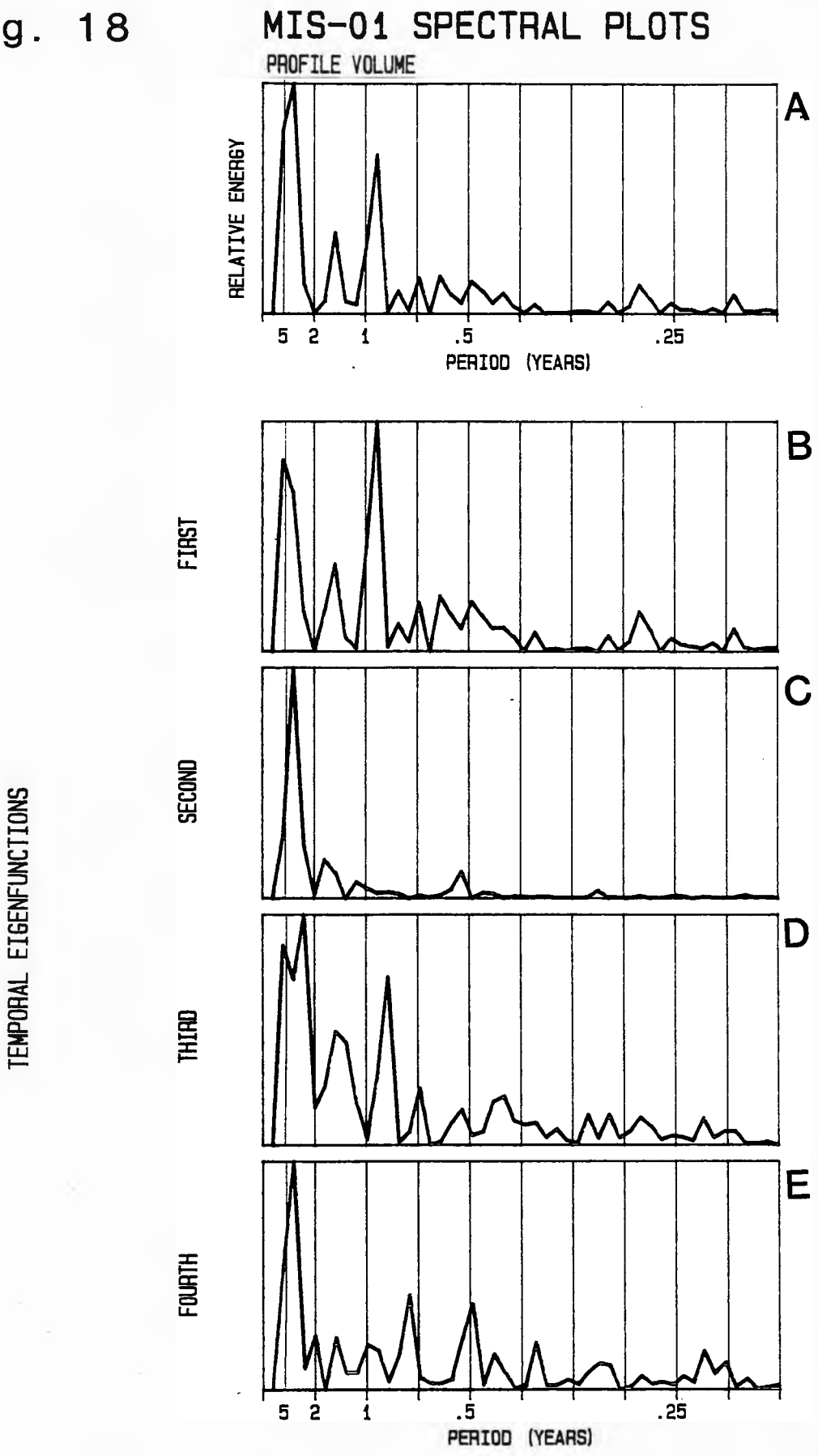
MIS-01 SPECTRAL PLOTS
PROFILE VOLUME
RELATIVE ENERGY
A
5 2 1 .5 .25
PERIOD (YEARS)
TEMPORAL EIGENFUNCTIONS
FIRST
B
SECOND
C
THIRD
D
FOURTH
E
5 2 1 .5 .25
PERIOD (YEARS)

Fig. 19

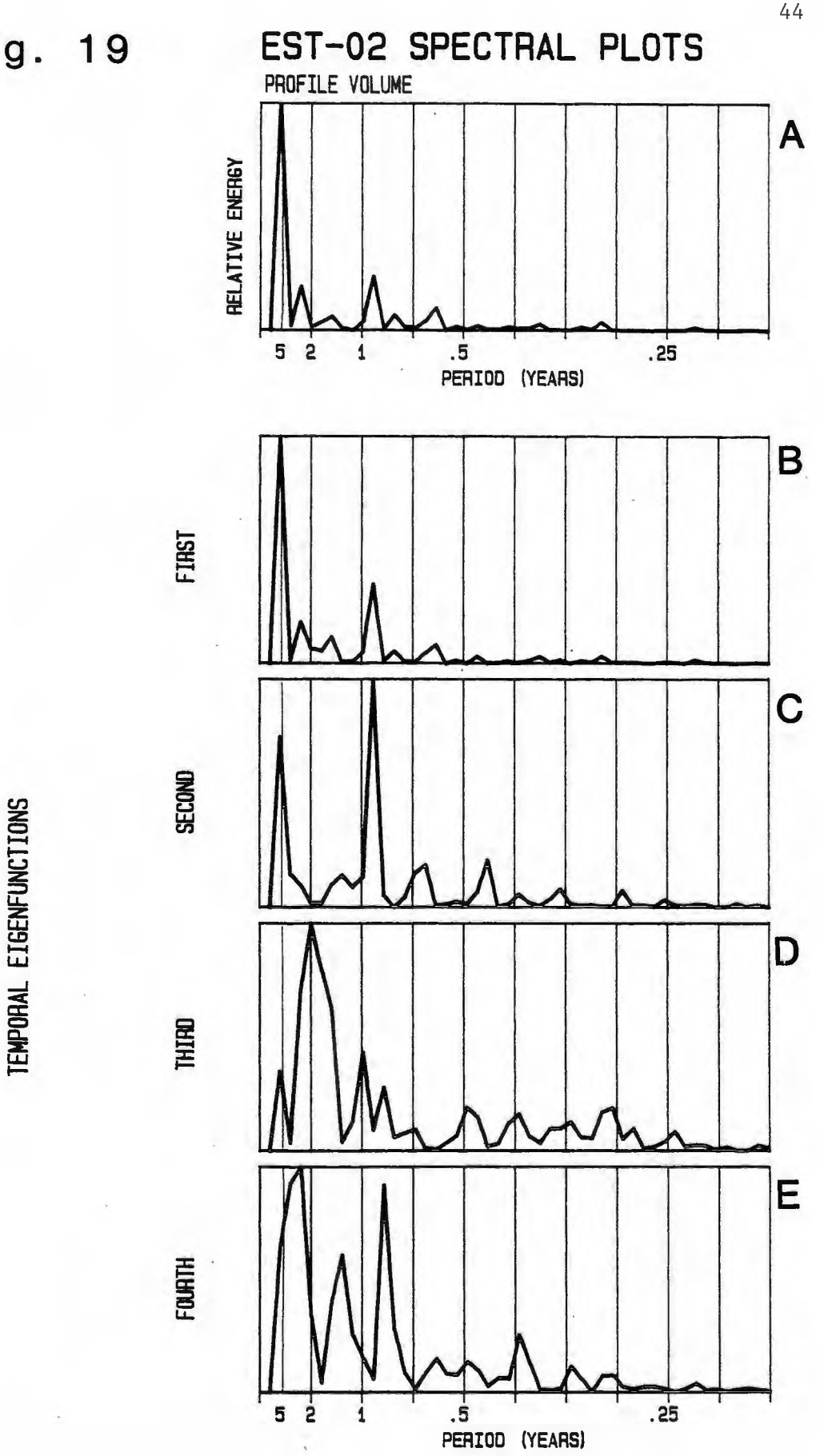
EST-02 SPECTRAL PLOTS
PROFILE VOLUME
RELATIVE ENERGY
A
5
2
1
.5
.25
PERIOD (YEARS)
TEMPORAL EIGENFUNCTIONS
FIRST
B
SECOND
C
THIRD
D
FOURTH
E
5
2
1
.5
.25
PERIOD (YEARS)

Fig. 20

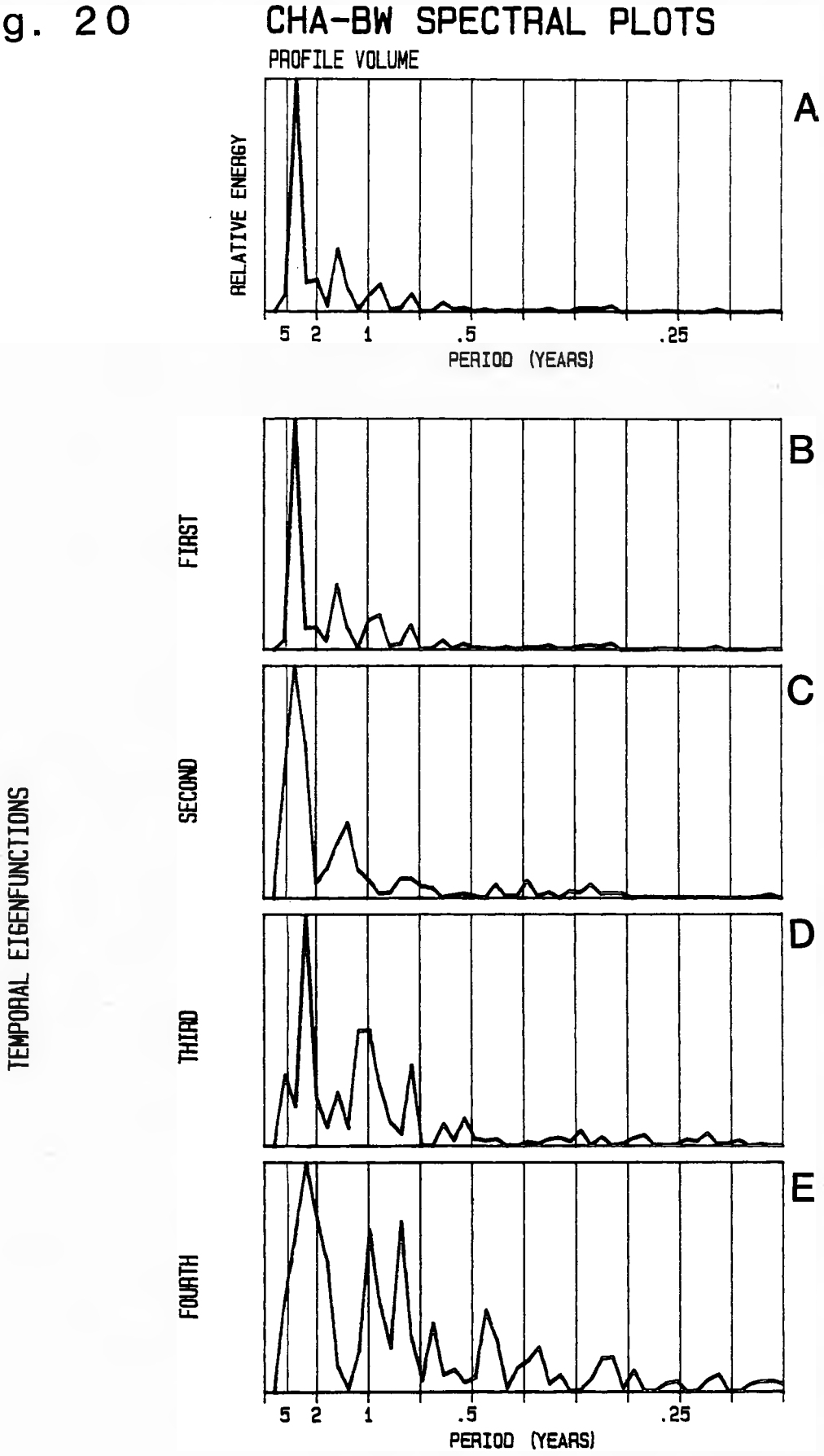
CHA-BW SPECTRAL PLOTS
PROFILE VOLUME
RELATIVE ENERGY
A
5
2
1
.5
.25
PERIOD (YEARS)
TEMPORAL EIGENFUNCTIONS
FIRST
B
SECOND
C
THIRD
D
FOURTH
E
5
2
1
.5
.25
PERIOD (YEARS)

Fig. 21

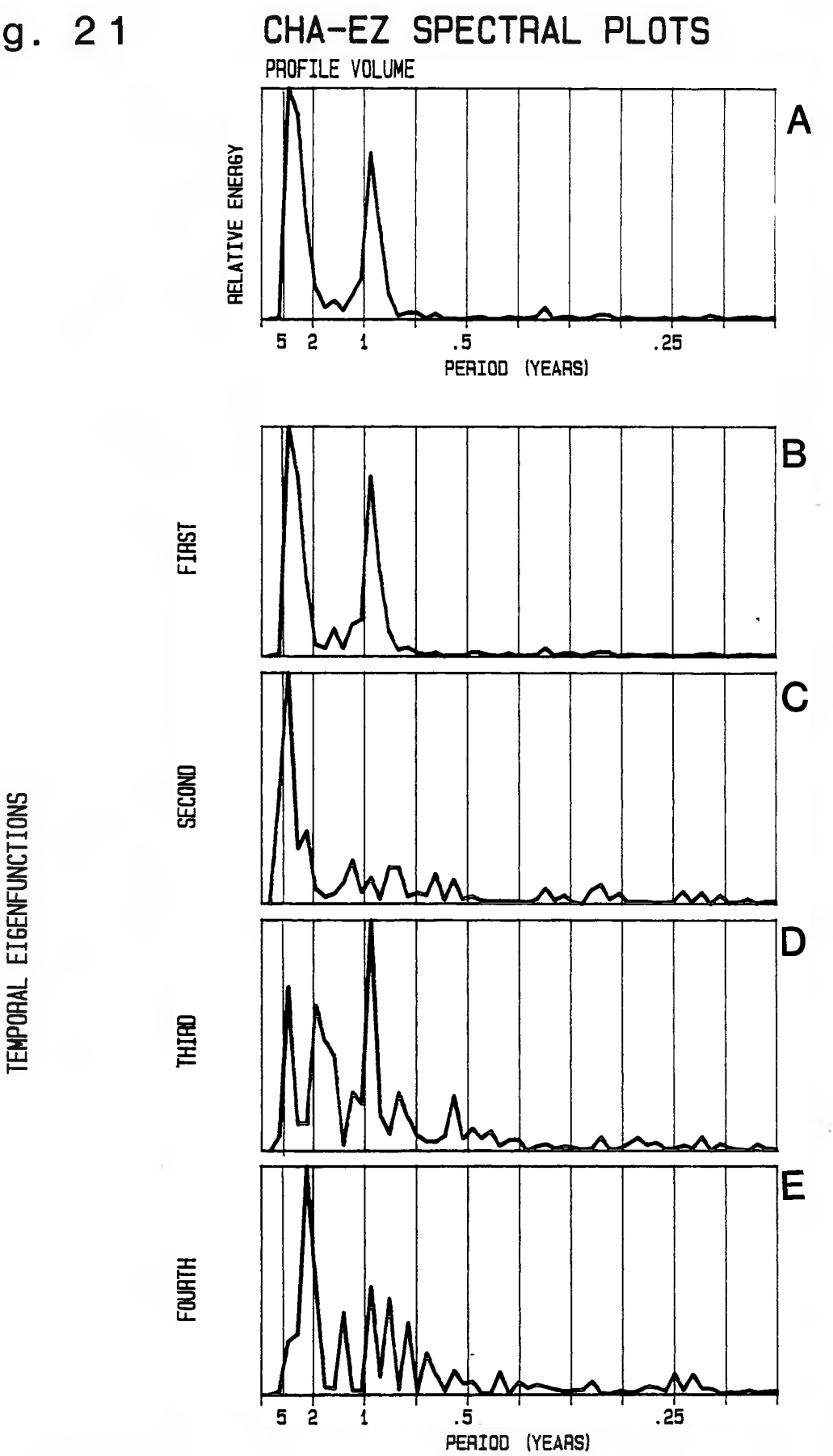
CHA-EZ SPECTRAL PLOTS
PROFILE VOLUME
RELATIVE ENERGY
A
5
2
1
.5
.25
PERIOD (YEARS)
TEMPORAL EIGENFUNCTIONS
FIRST
B
SECOND
C
THIRD
D
FOURTH
E
5
2
1
.5
.25
PERIOD (YEARS)

Fig. 22

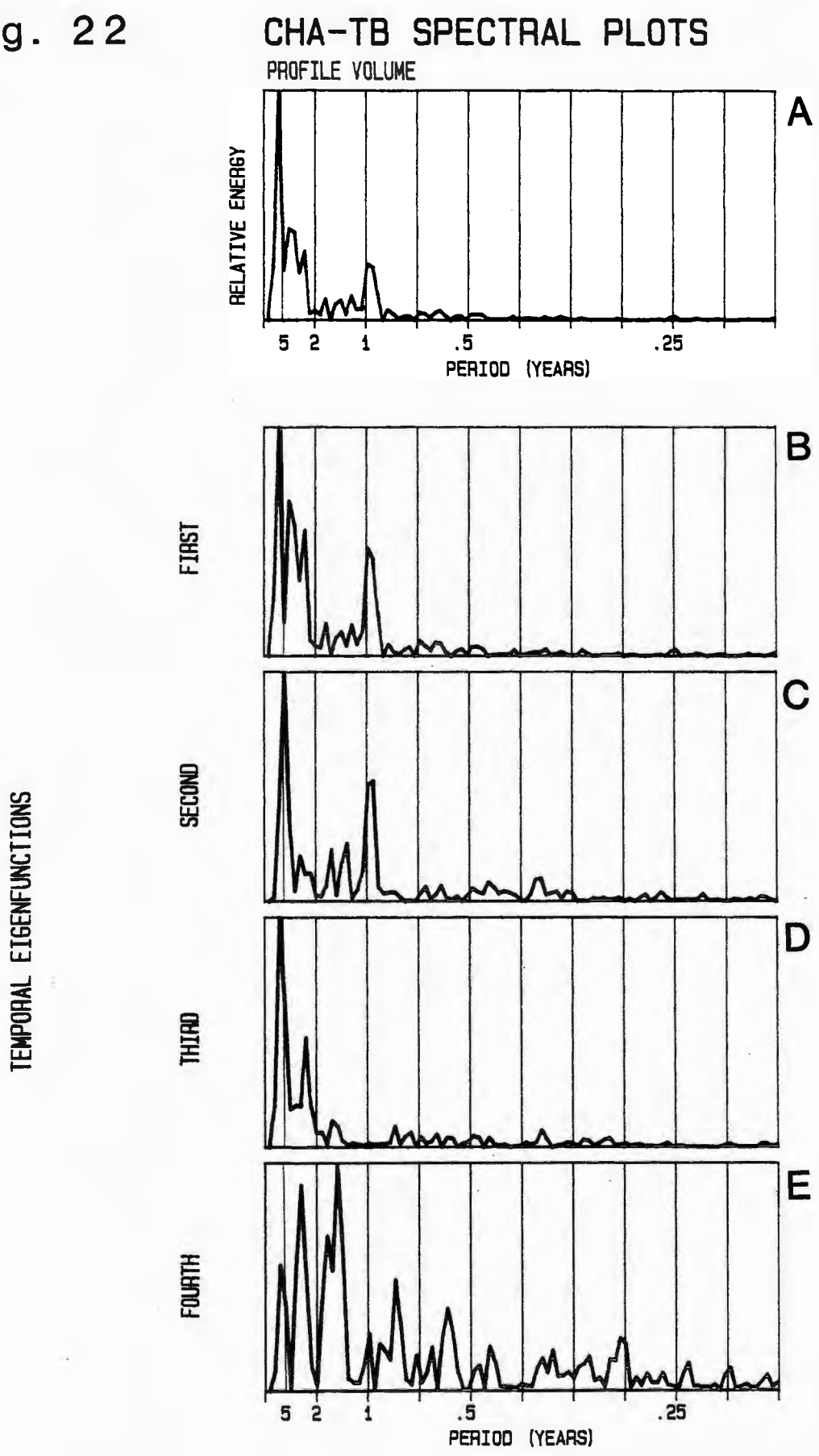
CHA-TB SPECTRAL PLOTS
PROFILE VOLUME
RELATIVE ENERGY
A
5
2
1
.5
.25
PERIOD (YEARS)
TEMPORAL EIGENFUNCTIONS
FIRST
B
SECOND
C
THIRD
D
FOURTH
E
5
2
1
.5
.25
PERIOD (YEARS)

Fig. 23

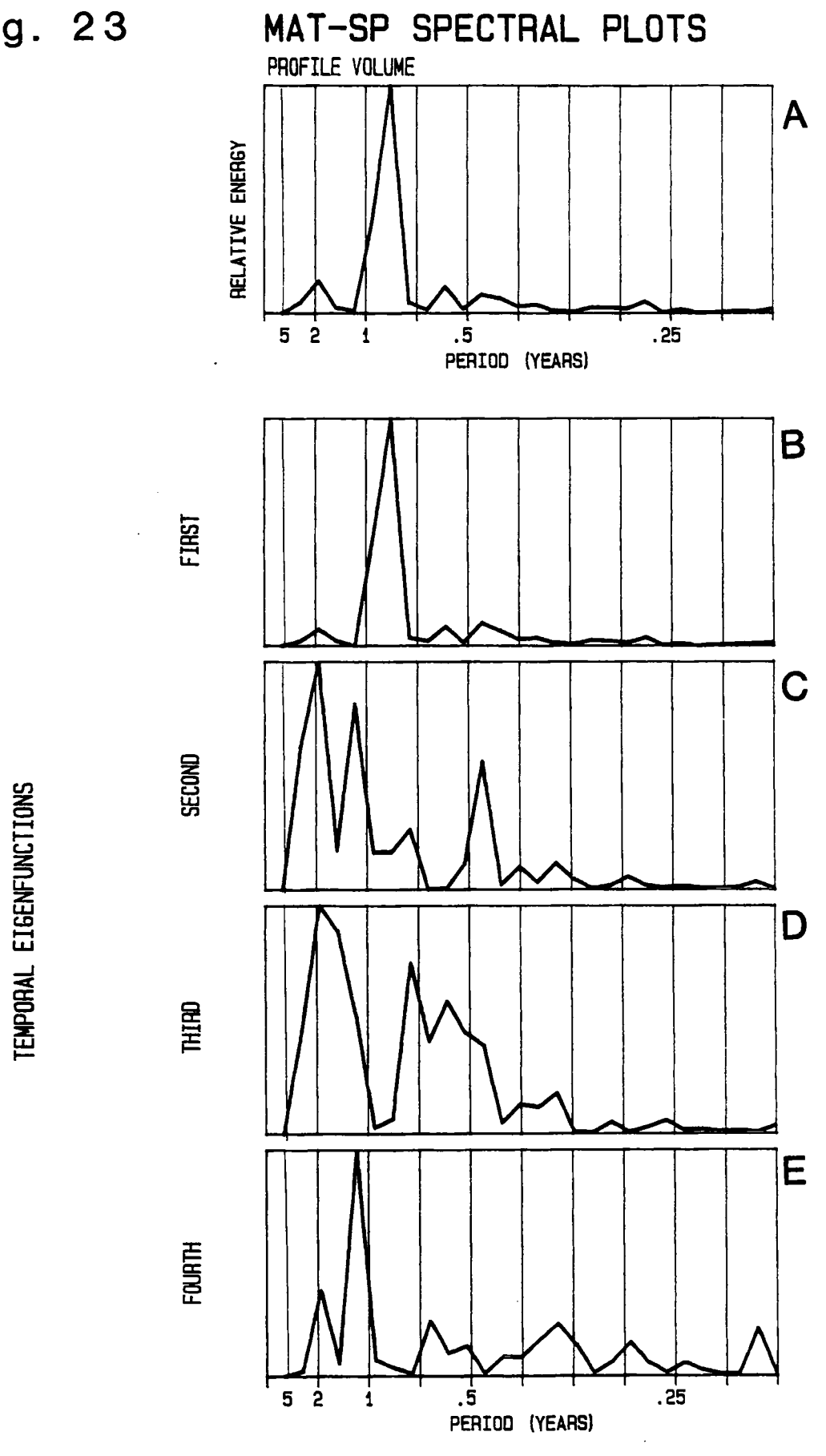
MAT-SP SPECTRAL PLOTS
PROFILE VOLUME
RELATIVE ENERGY
A
5 2 1 .5 .25
PERIOD (YEARS)
TEMPORAL EIGENFUNCTIONS
FIRST
B
SECOND
C
THIRD
D
FOURTH
E
5 2 1 .5 .25
PERIOD (YEARS)

such a significant drop, and in fact, the MIS-01 plot shows a volume increase during the 1982-83 winter. In the fall of 1972, GRH-01 experienced a permanent loss of sediment which did not occur at any other location.

From early 1983 to mid 1984, CHA-BW, which is just east of the jettied Charlestown inlet, and WKG-01, which is east of the protruding Weekapaug headland, significantly increased in volume. Over the same time period EST-02, which is west of the Charlestown inlet, and GRH-01, which is west of the Green Hill headland, decreased in volume (Gibeaut et al. 1986). From mid 1984 to 1986 these trends reversed and CHA-BW eroded while GRH-01 accreted; at WKG-01 and EST-02, the trends leveled off.

The spectra of the volume plots for the four long-running profiles show a very strong 10-year periodicity (Figs. 14a-17a). Qualitative inspection of the WKG-01, EST-01, and MST-01 volume plots show the 10-year cycles to be in phase with one another. Peaks occur in 1963, 1973-75, and 1984-85, and troughs in 1966-67, and 1979-81. The GRH-01 ten-year cycle appears to be slightly out of phase with the others and has peaks in 1971-72 and 1981-82 and troughs in 1963, 1975-76, and possibly one in 1986-87.

WKG-01, EST-01, GRH-01, and MST-01 have secondary peaks of varying importance at a 4-5 year period. WKG-01 and GRH-01 have the strongest 5-year peaks, whereas EST-01 and MST-01 have less important 5-year cycles. The phase relationship for this cycle is more complicated, but again

WKG-01, EST-01, and MST-01 appear to be in phase and have peaks at 1963, 1965-66, 1969-70, 1974-75, 1980-81, and 1984-85 and troughs in 1964, 1967, 1972, 1977, 1982, and possibly a future one in 1987. The 5-year-cycle phase relationship for GRH-01 is obscure but has corresponding peaks with the others in 1985 and 1981.

The volume spectra for WKG-01, EST-01, GRH-01, and MST-01 all have at least a small one-year, seasonal spike. EST-01, however, has by far the greatest seasonality and is the only beach which has a more important 1-year cycle than 5-year-cycle. On the other hand, seasonal volume change is of little importance at WKG-01 and MST-01. GRH-01 has a prominent seasonal peak, but the GRH-01 spectrum is much more broken up at the higher frequencies, which indicates a more complicated pattern of change. Also present at WKG-01 and EST-01 are minor 2.5 to 3.0-year cycles.

The volume spectra for the 6 shorter time series, except MAT-SP, have prominent 4-6-year spikes (Figs.18a-23a). The MAT-SP time series is only 4.5 years which may explain the absence of such a spike; however, a 4-6 year cycle is not even suggested in the volume plot (Fig. 23A, Plate MAT/SP-Vol). The MAT-SP spectra, however, has a minor 2-year spike. The 5-year cycles at CHA-BW, CHA-EZ, and CHA-TB are in phase with WKG-01, EST-01, and MST-01; MIS-01 and EST-02 are roughly in phase with GRH-01.

Of the six shorter-running profiles, all but CHA-BW have a prominent seasonal spike. Examination of the

volume plot for CHA-BW (Fig. 20A, Plate CHA/BW-Vol), however, reveals an equal amount of volume change on a seasonal basis compared to other profiles; it is the relative importance of the five-year cycle that overwhelms the seasonality.

Tide Gauge Data

Figure 24 is a time-series plot of weekly-averaged hourly water levels recorded by the Newport, Rhode Island tide gauge. Figure 24b is a plot of the yearly averages of the weekly averages. There are four temporal scales of variation apparent in the data. 1) High and low weekly spikes occur throughout the data and may stand out up to .25 m from the curve. 2) A yearly cycle, with lows in the winters and highs in the summers, has an amplitude of about .15 m. 3) An 11-to 14-year cycle, with lows centered on 1965 and 1979 and highs in 1972 and 1983-84. The amplitude of this long-term cycle is about .15 m. 4) A linear rise in sea level.

Eigenfunction Modes of Variance

Since eigenfunctions extracted from a symmetric covariance matrix are orthogonal, they theoretically describe independent modes of variance of the beach, and separate forcing functions may be identified that cause

Fig. 24.- Sea-level Plots (1961-1985) a) Weekly Average Sea Levels. b) Yearly Average Sea Levels.

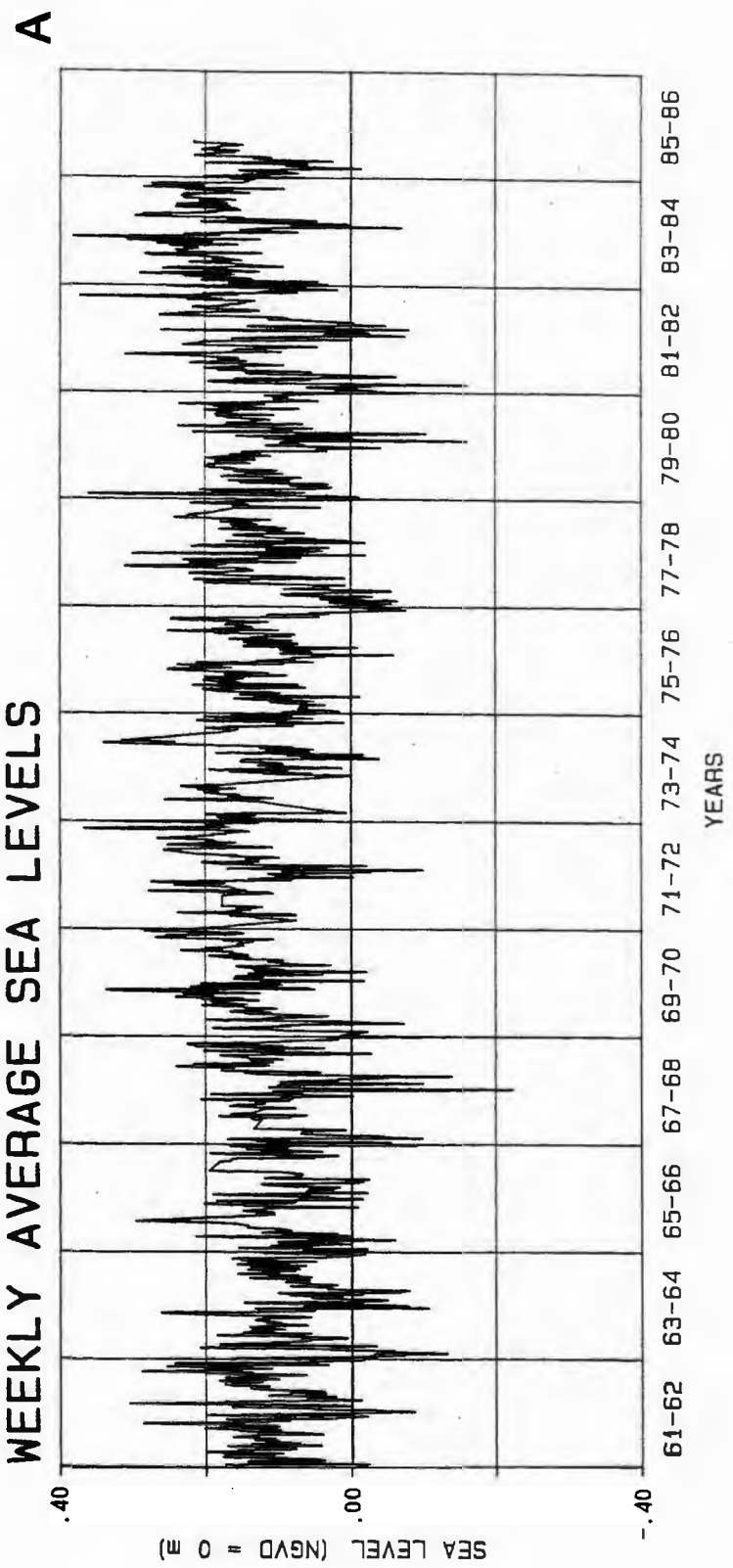
A
WEEKLY AVERAGE SEA LEVELS
SEA LEVEL (NGVD = 0 m)
.40
.00
-.40
61-62
63-64
65-66
67-68
69-70
71-72
73-74
75-76
77-78
79-80
81-82
83-84
85-86
YEARS

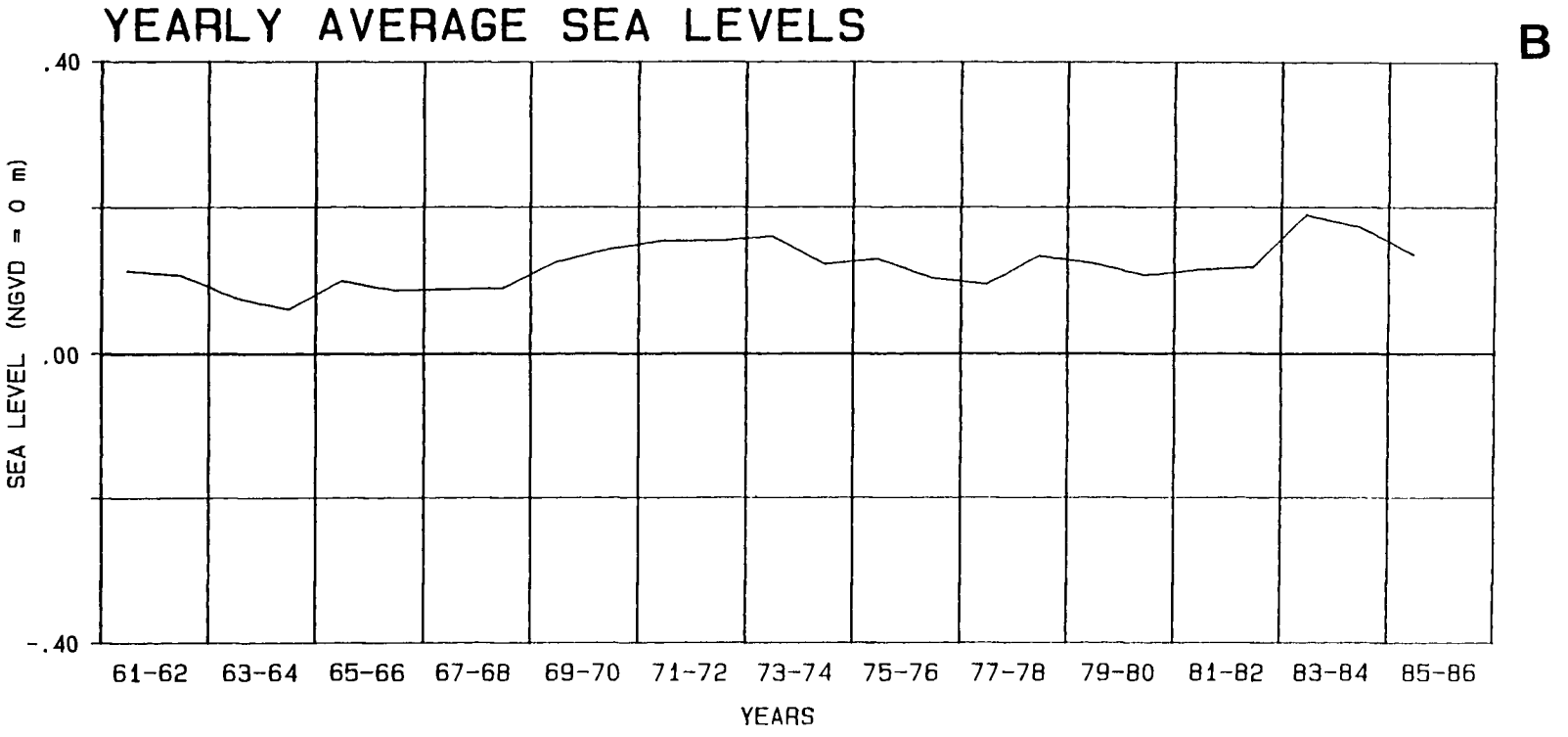
YEARLY AVERAGE SEA LEVELS
B
.40
.00
-.40
SEA LEVEL (NGVD = 0 m)
61-62
63-64
65-66
67-68
69-70
71-72
73-74
75-76
77-78
79-80
81-82
83-84
85-86
YEARS

trends in the temporal functions. In the present study, four characteristic modes of variance called beach-functions have been identified: the shoreface-berm-function; the beachface-function; the back-berm-function; and the foredune-function. Most beaches, however, do not have eigenfunctions that separate all these modes and some beach-functions may be combined to form hybrid functions. The identification of these beach functions requires an a priori knowledge of beach processes which, for this study, was greatly aided by a detailed five year analysis of CHA-EZ profiles by Rosenberg (1985). Following is a discussion of each beach function.

Shoreface-berm function.- Winant et al. (1975) analyzed 2 years of profile data from Torrey Pines Beach, California. The profiles extended from the backshore seaward to a depth of 7 m below sea level. In that study, the most important eigenfunction explaining the variance from the mean profile was identified as the bar-berm-function and displayed a pivotal point at 2-3 m depth through which sand passed on a seasonal basis. Landward of this point was a broad maximum where the summer berm formed; seaward was a minimum where the winter bar formed. In the present study, even though profiles extend to only mean low water, the first eigenfunctions for all locations suggest that a pivotal point exists below mean low water (Figs. 25b-34b). This function is therefore called the shoreface-berm-function and

Fig. 25-34.- Spatial Eigenfunctions.

25) Weekapaug Beach 1.
a) mean profile b) first spatial eigenfunction c) second spatial eigenfunction d) third spatial eigenfunction e) fourth spatial eigenfunction

26) East Beach 1.
a-e) same as above

27) Green Hill Beach 1.
a-e) same as above

28) Moonstone Beach 1.
a-e) same as above

29) Misquamicut Beach 1.
a-e) same as above

30) East Beach 2.
a-e) same as above

31) Charlestown Breachway Beach.
a-e) same as above

32) Charlestown EZ Beach.
a-e) same as above

33) Charlestown Town Beach.
a-e) same as above

34) Matunuck SP Beach.
a-e) same as above

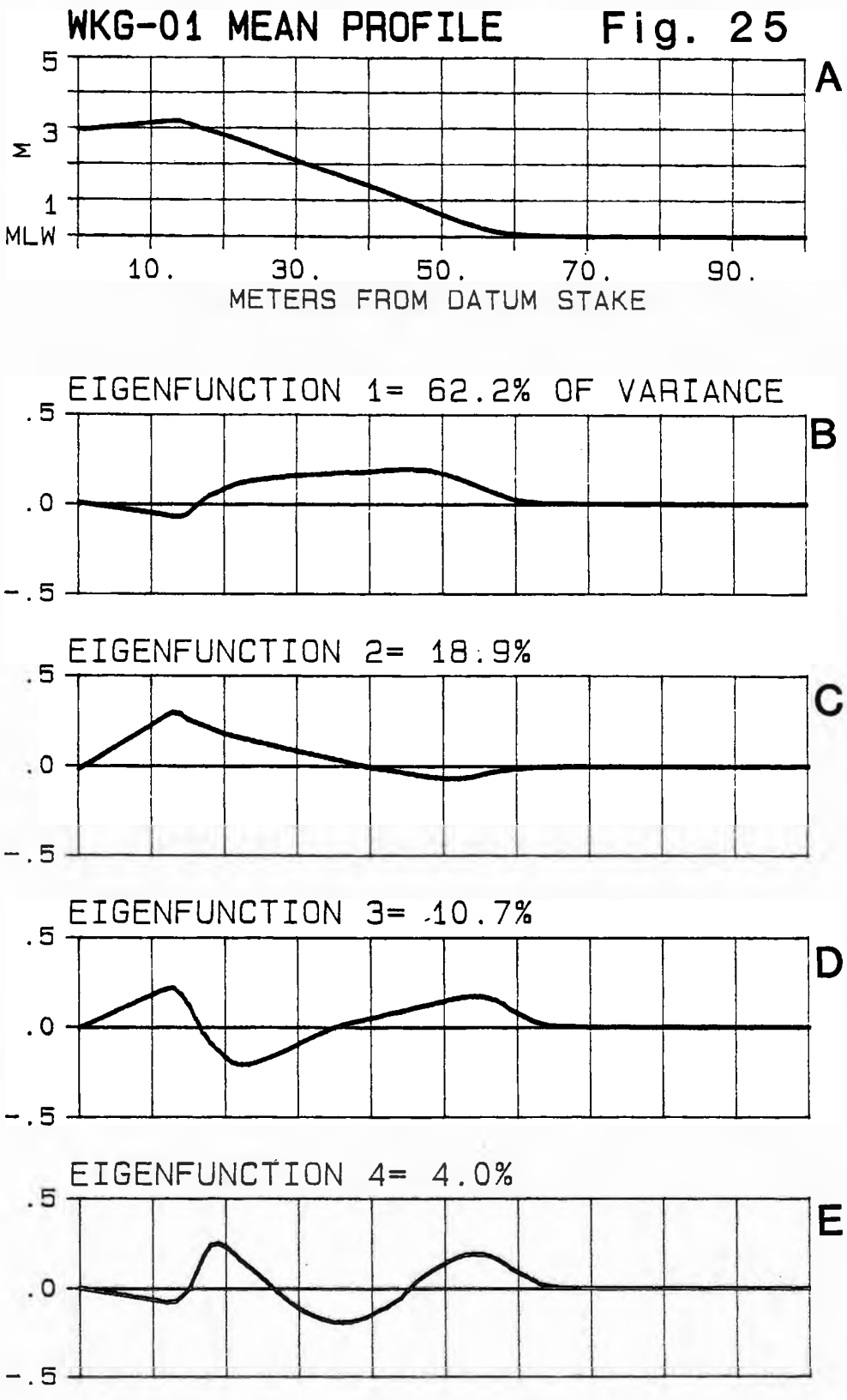
WKG-01 MEAN PROFILE
Fig. 25
A
5
3
1
MLW
M
10.
30.
50.
70.
90.
METERS FROM DATUM STAKE
EIGENFUNCTION 1= 62.2% OF VARIANCE
B
.5
.0
-.5
EIGENFUNCTION 2= 18.9%
C
EIGENFUNCTION 3= 10.7%
D
EIGENFUNCTION 4= 4.0%
E

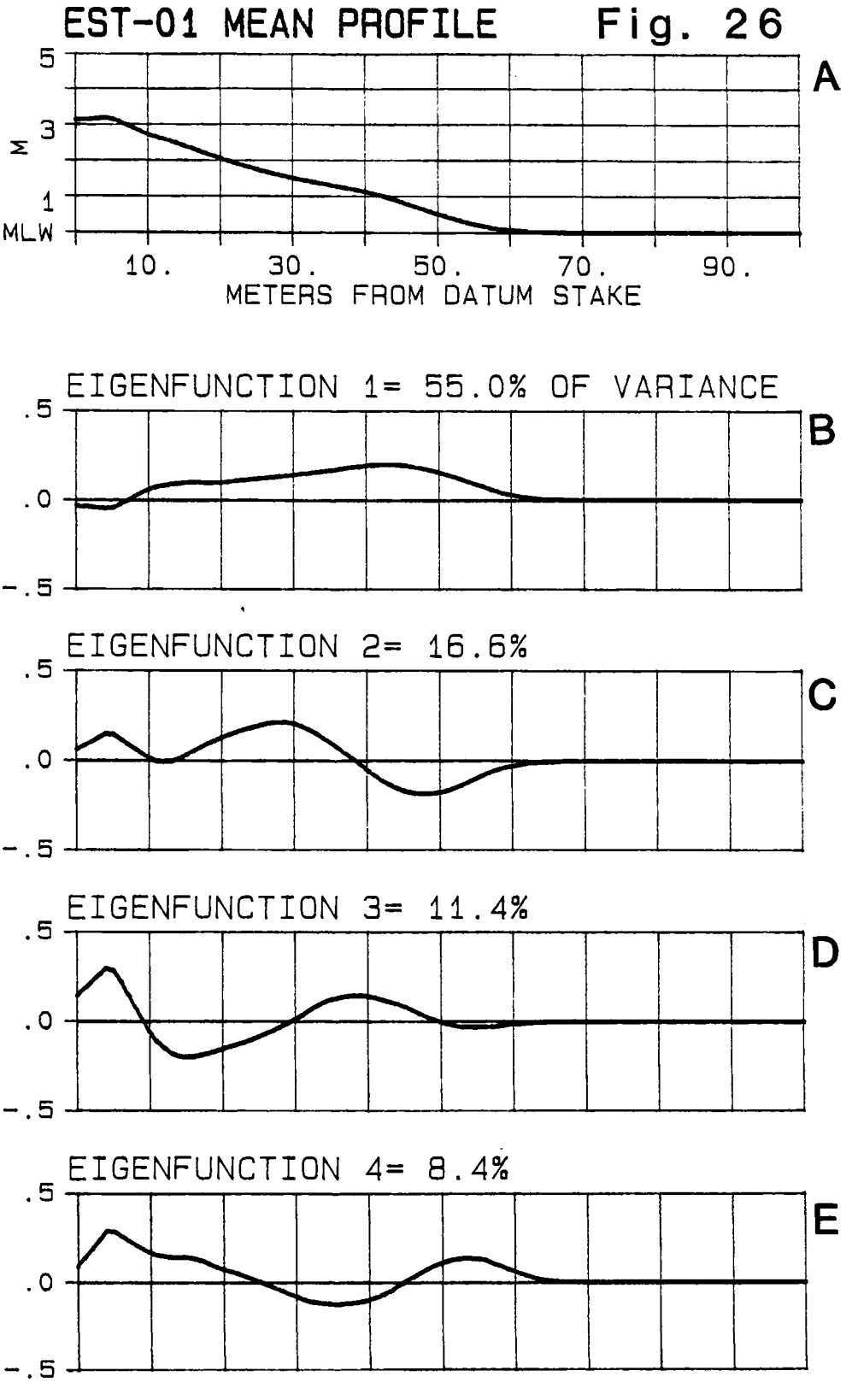
EST-01 MEAN PROFILE
Fig. 26
A
5
3
1
MLW
M
10.
30.
50.
70.
90.
METERS FROM DATUM STAKE
EIGENFUNCTION 1= 55.0% OF VARIANCE
B
.5
.0
-.5
EIGENFUNCTION 2= 16.6%
C
.5
.0
-.5
EIGENFUNCTION 3= 11.4%
D
.5
.0
-.5
EIGENFUNCTION 4= 8.4%
E
.5
.0
-.5

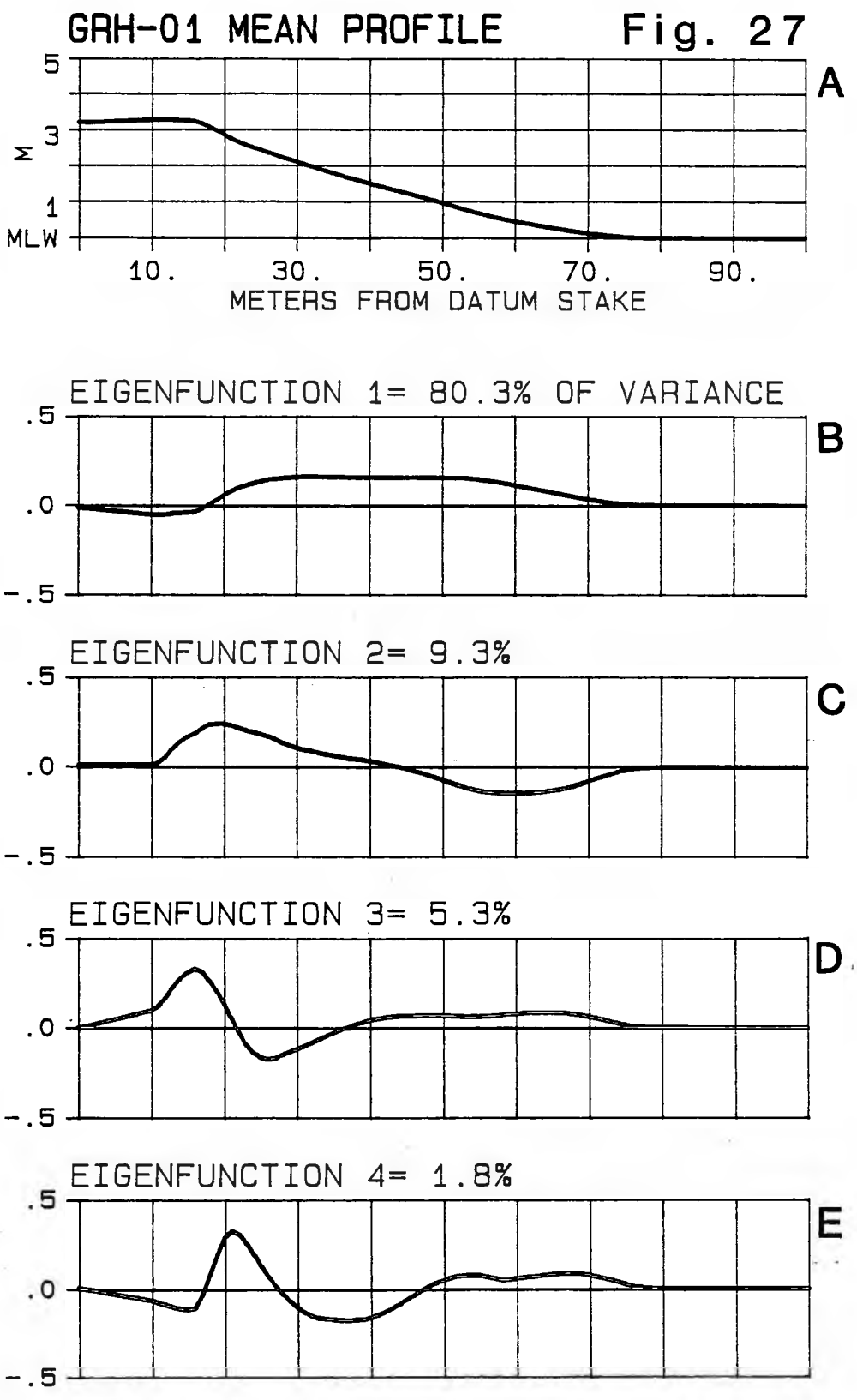
GRH-01 MEAN PROFILE
Fig. 27
A
5
3
1
M
MLW
10.
30.
50.
70.
90.
METERS FROM DATUM STAKE
EIGENFUNCTION 1= 80.3% OF VARIANCE
B
.5
.0
-.5
EIGENFUNCTION 2= 9.3%
C
.5
.0
-.5
EIGENFUNCTION 3= 5.3%
D
.5
.0
-.5
EIGENFUNCTION 4= 1.8%
E
.5
.0
-.5

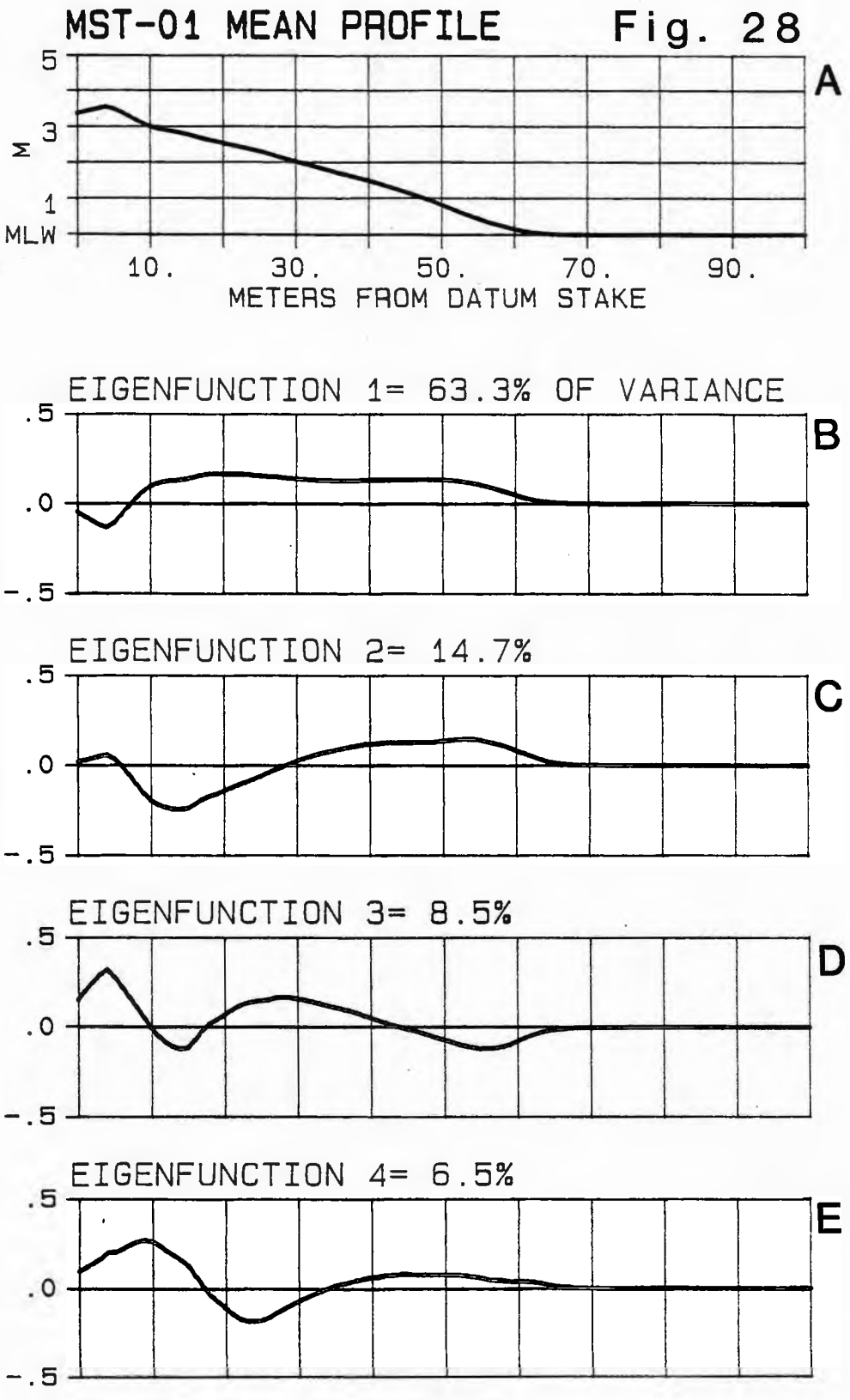
MST-01 MEAN PROFILE
Fig. 28
A
5
3
1
M
MLW
10.
30.
50.
70.
90.
METERS FROM DATUM STAKE
EIGENFUNCTION 1= 63.3% OF VARIANCE
B
.5
.0
-.5
EIGENFUNCTION 2= 14.7%
C
.5
.0
-.5
EIGENFUNCTION 3= 8.5%
D
.5
.0
-.5
EIGENFUNCTION 4= 6.5%
E
.5
.0
-.5

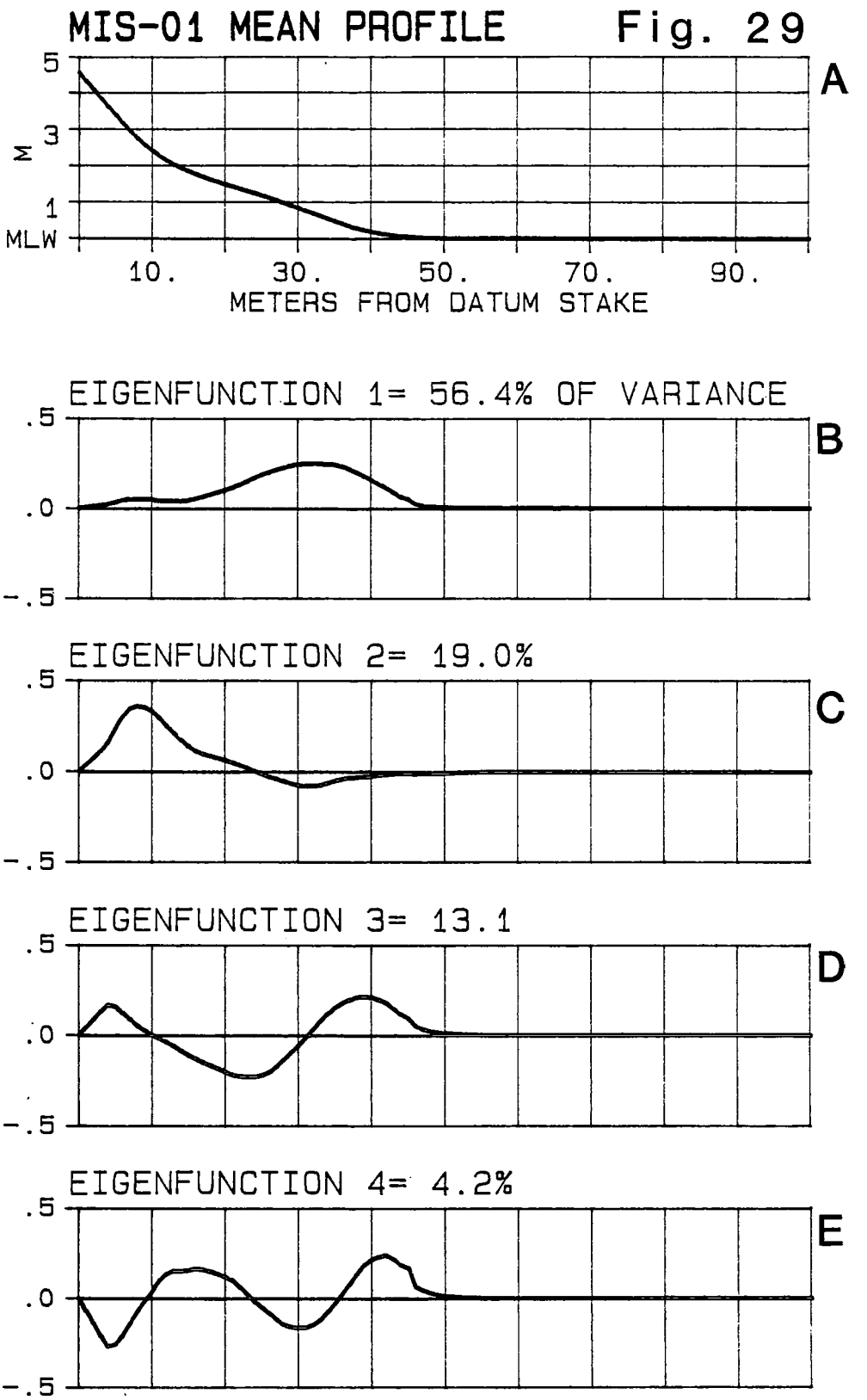
MIS-01 MEAN PROFILE
Fig. 29
A
5
3
1
M
MLW
10.
30.
50.
70.
90.
METERS FROM DATUM STAKE
EIGENFUNCTION 1= 56.4% OF VARIANCE
B
.5
.0
-.5
EIGENFUNCTION 2= 19.0%
C
.5
.0
-.5
EIGENFUNCTION 3= 13.1
D
.5
.0
-.5
EIGENFUNCTION 4= 4.2%
E
.5
.0
-.5

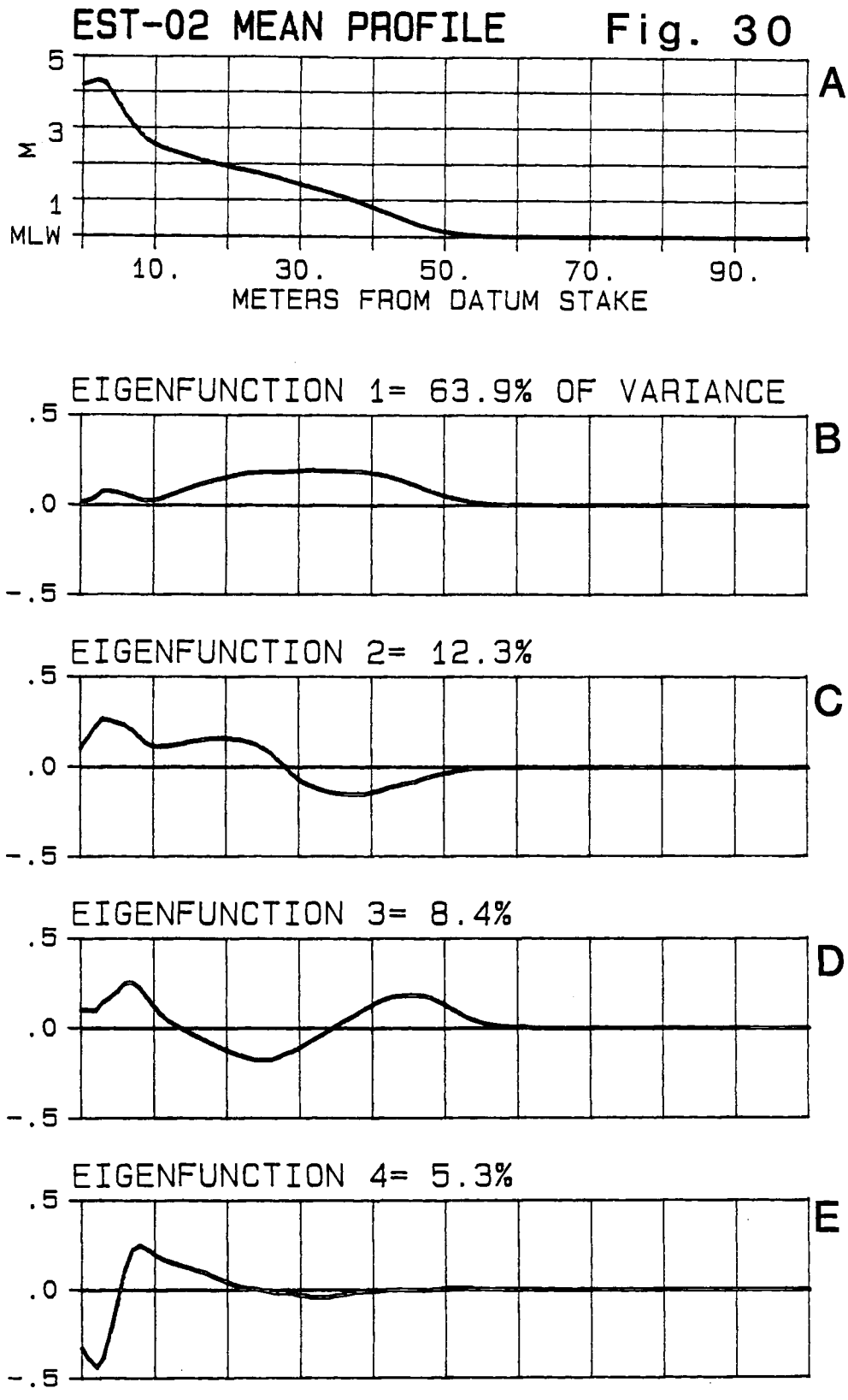
EST-02 MEAN PROFILE
Fig. 30
A
5
3
1
MLW
M
10.
30.
50.
70.
90.
METERS FROM DATUM STAKE
EIGENFUNCTION 1= 63.9% OF VARIANCE
B
.5
.0
-.5
EIGENFUNCTION 2= 12.3%
C
.5
.0
-.5
EIGENFUNCTION 3= 8.4%
D
.5
.0
-.5
EIGENFUNCTION 4= 5.3%
E
.5
.0
-.5

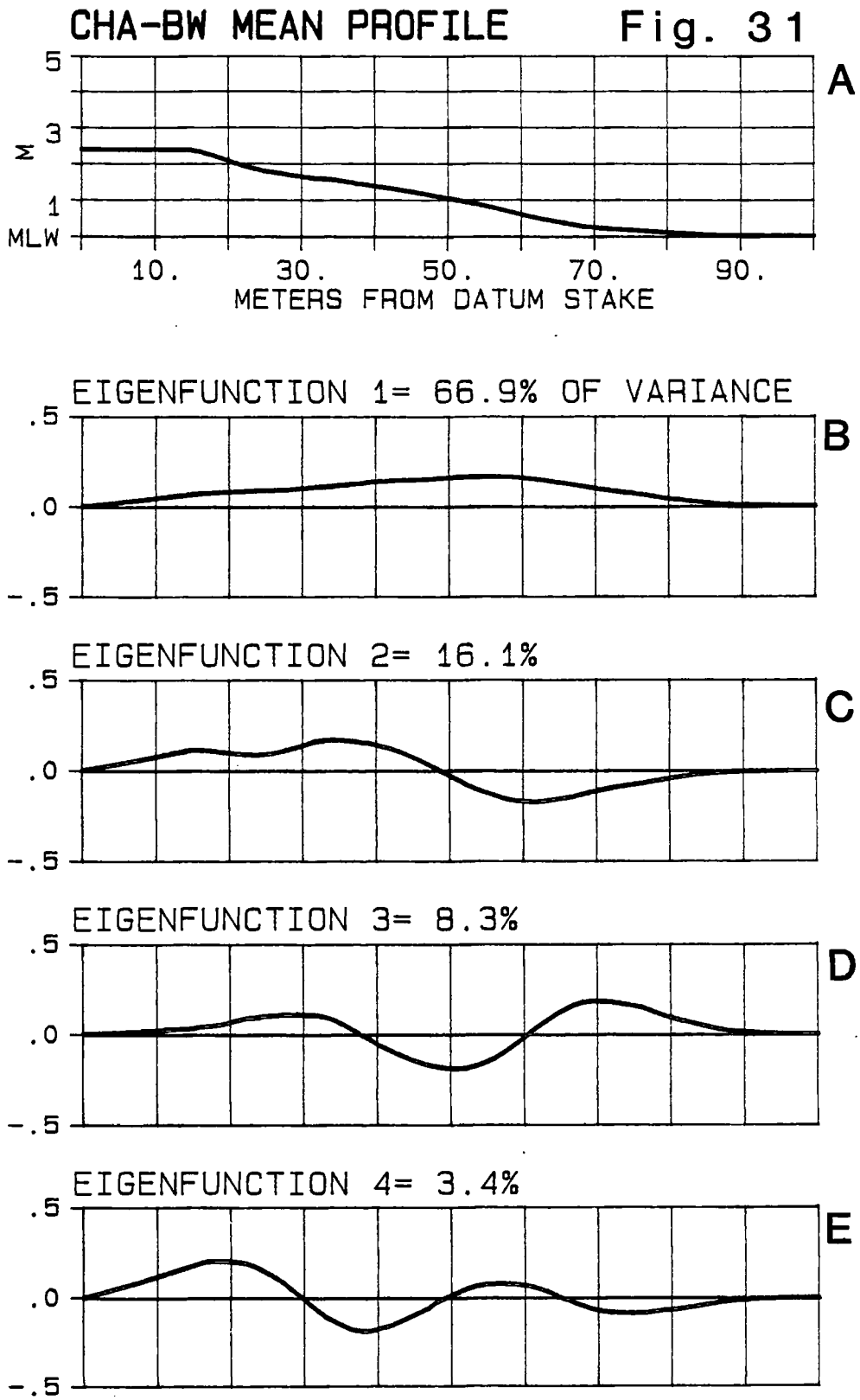
CHA-BW MEAN PROFILE
Fig. 31
A
5
3
1
M
MLW
10.
30.
50.
70.
90.
METERS FROM DATUM STAKE
EIGENFUNCTION 1= 66.9% OF VARIANCE
B
.5
.0
-.5
EIGENFUNCTION 2= 16.1%
C
.5
.0
-.5
EIGENFUNCTION 3= 8.3%
D
.5
.0
-.5
EIGENFUNCTION 4= 3.4%
E
.5
.0
-.5

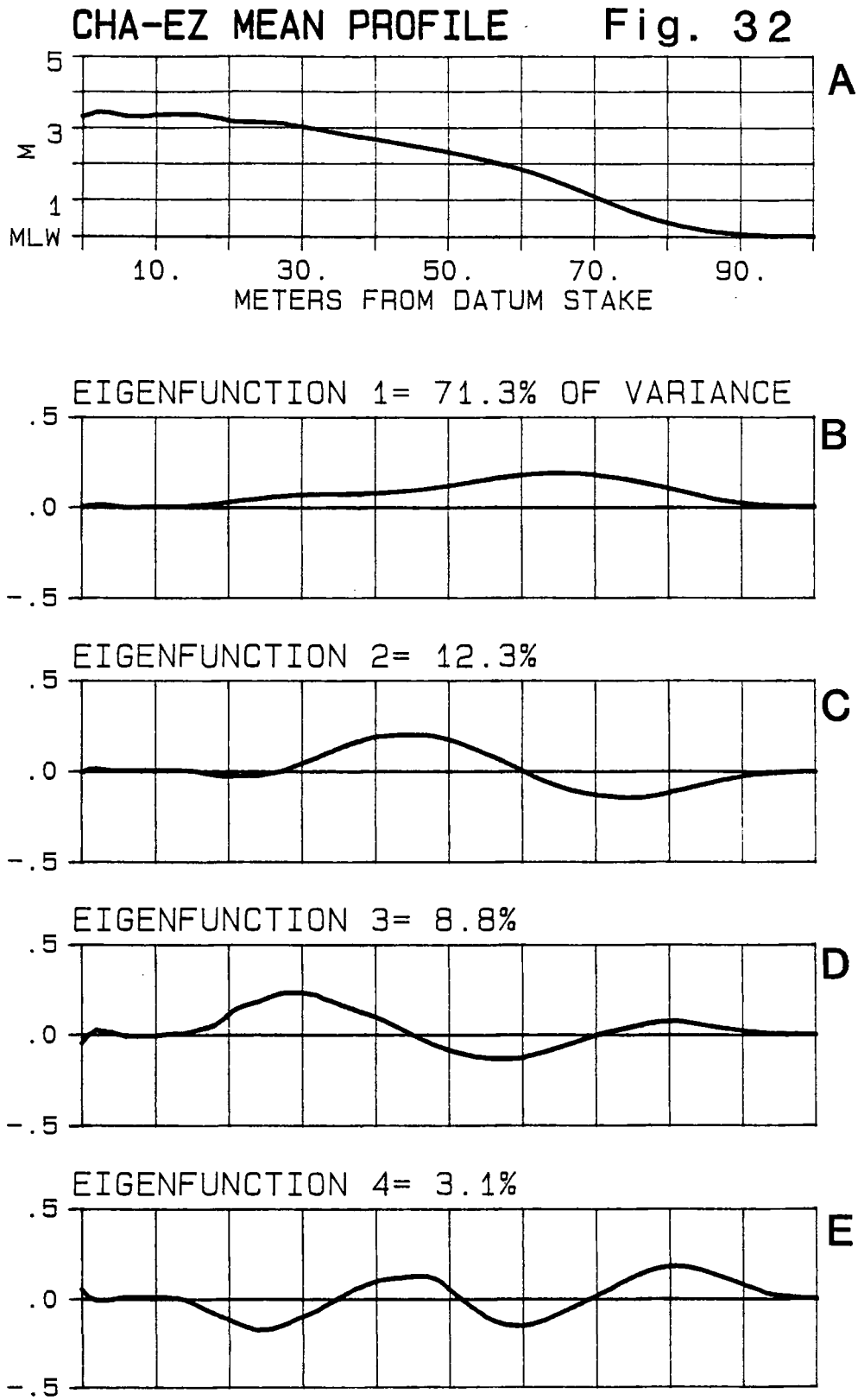
CHA-EZ MEAN PROFILE
Fig. 32
A
5
3
1
MLW
M
10.
30.
50.
70.
90.
METERS FROM DATUM STAKE
EIGENFUNCTION 1= 71.3% OF VARIANCE
B
.5
.0
-.5
EIGENFUNCTION 2= 12.3%
C
.5
.0
-.5
EIGENFUNCTION 3= 8.8%
D
.5
.0
-.5
EIGENFUNCTION 4= 3.1%
E
.5
.0
-.5

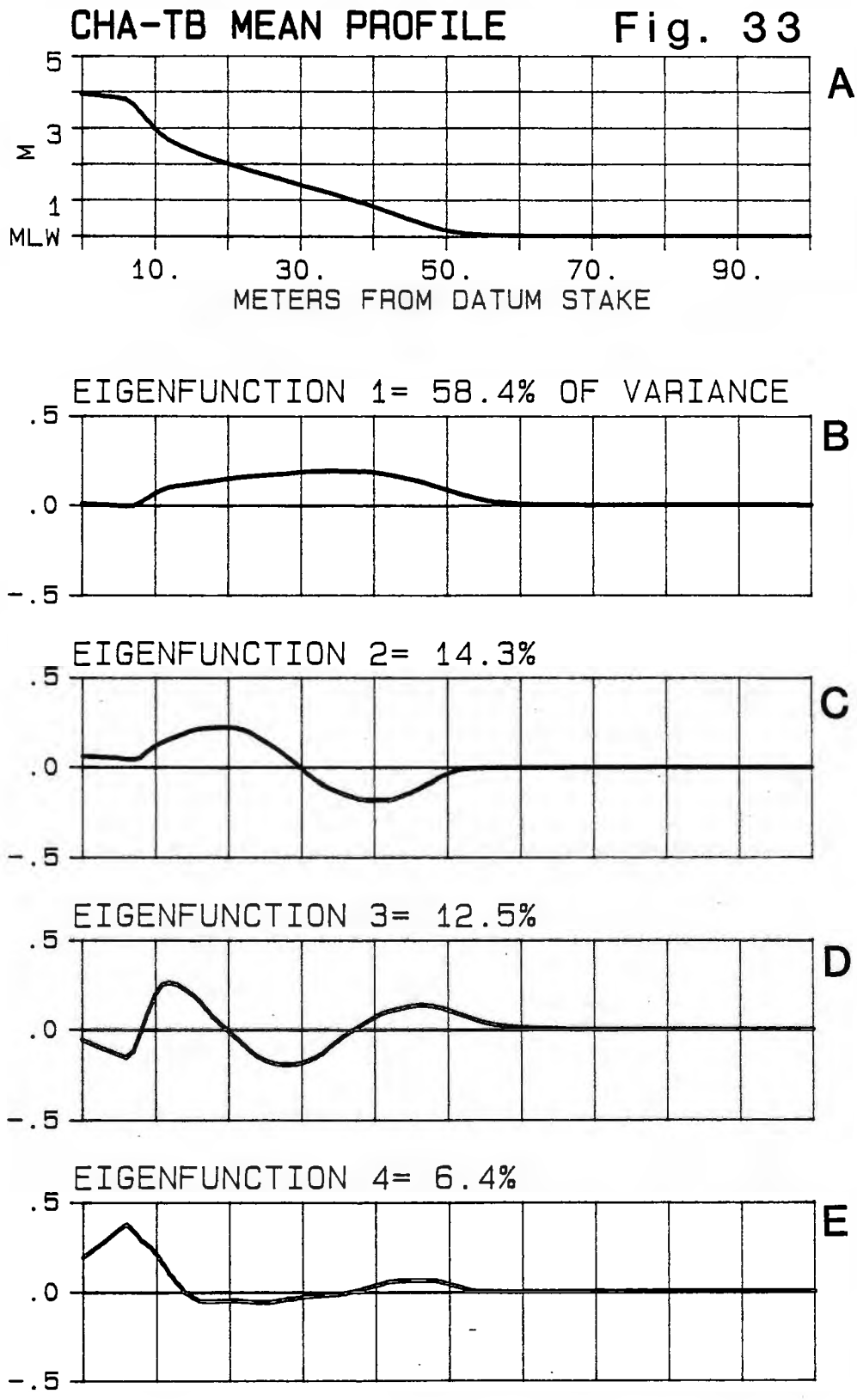
CHA-TB MEAN PROFILE
Fig. 33
A
5
3
1
M
MLW
10.
30.
50.
70.
90.
METERS FROM DATUM STAKE
EIGENFUNCTION 1= 58.4% OF VARIANCE
B
.5
.0
-.5
EIGENFUNCTION 2= 14.3%
C
.5
.0
-.5
EIGENFUNCTION 3= 12.5%
D
.5
.0
-.5
EIGENFUNCTION 4= 6.4%
E
.5
.0
-.5

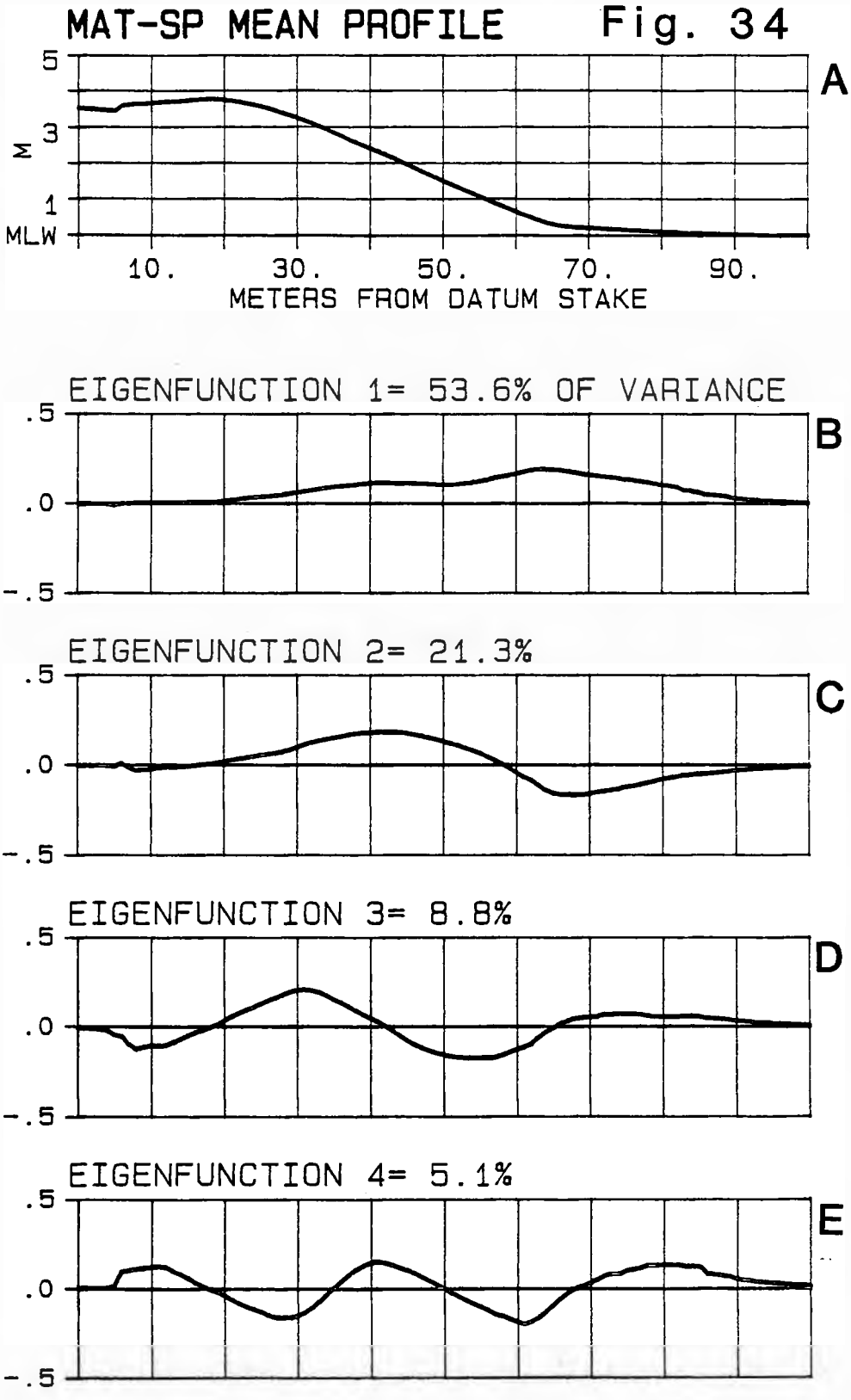
MAT-SP MEAN PROFILE
Fig. 34
A
5
3
1
M
MLW
10.
30.
50.
70.
90.
METERS FROM DATUM STAKE
EIGENFUNCTION 1= 53.6% OF VARIANCE
B
.5
.0
-.5
EIGENFUNCTION 2= 21.3%
C
.5
.0
-.5
EIGENFUNCTION 3= 8.8%
D
.5
.0
-.5
EIGENFUNCTION 4= 5.1%
E
.5
.0
-.5

represents the building and destruction of berms primarily caused by the onshore-offshore movement of sediment. The term shoreface in place of bar is preferred because it can be equally applied to non-barred as well as barred shorelines. The shoreface-berm-function does not well separate beach subenvironments in Rhode Island, differing from the measurements of Bowman (1981) for the equivalent function over a one year time period. This is probably caused by onshore-offshore sediment exchange occurring over a wider horizontal extent during the period of the Rhode Island study. Clarke and Eliot (1983) called the equivalent function the fundamental beach response.

Backberm-function.- The backberm-function is most pertinent to sediment exchange between the backberm and beachface and between the backberm and foredune areas. Ideally, this function has a prominent extremum centered in the backberm area, which usually includes the foredune ramp, and extrema of opposite sign in the dune and beachface areas. The nodal point seaward of the backberm zone separates the beachface and backberm zones and is taken as the modal berm crest position. The third eigenfunction of the EST-01 profile is a good example (Fig 26d).

This function is sensitive to profile shortening and steepening, for instance when sediment moves from the beachface to the backberm or in an opposite manner, or to berm-runnel development when major sediment accumulation is

centered seaward of the mean backberm position. This function may also be sensitive to sand movement from the bermtop to the dune/foredune ramp zones caused by wind, or to dune-scarp erosion feeding the foredune ramp and bermtop zones.

Beachface-function.- The beachface-function is similar to the backberm-function but the extrema are shifted seaward. The beachface-function involves swash-bar formation and migration up the low-tide terrace, and incipient berm evolution as described by Hine (1979), Davis et al. (1972), Dekay (1981), and Rosenberg (1985). This function, therefore, is sensitive to a more ephemeral mode of sediment exchange than the more permanent exchange shown by the backberm-function. The second eigenfunction for EST-01 (Fig. 26c) is a good example. The temporal dependence of this function is sensitive to individual storms, and to the neap-spring tidal cycle which largely determines the horizontal position of new or incipient berms (Rosenberg 1985).

Clarke and Eliot (1983a) called the equivalent function the swash-function; however, this name implies a process which in some cases may not be the most important factor causing beachface change, such as during storms when the entire beachface is in the breaking zone, or by changes induced by the neap-spring tidal cycle. Besides, the

spatial eigenfunctions only describe morphological shapes and not processes.

Foredune-function.- The foredune-function is most important during times of foredune and foredune ramp activity. Thus, this function describes on the one hand, episodic dune erosion by storm waves, but on the other, gradual foredune vertical and seaward accretion caused by wind deposition. Eigenfunction 4 of the CHA-TB profile (Fig. 33e) is a good example of a well- defined foredune-function.

In the present study, the foredune function may be difficult to identify and interpret because of low measurement resolution in the dune area and differing placements of the first elevation station as discussed above. When major foredune activity has occurred, however, the dune function shows significant trends.

Hybrid functions.- In some cases a set of eigenfunctions for a profile may not well separate the above defined beach-functions. One eigenfunction may be the most important in describing two or three of the modes of variance. The second eigenfunction of the GRH-01 location (Fig. 27c) is the most important in describing changes in the backberm and beachface areas. This is caused by extensive beachface erosion that results in the shifting of beach zones through time. On the other hand, two different functions may be

equally important in describing the variance in a single zone. An example of this is the second and third eigenfunctions of WKG-01 (Fig. 25C,D). The second function is important both in the dune and backberm area when the two areas are varying in the same direction. The third eigenfunction is also important in the dune and backberm areas, as well as, the beachface area. The third eigenfunction, however, explains backberm variance as an exchange of sand among the dune, backberm, and beachface zones.

Eigenfunction Analyses of Beach Profiles

The following sections give detailed results and discussion of the eigenfunction analyses for each location. The four longest-running profiles are discussed first, in west-to-east order; then the shorter time-span profiles are discussed in west-to-east order.

Weekapaug (WKG-01).- The shoreface-berm-function (first eigenfunction) has an asymmetric maximum covering 43 m of beach with most activity 12 m from the seaward extent of variability (Fig. 25b). This beach-function explains 62.2% of the variance.

The second eigenfunction contains 18.9% of the variance and is interpreted as a hybrid beach-function, including the backberm and foredune functions. This beach-

function shows a relatively broad 35 m maximum including the foredune, foredune-ramp, and backberm areas, with the peak centered at the mean foredune crest position (Fig. 25c). The temporal dependence of this function has a strong upward linear trend, which indicates net backberm and foredune vertical accretion since 1963 (Fig. 4c). Backberm and foredune erosion during the winters of 1977-78 and 1982-83 show in the temporal function as negative shifts, as does backberm erosion caused by Hurricane Gloria on September 27, 1985. The spectrum (Fig. 14c) displays a strong 10-year cycle which is in phase with the temporal shoreface-berm function. This phase relationship shows the importance of foredune and backberm activity on overall sediment volume at this location. The spectrum is divided into 2-4-year periods, and inspection of the time series reveals a prominent 2.5-3-year cycle.

It should be noted that the abrupt discontinuities in the first 13 years of the time series may be caused by differing placements of the first elevation station and may not be real; however, the linear trend, 10-year, and 2-4-year cycles are certainly significant.

The third eigenfunction (10.7% variance) includes three beach-functions: the foredune-function; the backberm-function; and the beachface-function (Fig. 25d). Whereas the second eigenfunction did not discriminate between the backberm and foredune areas, the third function does, and in addition, the third function is sensitive to the beachface-

bermtop exchange of sediment. This beach-function illustrates coupling between the foredune crest/foredune ramp area and the backberm area through a node 16m from the datum stake. The modal berm-crest position is the node 30 m from the seaward extent of variability. The associated temporal function (Fig. 4d) shows a downward trend from 1963 to 1977, caused by simultaneous profile shortening and steepening, with vertical accretion in the backberm area supplied by sand from both the beachface and foredune/foredune ramp areas. The discontinuities at the beginning of 1977 and 1978 are once again caused by elevation-station placement, but the trends between the discontinuities are accurate. The upward trend from 1977 to 1986 is caused primarily by berm widening and vertical accretion. The spectral plot (Fig. 14d) has a primary peak at about a 12-year period and a secondary peak at a 3-year period. Comparison of the second and third temporal functions reveals the 3-year cycles to be about 180 degrees out of phase. This is expected since the second function does not discriminate between the foredune and backberm areas, and therefore, backberm and foredune ramp accretion causes a positive trend in the second temporal function. The third function, however, shows that the sand for backberm and foredune ramp accretion comes from the foredune and beachface area. Thus during times of backberm and foredune ramp accretion, the third temporal trend has a negative slope.

The fourth spatial eigenfunction (4% of the variance) has 4 extrema (Fig. 25e). The spectrum of the associated fourth temporal function (Fig. 14e) has a major 10-year spike which is in phase with the shoreface-berm temporal function. The interpretation of this function is unclear but it may represent sediment exchange similar to the beachface-function during times of a wide berm profile.

Combining information from the second and third beach-functions, the following is evident: from 1963 to 1977 WKG-01 shortened overall and accreted in the foredune and backberm areas; from the winter of 1977 through the winter of 1978, the beach was greatly reduced in elevation across the entire width and the foredune crest cut back 7 m; from 1978 to 1986 the backberm and foredune accreted and the beach widened except for a brief period of erosion during the winter of 1982-83. Over the entire 23-year period, the foredune crest has had a net seaward growth of 1.2 m and vertical growth of about 1 m. On a shorter time scale, the beach tends to widen, and then shorten and steepen, on a 2- to 4-year cycle.

East Beach 1 (EST-01).- The shoreface-berm-function (first eigenfunction) explains 55% of the variance and covers 53 m of the beach. It is asymmetric with a maximum 19 meters from the seaward extent of variability (Fig. 26b). There is a step in the function between 12 and 20 meters from the

datum stake which is caused by a stable berm-runnel area often present at this site.

The second eigenfunction explains 16.6% of the variance and is the beachface-function (Fig. 26c). Profile shortening and backberm accretion cause positive shifts in the temporal function, and backberm erosion and/or profile lengthening cause negative shifts. The spectral plot of the beachface-function (Fig. 15c) has a major peak at about an 11-year periodicity and a suppressed seasonal peak relative to the shoreface-berm-function. The suppressed seasonal peak is caused by storm-recovery swash bars forming throughout the year. Also present are 6-and 2.5-3-year cycles.

Inspection of the shoreface-berm and beachface temporal plots (Figs. 5b,c) show them to be almost directly out of phase on the 10-11-year cycle . The out of phase relationship is caused by simultaneous berm width and elevation fluctuations. When the berm narrows, sand moves from the beachface to the bermtop causing a positive shift in the beachface temporal function, but at the same time the profile is also shortened, causing a negative shift in the shoreface-berm-function. In the winters of 1977 and 1978, however, the beach eroded across the entire length causing negative shifts in both functions.

The third function is the backberm-function and describes 11.4% of the variance (Fig. 26d). The modal berm crest position is 22 m from the seaward extent of

variability. The associated temporal plot (Fig. 5d) has an upward trend throughout the time period, caused by lowering of the backberm zone and a seaward shift of sedimentation giving a berm runnel configuration; the spectral plot (Fig. 15d) shows spectral splitting, possibly showing a significant cycle of about 6 years and another about 3 years. The very strong seasonal spike is most interesting, and demonstrates that the scale of seasonal fluctuations reaches to the backberm area. The third temporal plot generally has lows in the winter and highs in the summer. Thus the profile tends to shorten and the backberm increases in elevation during the winter months and every 2.5 and 6 years.

The fourth eigenfunction is the foredune-function (Fig. 26e) and explains 8.4% of the variance. In addition to being sensitive to foredune activity, the foredune-function is also sensitive to profile lengthening. The temporal function (Fig. 5e) shows that foredune erosion did not occur during the winter of 1976-77 such as at MST-01 and WKG-01, but about 5 m did erode during the winter of 1977-78. From 1978 to 1986, a steep, upward, linear trend is present and indicates unprecedented profile lengthening of about 10 m, and foredune ramp vertical accretion of about 0.4 m. The time series spectrum (Fig. 15e) has a strong 10-year cycle, a secondary peak at a 3-year period, and a third, less important seasonal spike.

In summary, EST-01 tends to widen and then shorten and steepen seasonally and at cycles of 2.5 and 6 years. The foredune crest and ramp areas remained fairly stable from 1963 to the winter of 1977-78, when much foredune and backberm erosion occurred. Since 1978, however, the foredune and backberm areas have undergone an accelerated rate of growth and the profile has lengthened. Nevertheless, the foredune crest eroded a net 6.3 m since 1963. Overall, the backberm area has lowered and the bulk of sediment has shifted seaward to form a berm runnel.

Green Hill (GRH-01).- The shoreface-berm-function explains a high 80.3% of the variance, is broad and flat, and covers 54 m of beach (Fig. 27b).

The second eigenfunction combines the beachface and backberm functions and has a berm crest 30 m from the seaward extent of variability (Fig. 27c). This hybrid beach-function explains 9.3% of the variance. Its temporal dependence has only one significant peak at 11 years (Fig. 6c). This 11-year cycle is out of phase with the 10-year cycle of the shoreface-berm-function for the same reason (berm width and elevation fluctuations) as is the EST-01 beachface-function (second eigenfunction). Positive trends are caused by backberm filling and/or profile shortening.

The third eigenfunction explains 5.3% of the variance and is most sensitive to, but not restricted to, foredune activity (Fig. 27d). Since this function also

describes activity across the backberm and beachface, shortening and steepening can cause negative trends in the associated temporal function. The third temporal function (Fig. 6d) has a sharp positive discontinuity at the beginning of 1977 caused by a change in the placement of the first elevation station. A negative discontinuity occurs in the fall of 1972, caused by foredune ramp erosion, and a sharp drop occurs on April 2, 1984 which is caused by 5 m of foredune erosion during a storm on March 29. When the erroneous discontinuity at the beginning of 1977 is subtracted out, the time series shows a strong erosional linear trend; however, backberm and profile-length changes affect the trend as well. The spectral plot (Fig. 16d) shows a 10-year peak, but the artificial positive discontinuity makes interpretation of the spectrum dubious.

The fourth eigenfunction explains only 1.8% of the variance and is not geologically interpretable.

In summary, from 1963 to late 1972, the volume and shoreface-berm time series plots remained stable while the hybrid beachface-backberm-function (second eigenfunction) shows profile lowering and widening from 1963 to 1967 and then steepening and shortening from 1967 to late 1972. Relatively moderate storms occurred in October and November of 1972; the effect of these storms on the steep beach was a large (30 m^3) and permanent loss of sediment. The beach has been consistently eroding since 1972 largely due to a lack of sediment. Backberm filling and profile steepening

stopped in 1972 and since then the beachface-backberm function displays a continuous trend of profile lowering. The severe foredune erosion on March 29, 1984 was preceded by a year of accelerated profile lowering as shown by the backberm-beachface-function. The foredune has consistently eroded since 1963 and the foredune crest has cut back a total of 10.5 m.

Moonstone Beach (MST-01).- The shoreface-berm-function is the first eigenfunction and explains 63.3% of the variance with a maximum extending over 54 m of the beach (Fig. 28b). The positive area of the function is broad and flat but has a slight low 33 m from the seaward extent.

The second eigenfunction is the backberm-function; it has a node 34 m from the seaward extent of the profile, which is the modal berm crest position (Fig. 28c). Negative trends in the temporal function indicate vertical accretion in the backberm area and profile shortening; positive trends indicate a rearrangement of sediment from the backberm to the beachface area (Fig. 7c). The time-series spectrum for this function also has a strong 10-year spike and a suppressed seasonal spike similar to the shoreface-berm-function, but in addition, it has a small peak at 2.5 years (Fig. 17c). The 10-year backberm cycle is out of phase with the 10-year cycle of the shoreface-berm-function, as expected. However, both functions generally show lows in the winter months and highs during the summer months, which

indicates most seasonal activity to be restricted to the seaward 35 m of the profile (positive area of the backberm-function).

From 1963 to 1978 the beach generally shortened and accreted in the backberm area. The sharp rise in the temporal function on February 17, 1978 is caused by the effect of the blizzard of February 6, 1978, when dune and backberm erosion occurred and subsequent deposition was shifted seaward of its pre-storm position. From 1981 to 1986 MST-01 has shortened and accreted in the backberm area.

The third eigenfunction is considered the beachface-function which explains 8.5% of the variance (Fig. 28d). The spectral plot has a major 9-year peak (Fig. 17d) which is approximately in phase with the shoreface-berm-function (Fig. 17D).

The fourth eigenfunction is most relevant to foredune activity, but because it is not restricted to the foredune it is difficult to interpret. It explains 6.5% of the variance (Fig. 28e). Generally, positive temporal trends represent vertical accretion, such as from 1967 to 1970, when 0.5 m was added vertically to the foredune area (Fig. 7e). On the other hand, seaward dune growth may cause negative trends, such as from 1970 to 1977, when the dune grew 10 m seaward. During the winter of 1976-77, the foredune crest was cut back 5 m, decreasing from 24 m to 19 m from the datum stake, causing a sharp positive jump. In early 1978, the crest was cut back another 12 m (from 16 to

4 m from the datum stake), which caused a negative shift. From 1978 to 1986, the foredune and foredune ramp widened about 5 m and accreted vertically about 1 m. Therefore, even though this function is the most sensitive to foredune activity, negative and positive trends in the temporal function are ambiguous and depend on the current position of the foredune.

In summary, MST-01 has shortened and steepened on 10-and 2.5-year cycles. The foredune, since 1963, has had a net vertical growth of 1 m and a 5 m seaward growth. The foredune was severely cut back during the winters of 1976-77 and 1977-78; thus all the resultant net growth is due to deposition since 1978.

Misquamicut (MIS-01).- The shoreface-berm function for MIS-01 contains 56.4% of the variance and shows a narrow 30 m area of activity (Fig. 29b). A step is present from 5 to 15 m from the datum stake, caused by workers placing the elevation stations differently, rather than it being due to dune activity. The volume plot and temporal shoreface-berm functions have a slight upward trend that yields a deposition rate of 0.8 $m^3 \cdot yr^{-1}$ by least squares linear regression (Table 2). Morton et al. (1982), also using linear regression, found for a single profile during the period from 1962 to 1973, a deposition rate of 0.4 $m^3 \cdot yr^{-1}$.

The second eigenfunction describes 19% of the variance and includes the foredune and backberm functions

(Fig. 29c). The modal berm crest is 16 m from the seaward extent of variability. The related temporal spectrum has one 3.3-year peak (Fig. 18c). The temporal function displays foredune and backberm accretion at the expense of the foreshore (positive trend), for the time period 1979 to 1984 (Fig. 18C). From 1984 to 1986, backberm lowering and berm widening prevailed (negative trend). The blizzard of February 6, 1978 did not cause severe backberm or foredune erosion; however, the backberm and foredune ramp were lowered about 0.5 m during the winter of 1979-80 . The effect of Hurricane Gloria on September 27, 1985 shows as a sharp negative trough in the temporal function caused by foredune-ramp and backberm lowering.

The third eigenfunction (13.1% of the variance) is the beachface-function (Fig. 29d). Berm formation and widening cause positive trends in the temporal function; berm narrowing and backberm deposition cause negative trends (Fig. 8d). The spectrum shows a prominent cycle of about 3 years and a seasonal cycle (Fig. 18d). Inspection of the temporal plot shows berm destruction to be rapid (sharp drops) and berm formation to be more gradual. The spectrum is broken up at higher frequencies, caused by low-tide terrace activity occurring throughout the seasons.

The fourth eigenfunction is not interpretable.

East Beach 2 (EST-02).- The shoreface-berm-function maximum (first eigenfunction) covers 43 m of beach and displays

63.9% of the variance (Fig. 30b). It has a very subtle step 22 to 28 m from the datum stake that represents a stable backberm zone.

The second eigenfunction (12.3% of the variance) is the backberm-function with the modal berm crest 23 m from the seaward extent of variability (Fig. 30c). The temporal function has a 5-6-year cycle (Fig. 9c) that is in phase with the shoreface-berm-function. Positive trends in the 5-year cycle are caused by sediment shifting from the beachface to the backberm and foredune ramp area (Fig. 9c). Thus, on a 5-year scale, profile-volume increases involve the shifting of sediment to the backberm area as it is supplied to the beachface. That is, there is a depositional backberm with a stable beachface, unlike the berm width fluctuations at EST-01. The second temporal (backberm) function also has a strong seasonal cycle (Fig. 9c) which is directly out of phase with the seasonal cycle of the shoreface-berm-function. Thus the seasonal fluctuations are largely restricted to the area seaward of the node in the backberm-function. A storm on March 29, 1984 lowered the foredune ramp and backberm about 2 m and shortened and lowered the beachface, causing a sharp drop in the temporal function.

The third eigenfunction displays 8.4% of the variance and is a hybrid beachface/backberm beach-function which is sensitive to profile steepening and narrowing on a shorter time scale (Fig. 30d). The related spectrum has a

prominent peak at 2 years (Fig. 19d). The effect of the March 29, 1984 storm is also evident in this function (Fig. 9D).

The fourth eigenfunction is the hybrid foredune-backberm function and explains 5.3% of the variance (Fig. 30e). It is sensitive to the foredune and foredune ramp exchange of sediment. From 1979 to the fall of 1984, the temporal function has a positive trend caused by foredune ramp accretion of about 5 m, while the foredune crest eroded back about 2 m (Fig. 9e). The blizzard of February 6, 1978 caused 2 m of horizontal foredune erosion and about .5 m of foredune ramp lowering. However, the drop in the temporal function is partly due to a change in the first elevation station placement. The March 29, 1984 storm shows up, but after that foredune ramp deposition had recommenced at a faster rate.

Charlestown Breachway (CHA-BW).- The shoreface-berm-function (first eigenfunction) includes 66.9% of the variance and has a broad and flat area of variability (80 m)(Fig. 31b). This attests to the dynamic behavior of this beach. A step occurs from 15 to 30 m from the datum stake and represents a more stable berm-runnel area.

The second eigenfunction (16.1% of the variance) is the backberm-function and displays the modal berm crest 35 m from the seaward extent of variability (Fig. 31c). The spectrum has one major peak at a 3.3-year cycle (Fig. 20c).

Profile lengthening from 35 to 55 m, and vertical accretion of about 1 m in the backberm area caused the positive trend from 1977 through 1981 (Fig. 10c). The negative shift from the beginning of 1982 to late 1983 is caused by dramatic lengthening from 55 to 90 m; the positive trend from late 1984 to 1986 is caused by shortening and vertical accretion in the foredune, foredune ramp, and backberm areas.

The third eigenfunction is the beachface-function and explains 8.3% of the variance (Fig. 31d). The temporal spectrum displays a 2.5-3-year peak (Fig. 10d). The 2.5-3-year cycles involve steepening and shortening, and then lengthening of the beachface.

The fourth eigenfunction (3.4% of the variance) is most sensitive to, but not restricted to, foredune and foredune- ramp activity (Fig. 31e). Its spectrum also displays a major 2.5-3-year peak involving the same type of activity as the beachface-function (Fig. 20e). From 1983 to 1986, foredune and foredune-ramp accretion caused a dramatic upward trend in the temporal function (Fig. 10e).

Charlestown Beach (CHA-EZ).- The CHA-EZ shoreface-berm-function (first eigenfunction, 71.3% of the variance) covers a wide (75 m) area of activity (Fig. 32b). There is a step, 28 to 42 m from the datum stake, that represents a stable backberm area.

The second eigenfunction is the beachface-function and includes 12.3% of the variance (Fig. 32c). The time-

series spectrum for this function has one strong 5-year cycle, but the spectrum is broken up at higher frequencies (shorter periods) (Fig. 21c). The cycle is out of phase with the shoreface-berm cycle; this shows that berm-width fluctuations across the seaward 30 m of the beach (minimum area of the beachface-function) is the major means of sediment volume changes. From 1977 to 1982, the beach generally kept the same berm width but increased in elevation about 1 m in the backberm area. From 1982 to the fall of 1984, the berm widened and grew out into the minimum area of the beachface-function (about 15 m), causing a negative shift in the temporal function (Fig. 11c). The berm eroded landward 15 m and downward about 1 m in the winter of 1984-85, causing a positive shift. Since 1985 the berm has remained fairly stable.

The third eigenfunction (8.8% of the variance) is the backberm-function (Fig. 32d). The modal berm-crest position is taken as the node 57 m from the seaward extent of variability. The related time series spectrum has a strong seasonal spike which suggests that seasonal cycling extends to the backberm area (Fig. 21d). Highs occur in the winter and lows in the summer; therefore, the beach tends to shorten in the winter and lengthen in the summer between 45 and 70 m from the datum stake (negative portion of the function). There are strong 2-and 5-year peaks in the spectrum as well. This function is more sensitive to backberm and foredune-ramp elevation changes than is the

beachface-function. From 1977 to the summer of 1978, the beach was lowered as indicated by the negative trend in the temporal function (Fig. 11d). From 1978 to 1982, the backberm generally increased in elevation; from 1982 to 1986, it has remained stable.

The fourth eigenfunction is not well defined in any particular area and is thus difficult to interpret.

Charlestown Beach (CHA-TB).- The shoreface-berm-function (first eigenfunction) covers 47 m of beach and includes 58.4% of the variance. It is narrow, steep, and asymmetric (Fig. 33b).

The second eigenfunction (14.3% of the variance) is the backberm-function with a modal berm crest 20 m from the seaward extent of variability (Fig. 33c). The spectrum has strong 5-year, and seasonal cycles (Fig. 22c). The 5-year cycle is in phase with the 5-year cycle of the shoreface-berm-function, which shows the importance of backberm elevation changes on overall sediment volume. The seasonal cycles, however, are directly out of phase. This is caused by the movement of sediment from the beachface to the shoreface and to the backberm zones during the winter months.

The third eigenfunction (12.5% of the variance) is the beachface-function, but also includes activity on the foredune ramp (Fig. 33d). A seasonal cycle is not present (Fig. 22d) due to low-tide terrace activity occurring

throughout the year as discussed above for other profiles. However, 2.5-and 5-year cycles occur.

The fourth eigenfunction (6.4% of the variance) is a well-defined foredune-function (Fig. 33e). The foredune eroded 3 m, and the foredune ramp lowered about 0.5 m, causing a trough in the temporal function during the winter of 1977-78 (Fig. 12e). The positive trend since 1978 is caused mostly by foredune ramp deposition; the foredune crest has not migrated horizontally. In the fall of 1978, workers began taking a side shot to yield the natural elevation of the dune crest as discussed in the methods section, hence the sharp rise in the temporal function. The sharp drop in the fall of 1985 is caused by a misplaced elevation station. The spectrum for the temporal function (Fig. 22e) is highly broken up showing the more aperiodic nature of foredune and foredune ramp activity.

East Matunuck State Beach (MAT-SP).- The first eigenfunction (53.6% of the variance) is the shoreface-berm-function (Fig. 34b). It has a wide area of activity covering 72 m, and displays a distinct step from 40 to 53 m from the datum stake.

The second eigenfunction is the beachface-function and explains a high (21.3%) percentage of the variance (Fig. 34c). This beach-function has a complicated temporal spectrum, probably caused by human alteration of the beach by bulldozers in the summer months (Fig. 13c). Generally,

the sand moves from the beachface to the shoreface and to the backberm during the winter by natural processes; and from the beachface to the backberm during the summer by human intervention with bulldozers.

The third eigenfunction is a hybrid-function including the foredune and backberm functions (Fig. 34d). The modal berm crest is 50 m from the seaward extent of variability. The temporal dependence was fairly stable until the fall of 1985, when Hurricane Gloria (September 27) caused a major shift of sediment from the backberm to the beachface area, as shown by the drop in the time-series plot (Fig. 13d). The spectral plot (Fig. 23d) is difficult to interpret, for the same reason discussed for the beachface-function-- human alteration.

The fourth eigenfunction is not geologically interpretable.

DISCUSSION

Characteristics of Beach-functions and Comparisons with other Studies

Eigenfunction analysis of profiles has shown remarkably similar results for profiles with similar morphology. CHA-BW and CHA-EZ are similar beaches and have similar first eigenfunctions (shoreface-berm-functions)(Figs. 31b, 32b), even though they have been surveyed by different methods and at different rates and times as discussed above. At the CHA-EZ location, the

second eigenfunction is the beachface-function, whereas the beachface-function for CHA-BW is the third eigenfunction. This switching of beach-functions is probably caused by the special effort to measure storm recovery profiles at CHA-EZ and thus to record more activity on the low-tide terrace.

Winant et al. (1976) found similar results with eigenfunction analysis when varying time-series lengths of one to four years were analyzed for a profile which extended offshore at Torrey Pines Beach, California. The 23-year data set of EST-01 and the 9.5-year data set of EST-02 also reveal similar first spatial eigenfunctions for these two locations (Figs. 26b,30b). The first function of EST-01, however, has a broader area of variation, indicating that over the longer time-span the berm has formed over a wider horizontal range. It should also be noted that the backberm-function is the third function for EST-01 but the second function for EST-02. This switch is caused by the higher relative influence that the backberm erosion during the winters of 1976-77 and 1977-78 has on the shorter time length EST-02 data set, and also by the erosional trend at EST-02 since 1982. In a similar manner, Rosenberg (1985) analyzed overlapping data from the CHA-EZ location and found that the foredune and beachface-functions reversed in importance. From October, 1977 to March, 1978, there was much foredune erosion and the second eigenfunction was the foredune function. When an additional 6 months, a period of berm building, was added to the analysis, the foredune-

function became the third eigenfunction. Such beach-function switching is inherent between subsets of the time series in the present study.

The first four eigenfunctions include the dominant modes of beach change. Together they describe from 83-95% of the variances from the mean profiles. The first beach-function accounts for 53.6-80.3% of the variance and in all cases is the shoreface-berm-function. This function has one broad extrema covering most of the beach length, excepting the dune area. The seaward tapering is partly an artifact of the analysis technique because the profile data are truncated at MLW which occurs at different points along the profile.

The shoreface-berm-function is always highly positively correlated with the volume time series. This correlation demonstrates that volume fluctuations occur mostly as unidirectional elevation changes across the entire beach. The spectra of the shoreface-berm-functions and volume plots are also very similar with one interesting exception. In all the shoreface-berm-function spectra, except for GRH-01 and MST-01, the seasonal peaks are more important than they are in the respective volume spectra; in the MIS-01 spectrum the 4-year and seasonal cycles reverse in importance. This clearly demonstrates the utility of the eigenfunction technique in separating modes of variance caused by forcing functions with different characteristics and cyclicities. The MST-01 spectral plots show little

variation among functions, whereas the 10-year cycle of the GRH-01 profile becomes more important in the shoreface-berm-function at the expense of the 4-year and seasonal cycles. At GRH-01, this is caused by much berm erosion on a 10-year time scale.

The relative importance of the shoreface-berm-function depends on the amount of onshore-offshore sediment movement compared to movement restricted to above MLW. The shoreface-berm-function is most important at GRH-01 (80.3% variance). The GRH-01 profile shows the greatest amount of erosion and volume change of the four long-running surveys (WKG-01,EST-01,GRH-01,MST-01). The shoreface-berm-function is least important at MAT-SP (53.6%). Swash-bars often form at MAT-SP , hence more of the variance is described by the beachface-function (21.3%).

Other workers have found that their beach-function equivalent to the shoreface-berm-function is the most important, and to describe about the same amount of variance from the mean profile. Bowman (1981) analyzed one-year of supratidal data from seven beaches composed of medium quartz sand on the southern Mediterranean coast of Israel. He found the second eigenfunction, which is equivalent to this study's first function because he did not remove the mean from the data, to describe 51-84% of the residual variance from the mean beach function. Clarke and Eliot (1983a) examined eighteen closely spaced profiles obtained over five years along a sandy beach in New South Wales, Australia.

Dividing the profiles into four segments above MLW and performing eigenfunction analysis using the volumes of each segment, they found that the first eigenfunction represents 67.6-95.1% of the variance. They also found the proportion of variance represented by this mode was generally higher along a section of the beach backed by reflective rock rip-rap which caused more onshore-offshore sediment transport.

The higher eigenfunctions may describe different beach-functions depending on the nature of the beach and the time covered. The second eigenfunction explains 9.3-21.3% of the variance. It includes the beachface-function at EST-01, CHA-EZ, GRH-01, and MAT-SP, and the backberm-function at all other locations. The third eigenfunction displays 5.3-13.1% of the variance and may be the foredune, backberm, or beachface functions. The fourth eigenfunction contains 1.8-8.4% of the variance from the mean profiles and may be uninterpretable. At EST-01, EST-02, CHA-BW, CHA-TB, and MST-01, however, the fourth eigenfunction is thought to be most sensitive to foredune activity, and at WKG-01 it may be important during times of a wide beach.

Sea-level Cycles

The four temporal scales of sea-level fluctuations previously noted have four different causes. The following is a discussion of the nature of the possible causes. It is

emphasized, however, that further research is required to confirm the hypotheses.

Weekly spikes in the data are caused by storm surge in the case of the highs or by strong offshore winds causing a set down in the case of the lows. These spikes show the greatest amplitude of the four scales, almost twice that of the other scales. Astronomical tides probably do not cause spikes, since unusually high tides are offset by unusually low tides in the same week.

The yearly cycle with lows in the winters and highs in the summers is probably caused by thermal contraction and expansion (Pattullo 1966).

The 11-to 14-year sea-level fluctuation is enigmatic; however, it is hypothesized that waves from the southeast and east created by local wind regimes, and waves arriving as swell generated by distal wind regimes cause a wave set-up at the coast. Since the shoreline is oriented northeast-southwest, waves out of the southeast impinge most directly on the shore, allowing for the set-up. Also, waves out of the southeast have a longer wave length and greater height than waves from any other direction (Raytheon Corp. 1975; Morton et al. 1982). The high sea levels in 1983 also coincide with an increase in winds from the southeast quadrant compared to the 1980-1982 period (Blais 1986; Rosenberg 1985).

Further evidence for predominant southeast waves causing the 11-to 14-year highs lies in the evidence of a

westward shift in the alongshore transport of sand coinciding with a sea-level high. From 1983 to 1985 profile volume greatly increased at WKG-01, which is just to the east of a headland, and at CHA-BW, which is just east of a jettied inlet. On the other hand, sediment volume decreased at EST-02, which is west of a jettied inlet, and at GRH-01, which is west of a headland (Gibeaut et al. 1986). This pattern of sedimentation is strong evidence for an overall shift of sediment transport to the west, induced by predominant southeast to east wave conditions which in turn caused a sea-level high.

The upward linear trend is explained by relative sea-level rise caused by melting glaciers and isostatic subsidence. Hicks (1981) performed a least squares linear regression on yearly mean tide data from Newport covering from 1931 to 1978. Hicks found a sea-level rise rate of .0027 m/yr. Over 25 years, this rate means a sea-level increase of .07 m, which is about half the sea-level variation on the 11-to 14-year scale. An importannt distinction must be made, however, in that the sea-level rise over the 25 years is eustatic and isostatic whereas the 11-to 14-year fluctuations are thought to be caused by a changing wave climate.

The above discussed causes of sea-level spikes and cycles need to be confirmed by further research and analyses. For the 11-to 14-year cycles, wave conditions required to create the observed amplitude must be

determined. Hindcast techniques should then be used to recreate the observed curve. As for the spikes, past storm surges must be correlated with the curve.

Beach Cycles

It is clear that in the last 24 years the barriers, particularly the beaches, of the southwest shore of Rhode Island have undergone changes in sediment volume on 10-11-, 4-5-, and 1-year cycles. Some locations show minor 2-4-year volume cycles. These cyclic volume changes are accompanied by unidirectional changes in elevation across the entire beach and changes in length or both. The 10-year cycle involves the most sediment movement with the 5- and 1-year cycles being less important.

High sea levels on an 11- to 14-year cycle generally coincide with high sediment volumes, as low sea levels coincide with low sediment volumes (Fig. 24) As stated earlier, it is hypothesized that high sea levels are caused by periods of predominant southeast swell conditions. Hence, the sediment volume highs could be a result of enhanced onshore sediment transport from the shoreface (about 8 m depth), caused by long wave length waves from the southeast.

Two previous studies provide evidence for a source and a mechanism for long-term onshore transport of sand from the shoreface. Morang and McMaster (1980) surveyed the south

shore with side scan sonar and discovered narrow, shore-normal bands of megarippled sand. The shore-normal bands merged and terminated in a sand sheet at 8 m depth, 300-400 m offshore; megaripple symmetry was not determined. DeKay (1981) reported a convex sand sheet running parallel to the shore in about 8 m of water off the EST-01 location. The formation of the shore parallel sand sheet is believed to occur during storms when sand transported from seaward of 8 m depth converges with sand eroded from the beach and upper shoreface. DeKay also discovered shore-normal lobes and troughs on the upper shoreface (<8 m depth). The relief between the lobes and troughs was on the order of 10's of cm, and the width of these features was on the order of 10's of m. Lobes and troughs formed during fairweather, swell wave conditions. Grain-wise onshore transport in narrow shore-normal zones nourishes the beach and creates troughs. DeKay hypothesized that the regular spacing of the lobes and troughs is controlled by edge waves. The DeKay (1981) and Morang and McMaster (1980) studies further the feasibility that periods of southeast swell conditions enhance onshore sediment transport and in turn cause coinciding high sea levels and beach volumes.

Beaches located near headlands or other features that interupt alongshore sediment transport, will be more sensitive to changes in the direction of transport than other beaches. Furthermore, beaches on opposite sides of obstructions will behave in an opposite manner. Of the four

long-term profiles, the volume time-series of WKG-01 and GRH-01, which are adjacent to headlands, but located on opposite sides, have more important 5-year cycles than EST-01 and MST-01, which have central barrier locations. Also, the 5-year cycles of WKG-01 and GRH-01 tend to be directly out of phase (this is most easily seen by comparing the two profiles since 1977). Accretion and erosion shifts on each side of the jettied Charlestown inlet occur on the order of 5 years (McMaster 1961-present). From these observations, it is deduced that the 5-year cyles are caused by shifts in alongshore sediment transport.

The importance of the seasonal cycle (1-year) varies but is always subordinant to the 10-year cycle. The seasonal cycle is caused primarily by the onshore-offshore sediment movement associated with the increased frequency of storms in winter. In many of the profiles, the backberm and beachface beach-functions show an increase in importance of the yearly cycle, indicating a seasonal exchange of sediment between the beachface and the backberm areas. However, the amount of seasonality may vary through time as storms may occur throughout the year or mild winters may prevail (Rosenberg 1985; Morton et al. 1982). Over the 24-year time period, WKG-01 has the least significant seasonal cycle but a relatively important 5-year cycle. The position of WKG-01, near a headland, makes it sensitive to alongshore transport which may mask an onshore-offshore yearly cycle.

EST-01 has by far the most important seasonal cycle; the reason for this is unknown.

Temporal dependences of the backberm and beachface functions often show 2-4-year cycles that represent backberm filling and profile shortening. These 2-4-year cycles in the higher temporal eigenfunctions do not involve important volume changes; they are probably caused by wave-climate cycles. Possibly these geomorphic cycles are caused by severe storms from which, volumetrically, the beach recovers quickly but with a downward and seaward shift in the locus of sedimentation. Subsequently, the center of sedimentation moves landward and the backberm is rebuilt over the next 2 or 3-years. A more detailed study of the profiles is needed to confirm this hypothesis.

The four long-term profiles display erosional trends over 24 years. The erosional trends may be related to the 7 cm increase in sea level discussed previously; however, storm surges commonly may be over 1 m. The storm surge from Hurricane Gloria, which struck New England at Bridgeport, Connecticut on September 27, 1985, was 2.5 m (Boothroyd et al. 1986). The "Blizzard of 78" storm surge (February 6) was m. (Boothroyd et al. 1986). The rise in sea level of 7 cm over the study period, therefore, is believed to be insignificant in causing erosion compared to the individual storms which occurred throughout the last 25 years. Hence, the long-term (24-year) erosional trends are caused by aperiodic storms and periods of closely spaced storms

(winter of 1976-77 and 1977-78) which occurred over 24 years. This is not to say that sea-level rise is unimportant in beach erosion but rather that it only becomes important on time scales greater than 25 years.

CONCLUSIONS

1) The shoreface-berm-function is the most important beach-function and describes onshore-offshore sediment transport. The amount of variance described by shoreface-berm-functions in this study agrees well with previous studies of other sandy beachs.

2) Profile volume time series are highly positively correlated with the shoreface-berm functions, which shows that volume changes occur as unidirectional changes in elevation across the entire beach or changes in length, or both.

3) The shapes of the shoreface-berm-functions may be able to discriminate modal profile configurations such as berm runnels; however, further detailed analysis is required on subsets of the time series.

4) The seaward node of the backberm-function is a good indicator of the modal berm-crest position because it involves a sediment exchange process and not just

morphology. This point can be used as a reference point in future studies.

5) With direction shifts of incoming waves, irregular offshore bathymetry will cause more variable wave conditions at the beach than at a beache with smooth offshore bathymetry. Offshore bars attenuate waves and create a more uniform wave climate than at non-barred locations.

From July, 1977 to 1986, CHA-BW has by far the greatest amount of volume variance of the McMaster profiles. Complicated offshore bathymetry and updrift accretion of sand on either side of the jettied inlet means that this beach is sensitive to different storm-wave climates, and to wave climates on a seasonal, and at least, a 5-year timescale. MIS-01, on the other hand, is located in the center of a barrier spit, and has an offshore bar system that attenuates the waves. Hence MIS-01 has a very low volume variance. CHA-TB also has a very low volume variance caused by sediment by-passing this central barrier location.

6) On a 24-year time scale, all four beaches measured show erosional trends, with a beach located to the west of a headland (GRH-01) having the greatest erosion, and WKG-01, located to the east of a headland, having the least erosion.

7) For the 24-year volume time series, all locations show a strong 10-year cycle of erosion and deposition. High

volumes existed at WKG-01, EST-01, and MST-01 in 1963, 1973-75, and 1984-85; low volumes existed in 1966-67 and 1979-81. The GRH-01 cycle is complicated and out of phase with the others.

8) For the long-running volume time series, all profiles have a secondary 5-year cycle. WKG-01, EST-01, and MST-01 have high volumes in 1963, 1965-66, 1969-70, 1974-75, 1980-81, and 1984-85, and lows in 1964, 1967, 1972, 1977, 1982, and possibly one to occur in 1987. The GRH-01 cycle appears to be more complicated and out of phase with the others.

9) The 6 shorter timespan profiles, except for MAT-SP, have prominent 4-6-year cycles, with the 3 locations on Charlestown Beach in phase with WKG-01, EST-01, and MST-01.

10) The shorter-running profiles usually have relatively more important seasonal cycles, but the longer-term profiles, except for EST-01, do not. This emphasizes the greater importance of beach sedimentation on 10- and 5-year time scales rather than on a yearly scale.

11) The temporal dependence of the backberm and beachface functions often show 2-4-year cycles that represent backberm filling and profile shortening. These 2-4-year cycles in the higher temporal eigenfunctions do not

involve important volume changes; therefore, they are primarily caused by wave- climate cycles.

12) The 10- and 5-year cycles involve sediment supply fluctuations. The 10-year cycle may be caused by onshore sediment movement from the shoreface, and the 5-year cycle may involve alongshore transport.

13) Sea-level highs on an 11- to 14-year cycle coincide with sediment volume highs on about the same cycle. It is proposed that periods of dominant southeast to east swells cause a set-up on the coast. These long wave length swells, in turn, enhance onshore sediment transport from the shoreface (about 8 m depth).

14) Long-term erosional trends (24 years) are caused by aperiodic storms and periods of closely spaced storms. Beach erosion caused by sea-level rise only becomes important on time scales of 25 years or more.

REFERENCES

ABELE, R.W., JR., 1977, Analysis of short-term variations in beach morphology (and concurrent dynamic processes) for summer and winter periods, 1971-72, Plum Island, Massachusetts: Misc. Rept. No. 77-5, U.S. Coastal Engineering Research Center, 101 p.

ASYST SCIENTIFIC SOFTWARE, 1985, Asyst: a Scientific System Module 2, Analysis: Macmillan Software Company, New York.

AUBREY, D.G., 1979, Seasonal patterns of onshore/offshore sediment movement: Jour. Geophys. Res., v.84, p. 6347-6354.

AUBREY, D.G., 1983, Beach changes on coasts with different wave climates, in: McLachlan, A., and Erasmus, T., (eds.), Sandy Beaches as Ecosystems: The Hague, D.W. Junk Publishers, p. 63-85.

AUBREY, D.G., INMAN, D.L. and WINAUT, C.D., 1980, The Statistical prediction of beach changes in southern California: Jour. Geophys. Res., v. 85 p. 3264-3276.

AUBREY, D.G., AND EMERY, K.O., 1983, Eigenanalysis of recent United States sea levels: Continental Shelf Research, V. 2, no. 1, p. 21-33.

AUBREY, D.G., AND ROSS, R.M., 1985, The Quantitative description of beach cycles: Marine Geology, V. 69, p. 155-170.

AUBREY, D.G., AND EMERY, K.O., 1986, Relative sea levels of Japan from tide-gauge records: Geol. Soc. of Am. Bull., V.97, no. 2, p. 194-205.

BLAIS, A. G., 1986, Spatial and temporal variations of a microtidal beach: Charlestown Beach, Rhode Island [M.S. thesis]: Univ. Rhode Island, 405 p.

BOOTHROYD, J.C., CABLE, M.S., MCCREERY, C.J., and RUSSELL, D., 1978, Beach erosion and recovery, Charlestown Beach, Rhode Island: 1978 Blizzard Symp. Proc., Boston State College, Boston Massachusetts, p. 81-90.

BOOTHROYD, J.C., FRIEDRICH, N.E., AND McGINN, S.R., 1985, Geology of microtidal coastal lagoons: Rhode Island: Marine Geology, v. 63, p. 35-76.

BOOTHROYD, J.C., GIBEAUT, J.C., DACEY, M.F., AND ROSENBERG, M.J., 1986, Geological Aspects of Shoreline Management: A Summary for Southern Rhode Island, Volume 1: Sea Grant Tech. Report, Univ. Rhode Island, Project no. R/CS-1, 104 p.

BOWMAN, D., 1981, Efficiency of eigenfunctions for discriminant analysis of subaerial non-tidal beach profiles: Marine Geology, v. 39, p. 243-258.

BRUUN, P., 1962, Sea level as a cause of shore erosion: Jour. of Waterways and Harbors Div., A.S.C.E., V. 88, p. 117-130.

CLARKE, D. J., and ELIOT, I. G., 1983a, Onshore-offshore patterns of sediment exchange in the littoral zone of a sandy beach: Journal of Geological Society of Australia, v. 30, p. 341-351.

CLARKE, D. J., and ELIOT, I. G., 1983b, Mean sea-level and beach-width variation at Scarborough, Western Australia: Marine Geology, V. 51, p. 251-267.

CLARKE, D.J., AND ELIOT, I.G., 1984, Variation in subaerial beach sediment volume on a small sandy beach over a monthly lunar tidal cycle: Marine Geology, V. 58, p. 319-344.

DAVIS, J.C., 1973, Statistics and Data Analysis: New York, NY, John Wiley and Sons, 550 p.

DAVIS, R.A., AND FOX, W.T., 1972, Four-dimensional model for beach and inner nearshore sedimentation: Journal of Geology, V. 80, p.484-493.

DAVIS, R.A., JR., FOX, W.T., HAYES, M.O., AND BOOTHROYD, J.C., 1972, Comparison or ridge and runnel systems in tidal and non-tidal environments: Journal of Sedimentary Petrology, v. 42, p. 413-421.

DEKAY, L.E., 1981, Morphodynamics of an undernourished barrier beach, East Beach, Rhode Island [M.S. thesis]: Univ. Rhode Island, 166 p.

EMERY, K.O., 1961, A simple method of measuring beach profiles: Limnology and Oceanography, v. 6, p. 90-93.

FISHER, J.J., and SIMPSON, E.J., 1979, Washover and tidal sedimentation rates as environmental factors in development of a transgressive barrier shoreline, in: Leatherman, S.P., (ed.), Barrier Island-Gulf of Mexico to Gulf of St. Lawrence, N.Y., Academic Press, 336 p.

FLICK, R.E., AND CAYAN, D.R., 1984, Extreme sea levels on the coast of California: Proceedings of the 19th Coastal Engineering Conference, A.S.C.E., Houston, TX, p. 886-898.

FOX, W.T., and DAVIS, R.A., JR., 1973, Simulation model for storm cycles and beach erosion on Lake Michigan: Geological Society of America Bull., v. 84, p. 1769-1790.

HASHIMOTO, H., UDA, T., AND TAKEBUCHI, T., 1981, Prediction of beach profile changes around structures by an empirical model: Coastal Engeneering of Japan, V. 24, p. 258.

HAYES, M.O., 1979, Barrier island morphology as a function of tidal and wave regime: in, Leatherman, S.P., (ed.), Barrier Islands from the Gulf of St. Lawrence to the Gulf of Mexico: New York, Academic Press, p. 1-28.

HEAPS, N.S., 1985, Tides, storm surges and coastal circulations: in, Dyke, P.P.G, Moscardini, A.O., and Robson, E.H., (eds.), Lecture Notes on Coastal and Estuarine Studies: New York, Springer-Verlag, p. 3-54.

HICKS, S. D., 1981, Long-period sea level variations for the United States through 1978: Shore and Beach, April, p. 26-29.

HINE, A.C., 1979, Mechanisms of berm development and resulting beach growth along a barrier spit complex: Sedimentology, v. 26, p. 333-351.

KOMAR, P.D., 1976, Beach Processes and Sedimentation: Englewood Cliffs, New Jersey, Prentice-Hall, Inc., 429 p.

LaFOND, E.C., 1938,Relationship between mean sea level and sand movements: Science, V. 88, no. 2274, p. 112-113.

McMASTER, R.L., (compiler) et al., 1961-present, Transit surveying of selected Block Island Sound beaches in Washington County, Rhode Island [unpub. Annual Reports]: Coastal Resources Center, Univ. Rhode Island, Kingston, RI.

McMASTER R.L. AND FRIEDRICH ,N.E., 1986, Southwestern Rhode Island Beaches and Shoreline Processes, 1938-1984: report prepared for Coastal Resources Center, Univ. Rhode Island Graduate School of Oceanography, 60 p.

MIZUGUCHI, S., OKADA, I., AND MORI, T., 1982, Empirical eigenfunction analysis of three-dimensional beach transformation: Coastal Engeneering of Japan, V. 25 p. 287.

MORANG, A., AND McMASTER, R. L., 1980, Nearshore bedform patterns along Rhode Island from side-scan sonar surveys: Jour. Sed. Petrol., V. 50, no. 3, p. 831-839.

MORTON, R. W., BOHLEN, W. F., and AUBREY, D. G., 1982, Beach changes at Misquamicut Beach, Rhode Island, 1962-73: report submitted to U. S. Army Coastal Engineering Research Center, Fort Belvoir, VA, Science Applications Inc., Newport, RI.

NOAA, 1986, Tide Tables 1986, High and Low Water Predictions: East Coast of North and South America Including Greenland: U.S. Dept. of Commerce, Washington, D.C., 285 p.

NUMMEDAL, D., and FISCHER, I.A., 1978, Process-response models for deposition shorelines: The German and Georgia Bights: Proc. 16th Conf. Coastal Engineering, American Soc. Civil Engineers, II, p. 1215-1231.

PATTULLO, J. G., 1966, Seasonal changes in sea level. In Hill, M. N., (ed.), The Sea, Interscience Publ., New York, p. 485-496.

RAYNER, J. N., 1971, An Introduction to Spectral Analysis: London, Pion Limited, 174 p.

ROSENBERG, M.J., 1985, Temporal variability of beach profiles, Charlestown Beach, Rhode Island [M.S. Thesis]: Univ. Rhode Island, 358 p.

STATISTICAL ANALYSIS SYSTEM (SAS) INSTITUTE, INC., 1985, SAS User's Guide: Statistics, Version 5 Edition, Cary, NC, SAS Institute, Inc., 956 p.

STRAHLER, A. N., AND STRAHLER, A. H., 1978, Modern Physical Geography: John Wiley and Sons, New York, Chapter 6, p. 76-89.

WRIGHT, L.P., and SHORT. A.D., 1984, Morphodynamic variability of surf zones and beaches: a synthesis*: Marine Geology, v. 56, p. 93-118.

APPENDIX 1

BEACH PHOTOGRAPHS

Weekapaug Beach 1 (WKG-01, May 1986).

East Beach 1 (EST-01, May 1986).

Green Hill Beach 1 (GRH-01, May 1986).

Moonstone Beach 1 (MST-01, May 1986).

Misquamicut Beach 1 (MIS-01, May 1986).

East Beach 2 (EST-02, May 1986).

Charlestown Breachway Beach (CHA-BW, Mar 1986).

Charlestown EZ Beach (CHA-EZ, Mar 1986).

Charlestown Town Beach (CHA-TB, May 1986).

Matunuck SP Beach (MAT-SP, Mar 1986).

APPENDIX 2

COMPUTER PROGRAMS

Program BEACH 3 uses beach profile data to create the profile plots in volumes 2 and 3. The Julian date and profile volumes are also calculated. The program is written in Fortran 66 and uses Calcomp graphic subroutines. The program is compiled on the TSO system and loaded into a load module (URI.EIL101.LOAD).

```
00010 //EIL101  JOB (EIL101),'BEACH3',MSGCLASS=A
00020 //  EXEC  FORTVCL,PARM.FORT='LANGLVL(66)',
00030 //  PARM.LKED='NCAL,LET,LIST,XREF'
00040 //FORT.SYSIN DD *
00050           INTEGER COUNT,TITLE(3),DATE(3),PROFIL(3),DATE2(3),RECORD(
5),
00060       1      COMP/'COMP'/,COMPAR/0/,COUNT2,COUNT3,Z,ZZ,JDAY,JMO,JYR
00070       1 ,JMOS(12),NMOS,NYRS,NLYR,MARG,LYRF,
00080       1 JM(12)/'JAN','FEB','MAR','APR','MAY','JUN','JUL','AUG','SEP
',
00090       1 'OCT','NOV','DEC'/
00100           REAL XMINC(200),XINC(200),YINC(200),X(200),Y(200),
00110       1     XDISP,YDISP,YHOLD(200),X2(200),Y2(200),A,B,C,D,M,
00120       1      YINT,XINT,XM,YM,XX,XXMINC,XX1,YY,YY1,VDSUM,MDVD,MNVD,V
D(999)
00130       1       ,DUM,JDATE
00140           CALL PLOTS(0.,0.,99)
00150           CALL FACTOR(0.5)
00160           WRITE(6,2000)
00170 2000      FORMAT(1X,'PROGRAM LOADED IS BEACH3')
00180 C
00190 C - - - - - - - -  READ PARAMETERS
00200 C
00210          Z=0
00220          VDSUM=0.
00230    5      REWIND 8
00240           COMPAR=0
00250    10     READ(5,100,END=999) PROFIL
00260    100    FORMAT(3A4)
00270           READ(5,100) DATE
00280 C
00290 C - - - - - - - - SCAN DATA FOR TITLE, DATE
00300 C
00310           IF(PROFIL(3).NE.COMP) GO TO 20
00320           COMPAR=1
00330           READ(5,100) DATE2
00340    20     READ(8,100,END=902) TITLE
00350           IF(TITLE(2).NE.PROFIL(2)) GO TO 20
00360           IF (TITLE(1).NE.PROFIL(1)) GO TO 20
00370           BACKSPACE 8
00380           BACKSPACE 8
00390    30     READ(8,200,END=903) RECORD
00400    200    FORMAT(5A4)
00410           IF(RECORD(1).NE.DATE(1)) GO TO 30
00420           IF(RECORD(2).NE.DATE(2)) GO TO 30
00430           IF(RECORD(3).NE.DATE(3)) GO TO 30
00440           WRITE(6,550) DATE
00450    550    FORMAT(1X,3A4)
00460 C
00470 C---------CONVERT DATE TO JULLIENNE DATE FOR CORRELATION AND
00480 C          VOLUME PLOT PROGRAM , 01 OCT 1961= DAY 1
00490 C
00500           BACKSPACE 8
00510           READ(8,101)JDAY,JMO,JYR
00520   101     FORMAT(I2,1X,A3,1X,I4)
00530           JMOS(1)=0
00540           JMOS(2)=31
00550           JMOS(3)=59
00560           JMOS(4)=90
00570           JMOS(5)=120
00580           JMOS(6)=151
```

```
00590           JMOS(7)=181
00600           JMOS(8)=212
00610           JMOS(9)=243
00620           JMOS(10)=273
00630          ¬MOS(11)=304
00640           JMOS(12)=334
00650           IF(JMO .EQ. JM(1))NMOS=1
00660           IF(JMO .EQ. JM(2))NMOS=2
00670           IF(JMO .EQ. JM(3))NMOS=3
00680           IF(JMO .EQ. JM(4))NMOS=4
00690           IF(JMO .EQ. JM(5))NMOS=5
00700           IF(JMO .EQ. JM(6))NMOS=6
00710           IF(JMO .EQ. JM(7))NMOS=7
00720           IF(JMO .EQ. JM(8))NMOS=8
00730           IF(JMO .EQ. JM(9))NMOS=9
00740           IF(JMO .EQ. JM(10))NMOS=10
00750           IF(JMO .EQ. JM(11))NMOS=11
00760           IF(JMO .EQ. JM(12))NMOS=12
00770           JDATE=0
00780           IF(JYR .EQ. 1961) GO TO 415
00790           NYRS=JYR-1961
00800           NLYR=NYRS/4
00810           MARG=NYRS+1
00820           JDATE=365*(NYRS-1)+NLYR+92
00830           IF(NMOS .GT. 2 .AND. MOD(MARG,4) .EQ. 0)JDATE=JDATE+1
00840           JDATE=JMOS(NMOS)+JDATE+JDAY
00850           GO TO 416
00860  415      JDATE=JDATE+JDAY
00870           IF(JMO .EQ. JM(11))JDATE=JDATE+31
00880           IF(JMO .EQ. JM(12))JDATE=JDATE+61
00890  416      CONTINUE
00900   50      READ(8,100) TITLE
00910           WRITE(6,550) TITLE
00920 C
00930 C - - - - - - - READ DATA FOR PROFILE
00940 C
00950           READ(8,900)STELEV,SLEVEL
00960   900     FORMAT(2F9.1)
00970           WRITE(6,666)STELEV,SLEVEL
00980   666     FORMAT(1X,'STAKE ELEVATION=',F9.1,'    STAKE LEVEL=',F9.1
)
00990 C
01000 C - - - - - - - FILL X, Y ARRAYS
01010 C
01020   80      DO 90 I=1,200
01030           READ(8,560)XINC(I),YINC(I)
01040   560     FORMAT(F4.0,5X,F4.0)
01050           IF(XINC(I).LT.-100.)GO TO 95
01060           WRITE(6,561)XINC(I),YINC(I)
01070   561     FORMAT(1X,2F9.1)
01080   90      CONTINUE
01090   95      COUNT=I-1
01100           Y(1)=STELEV-SLEVEL
01110           X(1)=0.
01120 C
01130 C - - - - - - -  SUM DATA AND P¬¬CE VERTICAL DISPLACEMENT IN AN AR
RAY
01140 C
01150           DO 110 I=2,COUNT
01160           Y(I)=Y(I-1)+YINC(I-1)
01170           X(I)=X(I-1)+XINC(I-1)
```

```
01180   110     CONTINUE
01190           Z=Z+1
01200           VD(Z)=Y(COUNT)
01210           VDSUM=VDSUM+VD(Z)
01220           WRITE(6,931)X(COUNT),Y(COUNT)
01230   931     FORMAT(1X,'HORIZONTAL DISPLACEMENT =',F14.7,/,
01240       11X,'VERTICAL DISPLACEMENT =',F14.7)
01250 C
01260 C - - - - - - - -  CONVERT TO METERS
01270 C
01280           DO 120 I=1,COUNT
01290           Y(I)=Y(I)*.01
01300           X(I)=X(I)*.01
01310           XMINC(I)=XINC(I)*.01
01320   120     CONTINUE
01350           AMET=0.
01360 C
01370 C - - - - - - - -  CALCULATE AREA UNDER CURVE, TRAPEZOID SUMMATION
01380 C
01390           DO 170 I=1,COUNT
01400           IF(Y(I).LE.0.) GO TO 69
01410   170     YHOLD(I)=Y(I)+2.
01420 C
01430 C ---------------EXTRAPOLATE SHORT PROFILE
01440 C ---------------FIND REGRESSION  LINE OF LAST 4 POINTS
01450 C
01460               A=X(COUNT)*Y(COUNT)
01470               B=X(COUNT)
01480               C=Y(COUNT)
01490               D=X(COUNT)**2
01500               DO 75 I=1,3
01510                  A=A+X(COUNT-I)*Y(COUNT-I)
01520                  B=B+X(COUNT-I)
01530                  C=C+Y(COUNT-I)
01540                  D=D+X(COUNT-I)**2
01550   75              CONTINUE
01560               M=(A-((B*C)/4.))/(D-((B**2)/4.))
01570           IF(M.GE.-.01) GO TO 888
01580           IF((M.GE.-.05).AND.(Y(COUNT).GE..5))GO TO 888
01590               YINT=Y(COUNT)-M*X(COUNT)
01600               XINT=-1.*YINT/M
01610               XX=XINT
01620               XXMINC=XX-X(COUNT)
01630           DO 130 I=2,COUNT
01640           AMET=AM¬¬+.5*(YHOLD(I-1)+YHOLD(I))*XMINC(I-1)
01641 130       CONTINUE
01670           AMET=AMET-(X(COUNT)*2.) + .5*(YHOLD(COUNT)-2.)*XXMINC
01680           WRITE(6,930)AMET
01690   930     FORMAT(' AREA UNDER CURVE =',F14.7)
01700           YY=0.
01710           IF(COMPAR.NE.1) GO TO 300
01720           GO TO 71
01730   888     DO 889 I=2,COUNT
01740              AMET=AMET+.5*(YHOLD(I-1)+YHOLD(I))*XMINC(I-1)
01741 889         CONTINUE
01760           AMET=AMET-(X(COUNT)*2.)
01770           WRITE(6,887)
01780   887     FORMAT('**CAUTION, EXTRAPOLATION MAY NOT BE RESONABLE; VO
LUME
01790       1 AND GRAPH ARE CALCULATED TO THE LAST DATA POINT**')
01800           WRITE(6,930)AMET
```

```
01810           XX=X(COUNT)
01820           YY=Y(COUNT)
01830           IF (COMPAR .NE. 1 ) GO TO 300
01840           GO TO 71
01850    69     CONTINUE
01851  C
01852  C ------------DETERMINE THE LINE OF THE LAST 2 POINTS SPANNING MLW
01853  C-------------AND FIND THE X INTERCEPT
01854  C
01855            COUNT3=I-1
01856           M=(Y(COUNT3)-Y(COUNT3+1))/(X(COUNT3)-X(COUNT3+1))
01857           YINT=Y(COUNT3)-(M*X(COUNT3))
01858           XM=-1.*YINT/M
01859           YM=0.
01860           YHOLD(COUNT3+1)=YM+2.
01870           XMINC(COUNT3)=XM-X(COUNT3)
01880           COUNT3=COUNT3+1
01890           DO 152 I=2,COUNT3
01900           AMET=AMET+.5*(YHOLD(I-1)+YHOLD(I))*XMINC(I-1)
01901  152      CONTINUE
01930           AMET=AMET-(XM*2.)
01940           WRITE(6,935)AMET
01950    935    FORMAT(' AREA UNDER CURVE =',F14.7)
01960           XX=X(COUNT)
01970           YY=Y(COUNT)
01980           IF(COMPAR.NE.1) GO TO 300
01990    71     CONTINUE
02000  C
02010  C - - - - - - - SAVE FIRST PROFILE DATA
02020  C
02030           DO 133 I=1,COUNT
02040           Y2(I)=Y(I)
02050    133    X2(I)=X(I)
02060           COUNT2=COUNT
02070           DIFF=AMET
02080           COMPAR=2
02090           XX1=XX
02100           YY1=YY
02110    40     READ(8,200,END=904) RECORD
02120           IF(RECORD(1).NE.DATE2(1)) GO TO 40
02130           IF(RECORD(2).NE.DATE2(2)) GO TO 40
02140           WRITE(6,550) DATE2
02150           GO TO 50
02160  C
02170  C - - - - - - - CALCULATE AREA CHANGE
02180  C
02190    300    IF(COMPAR.NE.2) GO TO 220
02200           AAAA=AMET
02210           AMET=AMET-DIFF
02220  C
02230  C - - - - - - -  PLOT PROFILES
02240  C
02250    220   WRITE(9,104)JDATE,DATE,AMET
02260    104   FORMAT(F5.0,3X,3A4,3X,F5.1)
02270          CALL PROPLT(X,Y,X2,Y2,COUNT,COUNT2,TITLE,DATE,DATE2,AMET,
02280         *AAAA,DIFF,COMPAR,XX,XX1,YY,YY1)
02290           GO TO 5
02300  C
02310  C----------FIND MEAN AND MEDIAN V.D.
02320  C
02330    999    MNVD=VDSUM/Z
```

```
02340           ZZ=Z
02350           DO 315 I=1,ZZ
02360              Z=Z-1
02370              DO 316 J=1,Z
02380                 IF(VD(J).LT.VD(J+1)) GO TO 316
02390                 DUM=VD(J)
02400                 VD(J)=VD(J+1)
02410                 VD(J+1)=DUM
02420  316         CONTINUE
02430  315       CONTINUE
02440               DO 147 I=1,ZZ
02450                  WRITE (6,148) VD(I)
02460 148              FORMAT (1X,F7.1)
02470 147           CONTINUE
02480            IF (MOD(ZZ,2) .EQ. 0) GO TO 318
02490            MDVD=VD(ZZ/2+1)
02500            GO TO 319
02510  318       MDVD=(VD(ZZ/2)+VD(ZZ/2+1))/2.
02520                  WRITE (6,111) ZZ,VD(ZZ/2),VD(ZZ/2+1),VDSUM
02530 111              FORMAT(1X,I4,2X,3(F7.1,2X))
02540  319       WRITE(6,317) ZZ,MNVD,MDVD
02550  317       FORMAT(1X,'# PROFILES = ',I4,3X,'MEAN V.D. = ',F5.1,3X,
02560      1       'MEDIAN V.D. = ',F5.1)
02570 C
02580 C - - - - - ¬¬- ERROR MESSAGES
02590 C
02600           CALL PLOT(0.,0.,999)
02610           WRITE(6,9011)
02620  9011     FORMAT(' END OF RUN.....')
02630           STOP
02640   902     WRITE(6,9022)
02650  9022     FORMAT(' END OF DATA; SEARCHING FOR PROFILE TITLE.')
02660           STOP 333
02670   903     WRITE(6,9033)
02680  9033     FORMAT(' END OF DATA; SEARCHING FOR DATE 1.')
02690           STOP 333
02700   904     WRITE(6,9044)
02710  9044     FORMAT(' END OF DATA, SEARCHING FOR DATE 2.')
02720           STOP 333
02730           END
02740           SUBROUTINE PROPLT(X,Y,X2,Y2,COUNT,COUNT2,TITLE,DATE,DATE2
,AMET,
02750      1       AAAA,DIFF,COMPAR,XX,XX1,YY,YY1)
02760           REAL X(200),Y(200),XORG/0.0/,NWXORG,XLEN,X2(200),Y2(200)
02770      1     ,XX,YY,YY1,XX1
02780           INTEGER COUNT,DATE(3),TITLE(3),COUNT2,DATE2(3),COMPAR
02790   1       NWXORG=0.0
02800 C
02810 C - - - - - - - -  FIND LENGTH OF X AXIS
02820 C
02830         IF ((COMPAR .EQ. 2) .AND. (XX1 .GT. XX)) GO TO 4000
02840           IF(X(1).GE.0.) GO TO 100
02850           XLEN=(XX-X(1))/5 + 1
02860           XORG=X(1)/5 - 1
02870           NWXORG=XORG*(-1.)
02880           CALL PLOT(NWXORG,0.0,-3)
02890           GO TO 101
02900    100    XLEN=XX/5 + 1
02910           GO TO 101
02920 4000    CONTINUE
02930         IF (X(1) .GE. 0.) GO TO 4010
```

```
02940          XLEN=(XX1-X(1))/5 + 1
02950          XORG=X(1)/5 -1
02960          NWXORG=XORG*(-1.)
02970          CALL PLOT(NWXORG,0.0,-3)
02980          GO TO 101
02990 4010     XLEN=XX1/5 + 1
03000 C
03010 C - - - - - - - -  SCALE DATA
03020 C
03030    101     X(COUNT+1)=0.
03040            X(COUNT+2)=5.
03050            Y(COUNT+1) = -1.
03060            Y(COUNT+2) = 1.
03070            IF(COMPAR.EQ.3) GO TO 107
03080 C
03090 C - - - - - - ¬ -  PLOT AXES
03100 C
03110            CALL AXIS(XORG,0.0,'METERS ABOVE MLW',16,7.,90.,
03120         1     Y(COUNT+1),Y(COUNT+2))
03130            CALL AXIS(XORG,0.0,'METERS FROM DATUM STAKE',-23,XLEN,0.,
03140         1     X(COUNT+1),X(COUNT+2))
03150 C
03160 C - - - - - - - -  PLOT SCALE OF PROFILE
03170 C
03180             CALL PLTLN(.75,1.5,1.75,1.5)
03190             CALL PLTLN(1.75,1.45,1.75,1.55)
03200             CALL SYMBOL(0.88,1.3,0.15,'5.0 M',0.0,5)
03210             CALL PLTLN(.75,1.5,.75,2.5)
03220             CALL PLTLN(.7,2.5,.8,2.5)
03230             CALL SYMBOL(.65,1.63,0.15,'1.0 M',90.0,5)
03240             CALL SYMBOL(0.89,2.25,0.15,'V.E.=',0.0,5)
03250             CALL SYMBOL(1.04,2.00,0.15,'5:1',0.0,3)
03260 C
03270 C - - - - - - - -  PLOT I.D. BOX
03280 C
03290            CALL SYMBOL((XLEN-6.75),7.0,.48,TITLE,0.,12)
03300            CALL SYMBOL((XLEN-6.75),6.7,.25,1,0.,-1)
03310            CALL SYMBOL((XLEN-6.4),6.6,.25,45,0.,-1)
03320            CALL SYMBOL((XLEN-6.1),6.6,.25,DATE,0.,12)
03330            IF(COMPAR.NE.0) GO TO 102
03340            CALL SYMBOL((XLEN-6.75),5.8,.23,'AREA IN SQ METERS=',0.,1
8)
03350            GO TO 103
03360    102     CALL SYMBOL((XLEN-6.75),6.3,.25,2,0.,-1)
03370            CALL NUMBER((XLEN-2.9),6.6,.25,DIFF,0.,1)
03380            CALL SYMBOL((XLEN-1.3),6.6,.25,'SQ. METERS',0.,10)
03390            CALL SYMBOL((XLEN-6.4),6.2,.25,45,0.,-1)
03400            CALL SYMBOL((XLEN-6.1),6.2,.25,DATE2,0.,12)
03410            CALL NUMBER((XLEN-2.9),6.2,.25,AAAA,0.,1)
03420            CALL SYMBOL((XLEN-1.3),6.2,.25,'SQ. METERS',0.,10)
03430            CALL SYMBOL((XLEN-6.75),5.8,.23,'AREA CHANGE IN SQ. METER
S=',
03440         1     0.,26)
03450    103     CALL NUMBER((XLEN-.6),5.8,.25,AMET,0.,1)
03460            CALL REC¬((XLEN-7.0),5.6,2.0,8.4,0.,3)
03470 C
03480 C - - - - - - - -  PLOT MLW LINE
03490 C
03500    104     Q=-0.1
03510            DO 105 I=1,200
03520            Q=Q+.2
```

```
03530           CALL PLTLN(Q,1.0,(Q+.1),1.0)
03540           IF(Q.GT.(XLEN+1.0))GO TO 106
03550    105    CONTINUE
03560    106    CALL SYMBOL((Q-.25),1.0,.2,'MLW',0.,3)
03570 C
03580 C - - - - - - - -  PLOT PROFILE
03590 C
03600    107  FX=X(COUNT+1)
03610         DX=X(COUNT+2)
03620         FY=Y(COUNT+1)
03630         DY=Y(COUNT+2)
03640 C
03650         IF(COMPAR.EQ.2) GO TO 1072
03660 C
03670 C ------ COMPAR = 0 OR 3, SYMBOL # 1
03680 C
03690         CALL SYMBOL((X(1)-FX)/DX,(Y(1)-FY)/DY,0.2,1,0.0,-1)
03700         DO 1071 I=2,COUNT
03710         CALL SYMBOL((X(I)-FX)/DX,(Y(I)-FY)/DY,0.2,1,0.0,-2)
03720    1071 CONTINUE
03730           CALL PLOT ((X(COUNT)-FX)/DX,(Y(COUNT)-FY)/DY,3)
03740           CALL DASHP ((XX-FX)/DX,(YY-FY)/DY,.04)
03750           CALL SYMBOL ((XX-FX)/DX,(YY-FY)/DY,0.2,1,0.0,-1)
03760         GO TO 1074
03770 C
03780 C ------ COMPAR = 2, SYMBOL # 2
03790 C
03800    1072 CALL SYMBOL((X(1)-FX)/DX,(Y(1)-FY)/DY,0.2,2,0.0,-1)
03810         DO 1073 I=2,COUNT
03820         CALL SYMBOL((X(I)-FX)/DX,(Y(I)-FY)/DY,0.2,2,0.0,-2)
03830    1073 CONTINUE
03840           CALL PLOT ((X(COUNT)-FX)/DX,(Y(COUNT)-FY)/DY,3)
03850           CALL DASHP ((XX-FX)/DX,(YY-FY)/DY,.04)
03860           CALL SYMBOL ((XX-FX)/DX,(YY-FY)/DY,0.2,2,0.0,-1)
03870 C
03880    1074 IF((COMPAR.EQ.0) .OR. (COMPAR.EQ.3)) GO TO 109
03890 C
03900 C - - - - - - - PROCESS DATA FROM OTHER PROFILE
03910 C
03920           DO 108 I=1,COUNT2
03930           X(I)=X2(I)
03940    108    Y(I)=Y2(I)
03950           XX=XX1
03960           YY=YY1
03970           COUNT=COUNT2
03980           COMPAR=3
03990           GO TO 100
04000 C
04010 C - - - - - - - REDEFINE ORIGIN FO¬¬NEXT PLOT
04020 C
04030    109    CALL PLOT((XLEN+5.5),0.0,-3)
04040           RETURN
04050           END
04060         SUBROUTINE AXIS(XX,YY,IBCD,NCHAR,AXLEN,ANGLE,FIRSTV,DELTAV)
04070         DIMENSION IBCD(2)
04080         XPAGE=XX
04090         YPAGE=YY
04100         KN=NCHAR
04110         A=1.0
04120         IF (KN) 1,2,2
04130    1    A=-A
```

```
04140       KN=-KN
04150    2  EX=0.0
04160       ADX= ABS  (DELTAV)
04170       IF (ADX) 3,7,3
04180    3  IF (ADX- 99.0) 6,4,4
04190    4  ADX=ADX/10.0
04200       EX=EX+1.0
04210       GO TO 3
04220    5  ADX=ADX*10.0
04230       EX=EX-1.0
04240    6  IF (ADX-0.01) 5,7,7
04250    7  XVAL=FIRSTV*10.0**(-EX)
04260       ADX= DELTAV*10.0**(-EX)
04270       STH=ANGLE*0.0174533
04280       CTH=COS(STH)
04290       STH=SIN(STH)
04300       DXB=-0.25
04310       DYB=0.35*A-0.05
04320       XN=XPAGE+DXB*CTH-DYB*STH
04330       YN=YPAGE+DYB*CTH+DXB*STH
04340       NTIC=AXLEN+1.0
04350       NT=NTIC/2
04360       DO  20  I=1,NTIC
04370       IF(I.EQ.1) GO TO 15
04380       IF(MOD(I,2).EQ.0 .AND. ANGLE.EQ.0.0) GO TO 15
04390         IF(ANGLE.EQ.0.0) CALL NUMBER(XN+.044,YN,0.21,XVAL,0.0,-1)
04400         IF(ANGLE.NE.0.0)
04410      *    CALL NUMBER(XN-.06,YN+.13,.21,XVAL,0.0,-1)
04420   15    XVAL=XVAL+ADX
04430         XN=XN+CTH
04440         YN=YN+STH
04450         IF (NT) 20,11,20
04460   11      Z=KN
04470           IF (EX)  12,13,12
04480   12      Z=Z+7.0
04490   13      DXB=-.07*Z+AXLEN*0.5
04500           DYB=0.70*A-0.075
04510           XT=XPAGE+DXB*CTH-DYB*STH
04520           YT=YPAGE+DYB*CTH+DXB*STH
04530         IF(ANGLE.EQ.0.0) CALL SYMBOL(XT,YT-.1,0.21,IBCD(1),ANGLE,K
N)
04540         IF(ANGLE.NE.0.0)
04550      *    CALL SYMBOL(XT-.01,Y¬¬0.21,IBCD(1),ANGLE,KN)
04560           IF (EX)  14,20,14
04570   14        Z=KN+2
04580             XT=XT+Z*CTH*0.14
04590             YT=YT+Z*STH*0.14
04600             CALL SYMBOL(XT,YT,0.14,3H*10,ANGLE,3)
04610             XT=XT+(3.0*CTH-0.8*STH)*0.14
04620             YT=YT+(3.0*STH+0.8*CTH)*0.14
04630             CALL NUMBER(XT,YT,0.07,EX,ANGLE,-1)
04640   20  NT=NT-1
04650       CALL PLOT(XPAGE+AXLEN*CTH,YPAGE+AXLEN*STH,3)
04660       DXB=-0.07*A*STH
04670       DYB=+0.07*A*CTH
04680       A=NTIC-1
04690       XN=XPAGE+A*CTH
04700       YN=YPAGE+A*STH
04710       DO  30  I=1,NTIC
04720         CALL PLOT(XN,YN,2)
```

```
04730          CALL PLOT(XN+DXB,YN+DYB,2)
04740          CALL PLOT(XN,YN,2)
04750          XN=XN-CTH
04760          YN=YN-STH
04770   30    CONTINUE
04780         RETURN
04790         END
04800 /*
04810 //LKED.SYSLMOD  DD  DSN=URI.EIL1.LOAD,DISP=SHR
04820 //LKED.SYSIN  DD  *
04830  NAME SMLBEACH(R)
04840 /*
04850 //
04860 7890123456789012345678901234567890123456789012345678901234567890123456789
END OF DATA
```

Program COLE.SMALL is a JCL program which routes profile data from a data set to the compiled version of BEACH 3 in the load module. It also routes output plots and julian date and volume calculations to TSO files.

```
   L 'URI.EIL101.MIS01.COMP.PROG'
 'URI.EIL101.MIS01.COMP.PROG'
00010 //EIL101S JOB (EIL101),'COLE.SMALL BEACH',TIME=2,MSGCLASS=A
00020 /*JOBPARM L=20
00030 //SMALL         EXEC  PGM=LOADER,REGION=512K
00040 //SYSLIN        DD  DSN=URI.EIL1.LOAD(SMLBEACH),DISP=SHR
00050 //SYSLOUT      DD  SYSOUT=A
00060 //SYSLIB       DD  DSN=SYSP.FORTLIB,DISP=SHR
00070 //             DD  DSN=UCC.LC01.CPLOTLIB,DISP=SHR
00080 //FT06F001     DD  SYSOUT=A
00090 //FT07F001     DD  DUMMY
00100 //FT08F001     DD  DSN=URI.EIL101.MIS01.DATA,DISP=OLD
00110 //FT09F001     DD  DSN=URI.EIL101.MIS01.VOL.DATA,DISP=OLD
00120 //FT99F001     DD  DSN=URI.EIL101.MIS01.COMP.PLOT,DISP=OLD
00130 //FT05F001     DD  *
00140 MIS-01  COMP
00150 26 JUL 1977
00160 11 AUG 1977
00170 MIS-01  COMP
00180 11 AUG 1977
00190 24 AUG 1977
00200 MIS-01  COMP
00210 24 AUG 1977
00220 13 SEP 1977
00230 MIS-01  COMP
00240 13 SEP 1977
00250 06 OCT 1977
00260 MIS-01  COMP
00270 06 OCT 1977
00280 20 OCT 1977
00290 MIS-01  COMP
00300 20 OCT 1977
00310 10 NOV 1977
00320 MIS-01  COMP
00330 10 NOV 1977
00340 22 NOV 1977
00350 MIS-01  COMP
```

Program INTERP3 is a Fortran 66 program which interpolates data using least squares linear regression. The bulk of the code is from Davis (1973). The program is modified to accept input and create output as desired. The version shown is for interpolating volume time series data.

```
'URI.EIL101.INTERP3.PROG'
)0010 //EIL101S JOB (EIL101),'INTERP3',NOTIFY=EIL101,TIME=2,MSGCLASS=A
)0020 /*PASSWORD RGHC
)0030 /*JOBPARM L=50
)0040 // EXEC FORTVCG,PARM.FORT='LANGLVL(66)',LIB1=CPLOT,REGION.GO=1000K
)0050 //FORT.SYSIN  DD  *
)0060         REAL XIN(2000,2),AIN(2000,2),BIN(2000,2),CIN(2000,2),DIN(20
)0,2)
)0070        1,AOUT(2000,2),BOUT(2000,2),COUT(2000,2),DOUT(2000,2)
)0080        1,XOUT(2000,2),JIN(2000,2)
)0090          INTEGER COUNT
)0100          ID=0
)0110          DO 50 I=1,2000
)0120             READ(8,*,END=900)JIN(I,1),AIN(I,2)
)0130 50       CONTINUE
)0140 900       COUNT=I-1
)0150          DO 55 I=1,COUNT
)0160              XIN(I,1)=JIN(I,1)
)0170 55       CONTINUE
)0180          DO 60 I=1,COUNT
)0190              WRITE(6,*) XIN(I,1),AIN(I,2),
)0200 60       CONTINUE
)0210          DO 70 I=1,COUNT
)0220             XIN(I,2)=AIN(I,2)
00230 70       CONTINUE
00350 C
00360 C  INITIALIZE INDEXING PARAMETERS AND X COORDINATES OF FIRST DATA
00370 C  POINT TO INTERPLOLATE
00380 C
00390 212       IS=0
00400           XI=7.
00410          JS=1
00420          XB=5164.
00430          XL=8881.
00440          X=XB-XI
00450  1        X=X+XI
00460 C
00470 C  IF THE VARIABLE IS GREATER THAN THE FINAL POINT XL, STOP
00480 C
00490          IF (X-XL) 2,2,99
00500 2        IS=IS+1
00510          XOUT(IS,1)=X
00520 C
00530 C  ASSIGN THE FIRST Y VALUE IN XIN TO XOUT(IS,2)
00540 C
00550          IF(X-XIN(1,1)) 3,3,4
00560 3        XOUT(IS,2)=XIN(1,2)
00570          GO TO 1
00580 C
00590 C  IF THE VARIABLE X IS GREATER THAN THE LAST Y VALUE IN THE
00600 C  INPUT DATA, THEN 0. IS ASSIGNED TO XOUT(IS,2)
00610 C
00620 4        IF(X-XIN(COUNT,1)) 6,5,5
00630 5        XOUT(IS,2)=0.
00640          GO TO 1
00650 C
00660 C  FIND THE TWO DATA POINTS OF XIN SUCH THAT XOUT(IS,1) LIES IN
00670 C  THE INTERVAL (XIN(JS,1), XIN(JS+1,1)). USE THE Y VALUES OF THES
E
00680 C  TWO DATA POINTS TO INTERPOLATE THE VALUE OF XOUT(IS,2).
```

```
00690 C
00700 6       IF (X-XIN(JS,1)) 9,8,7
00710 7       IF (X-XIN(JS+1,1)) 8,8,9
00720 8       XOUT(IS,2)=XIN(JS,2)+(XIN(JS+1,2)-XIN(JS,2))*
00730       1  (X-XIN(JS,1))/(XIN(JS+1,1)-XIN(JS,1))
00740         GO TO 1
00750 9       JS=JS+1
00760         IF (JS-COUNT) 6,10,10
00770 10      JS=JS-1
00780         GO TO 5
00820 C
00830 C  OUTPUT TO A DATA FILE THE Y VALUES OF XOUT
00840 C
00850 99      DO 204 I=1,IS
00860            AOUT(I,2)=XOUT(I,2)
00870 204     CONTINUE
01012          DO 208 I=1,IS
01013           WRITE(10,107)XOUT(I,1),AOUT(I,2)
01014 208      CONTINUE
01020 C
01030 C  FORMATS
01040 C
01050 100     FORMAT(I2,1X,A3,1X,I4)
01060 101     FORMAT(1X,I2,1X,A3,1X,I4)
01070 102     FORMAT(2A4)
01080 103     FORMAT(1X,2A4)
01090 104     FORMAT(1X,F8.0)
01100 105     FORMAT(2F9.1)
01110 1¬¬     FORMAT(F5.0,5X,F5.0)
01111 107     FORMAT(F5.0,1X,F5.1)
01140 999      STOP
01150         END
01160 /*
01170 //GO.FT08F001  DD  DSN=URI.EIL101.CHATB.VOL.DATA.COR,DISP=OLD
01180 //GO.FT10F001  DD  DSN=URI.EIL101.CHATB.VOL.DATA.INTERP,DISP=OLD
```

Program SAS2 is a SAS program which calculates spatial and temporal eigenfunctions from interpolated beach profile data.

```
 'URI.EIL101.SAS2.PROG'
00010 //EIL101S JOB (EIL101),'SAS2',TIME=5,MSGCLASS=A
00020 /*JOBPARM LINES=30
00030 /*PASSWORD RGHC
00040 // EXEC SAS
00050 //GO.DATAIN1 DD DSN=URI.EIL101.CHAEZ.INTERP,DISP=OLD
00060 //GO.DATAOUT1 DD DSN=URI.EIL101.PRIN,DISP=OLD
00061 //GO.DATAOUT2 DD DSN=URI.EIL101.EVAL,DISP=OLD
00070 //GO.SYSIN DD *
00090     DATA INTERP;
00100        INFILE DATAIN1;
00101     INPUT DATE / M0 /  M1 / M2 / M3 / M4 / M5 / M6 /M7 / M8 / M9 /
M10
00102             / M11 / M12 / M13 / M14 / M15 / M16 / M17 / M18 / M19 /
 M20 /
00103              M21 / M22 / M23 / M24 / M25 / M26 / M27 / M28 / M29 /
M30 /
00104              M31 / M32 / M33 / M34 / M35 / M36 / M37 / M38 / M39 /
M40 /
00105              M41 / M42 / M43 / M44 / M45 / M46 / M47 / M48 / M49 /
M50 /
00106              M51 / M52 / M53 / M54 / M55 / M56 / M57 / M58 / M59 /
M60 /
00107              M61 / M62 / M63 / M64 / M65 / M66 / M67 / M68 / M69 /
M70 /
00108              M71 / M72 / M73 / M74 / M75 / M76 / M77 / M78 / M79 /
M80 /
00109              M81 / M82 / M83 / M84 / M85 / M86 / M87 / M88 / M89 /
M90 /
00110              M91 / M92 / M93 / M94 / M95 / M96 / M97 / M98 / M99 /
M100 ;
00120     PROC PRINT;
00130        TITLE 'INTERPOLATED PROFILES (1 METER INTERVALS)';
00140     PROC MEANS;
00141        VAR M0 M1-M100;
00160     PROC CORR;
00170        VAR M0 M1-M100;
00180     PROC PRINCOMP COV OUT=DATAOUT1.PRIN OUTSTAT=DATAOUT2.EVAL STD
N=4 ;
00190        VAR M0 M1-M100;
00280 /*
00290 //
```

Program SPECT is an ASYST program used to remove the linear trend in a data array and then to calculate the data's Fourier spectrum.

```
: SPECT
\  PROGRAM WRITTEN BY JAMES C. GIBEAUT
\
\  PROGRAM DESCRIPTION
\
\ THIS PROGRAM PLOTS AN ARRAY CALLED Y AGAINST AN ARRAY
CALLED X
\  THIS PROGRAM THEN TAKES THE LEAST SQUARE LINEAR FIT OF
DATA IN ARRAYS
\    CALLED X AND Y AND PLOTS THE LINE OVER THE ORIGINAL
DATA.
\    THIS LINE IS THEN SUBTRACTED FROM THE ORIGINAL DATA TO
YIELD DATA
\    WITH NO LINEAR TREND, AND THE RESULTS OF THE
SUBTRACTION ARE PLOTTED
\    OVER THE ORIGINAL DATA.  THE RESULTS ARE EMBEDDED IN A
ZERO ARRAY
\    WITH THE # OF ELEMENTS BEING A POWER OF 2 FOR THE FFT
ROUTINE.
\     THE SPECTRA IS
\    THEN PLOTTED AGAINST THE FREQUENCY. THE SPECTRA REMAINS
ON TOP OF THE
\    STACK.
\
\    PROGRAM REQUIREMENTS
\
\    GRAPHICS DISPLAY MODE 5 MUST BE INVOKED
\    X AND Y ARRAYS WITH DATA SAMPLED EVENLY SPACED IN TIME
MUST BE DEFINED
\      BEFORE LOADING.
\    A 1D ARRAY CALLED XE WITH THE # OF ELEMENTS BEING A
POWER OF 2 OF THE
\      PROPER SIZE ACCORDING TO THE SIZE OF Y MUST BE
DEFINED BEFORE
\      LOADING.
\    PROPER SCALING OF THE X AXIS OF THE SPECTRAL PLOT MUST
BE FIGURED AND
\    ENTERED IN THE PROGRAM WHERE NOTED BELOW.
\
3 COLOR XY.AUTO.PLOT
X Y 1 LEASTSQ.POLY.FIT  X SWAP
POLY[X] DUP X SWAP 1 COLOR XY.DATA.PLOT
Y SWAP - DUP  X SWAP  2 COLOR XY.DATA.PLOT
0. XE :=
\ THE NUMBERS IN THE BRACKETS BELOW DEPEND ON THE SIZE OF
THE Y AND XE ARRAYS
\ THE DATA SHOULD BE EMBEDDED IN THE MIDDLE OF THE XE (ZERO)
ARRAY
XE SUB[ 10 , 492 ] :=
XE  FFT
\ THE SECOND NUMBER IN THE BRACKET BELOW DEPENDS ON THE
AMOUNT OF THE SPECTRUM
\ IT IS DESIRED TO PLOT
ZMAG DUP * SUB[ 1 , 49 ] DUP
```

```
\ THE NUMBER BELOW SHOULD BE THE SAME AS THE 2ND NUMBER
ABOVE
49 REAL RAMP
\ THE 1ST NUMBER BELOW IS A SCALING FACTOR (SEE ASYST NEWS
LETTER V#1 ISSUE #1)
\ THE 2ND NUMBER BELOW SHOULD BE THE SIZE OF THE XE ARRAY
.019178 1024. * /
SWAP XY.AUTO.PLOT ;
```

The following ASYST program was used to create figures 4-7.

```
:  EIGENPLOT
\
\  WRITTEN BY JAMES C. GIBEAUT
\
\ PROGRAM DESCRIPTION
\
\   THIS PROGRAM PLOTS VOLUMES AND TEMPORAL COEFFICIENTS IN
A COLUMN
\
\   PROGRAM REQUIREMENTS
\
\    5 PAIRS OF ARRAYS ON TOP OF THE STACK WITH THE TOP PAIR
THE DATA
\    TO BE PLOTTED AT THE TOP OF THE PAGE.
\    PROPER LABELS INSERTED BELOW.
\
3 PLOTTER.PENS
AXIS.FIT.OFF
NORMAL.COORDS
0 0  DATA.ORIG
.4125 .15 AXIS.SIZE
.2  .76 AXIS.ORIG
.2 .835 AXIS.POINT
.0 IN. .05 IN. TICK.SIZE
1. 1. TICK.JUST
VERTICAL GRID.ON
HORIZONTAL GRID.ON
12 4 AXIS.DIVISIONS
HORIZONTAL NO.LABELS
VERTICAL -1.3 0. 4 LABEL.FORMAT
VERTICAL 0 2 LABEL.POINTS
VERTICAL -100 100 WORLD.SET
HORIZONTAL 457. 9223. WORLD.SET
.07 IN. .255 IN. CHAR.SIZE
XY.AXIS.PLOT
2 COLOR XY.DATA.PLOT 1 COLOR
WORLD.COORDS
.08 IN. .27 IN. CHAR.SIZE
847 -120  POSITION " 63-64" CENTERED.LABEL
1577 -120 POSITION " 65-66" CENTERED.LABEL
2307 -120 POSITION " 67-68" CENTERED.LABEL
3037 -120 POSITION " 69-70" CENTERED.LABEL
3767 -120 POSITION " 71-72" CENTERED.LABEL
4497 -120 POSITION " 73-74" CENTERED.LABEL
5230 -120 POSITION " 75-76" CENTERED.LABEL
5961 -120 POSITION " 77-78" CENTERED.LABEL
6691 -120 POSITION " 79-80" CENTERED.LABEL
7422 -120 POSITION " 81-82" CENTERED.LABEL
8152 -120 POSITION " 83-84" CENTERED.LABEL
8883 -120 POSITION " 85-86" CENTERED.LABEL
4865 -145 POSITION " YEARS" CENTERED.LABEL
90 LABEL.DIR 90 CHAR.DIR
-383 -15 POSITION " VOLUME (meters)" CENTERED.LABEL
0 LABEL.DIR 0 CHAR.DIR
```

```
3 COLOR
.16 IN. .49 IN. CHAR.SIZE 470 125 POSITION " GRH-01" LABEL
1 COLOR
\
NORMAL.COORDS
.4125 .15 AXIS.SIZE
.2 .54 AXIS.ORIG
.2 .615 AXIS.POINT
12 2 AXIS.DIVISIONS
.07 IN. .255 IN. CHAR.SIZE
VERTICAL 0 1 LABEL.POINTS
HORIZONTAL NO.LABELS
VERTICAL -1.3 0. 3 LABEL.FORMAT
0. IN. .03 IN. TICK.SIZE
VERTICAL -4 4 WORLD.SET
XY.AXIS.PLOT
WORLD.COORDS
.08 IN. .27 IN. CHAR.SIZE
90 LABEL.DIR 90 CHAR.DIR
-383 .0 POSITION " FIRST" CENTERED.LABEL
0 LABEL.DIR 0 CHAR.DIR
2 COLOR XY.DATA.PLOT 1 COLOR
\
NORMAL.COORDS
.4125 .15 AXIS.SIZE
.2 .38 AXIS.ORIG
.2 .455 AXIS.POINT
12 2 AXIS.DIVISIONS
.07 IN. .255 IN. CHAR.SIZE
VERTICAL -1.3 0. 3 LABEL.FORMAT
VERTICAL -4 4 WORLD.SET
XY.AXIS.PLOT
WORLD.COORDS
.08 IN. .27 IN. CHAR.SIZE
90 LABEL.DIR 90 CHAR.DIR
-383 .0 POSITION " SECOND" CENTERED.LABEL
0 LABEL.DIR 0 CHAR.DIR
2 COLOR XY.DATA.PLOT 1 COLOR
\
NORMAL.COORDS
.4125 .15 AXIS.SIZE
.2 .220 AXIS.ORIG
.2 .2950 AXIS.POINT
12 2 AXIS.DIVISIONS
.07 IN. .255 IN. CHAR.SIZE
VERTICAL -1.3 0. 3 LABEL.FORMAT
VERTICAL -4 4 WORLD.SET
XY.AXIS.PLOT
WORLD.COORDS
.08 IN. .27 IN. CHAR.SIZE
90 LABEL.DIR 90 CHAR.DIR
-383 .0 POSITION " THIRD" CENTERED.LABEL
0 LABEL.DIR 0 CHAR.DIR
2 COLOR XY.DATA.PLOT 1 COLOR
```

```
\
NORMAL.COORDS
.4125 .15 AXIS.SIZE
.2 .060 AXIS.ORIG
.2 .1350 AXIS.POINT
12 2 AXIS.DIVISIONS
.08 IN. .27 IN. CHAR.SIZE
VERTICAL -1.3 0. 3 LABEL.FORMAT
VERTICAL -4 4 WORLD.SET
XY.AXIS.PLOT
WORLD.COORDS
.08 IN. .27 IN. CHAR.SIZE
90 LABEL.DIR 90 CHAR.DIR
-383 .0 POSITION " FOURTH" CENTERED.LABEL
0 LABEL.DIR 0 CHAR.DIR
2 COLOR XY.DATA.PLOT 1 COLOR
.09 IN. .295 IN. CHAR.SIZE
90 LABEL.DIR 90 CHAR.DIR
-1183 12 POSITION " TEMPORAL EIGENFUNCTIONS" CENTERED.LABEL
AXIS.DEFAULTS ;
```

The following ASYST program was used to create figures 8-13.

```
:  EIGENPLOT
\
\ WRITTEN BY JAMES C. GIBEAUT
\
\THIS PROGRAM PLOTS VOLUME AND TEMPORAL COEFICIENTS IN A
COLUMN
\
\ PROGRAM REQUIREMENTS
\
\  5 PAIRS OF ARRAYS ON TOP OF THE STACK WITH THE TOP PAIR
THE
\    PAIR TO BE PLOTTED FIRST.
\  PROPER LABELS MUST BE INSERTED BELOW.
\
3 PLOTTER.PENS
AXIS.FIT.OFF
NORMAL.COORDS
0 0  DATA.ORIG
.45 .15 AXIS.SIZE
.5  .76 AXIS.ORIG
.5 .835 AXIS.POINT
.0 IN. .05 IN. TICK.SIZE
1. 1. TICK.JUST
VERTICAL GRID.ON
HORIZONTAL GRID.ON
6 4 AXIS.DIVISIONS
HORIZONTAL NO.LABELS
VERTICAL -1.3 -.20 4 LABEL.FORMAT
VERTICAL 0 2 LABEL.POINTS
VERTICAL -100 100 WORLD.SET
HORIZONTAL 4840. 9223. WORLD.SET
.06 IN. .12 IN. CHAR.SIZE
XY.AXIS.PLOT
2 COLOR XY.DATA.PLOT 1 COLOR
WORLD.COORDS
.07 IN. .13 IN. CHAR.SIZE
5255 -125 POSITION " 75-76" CENTERED.LABEL
5986 -125 POSITION " 77-78" CENTERED.LABEL
6716 -125 POSITION " 79-80" CENTERED.LABEL
7447 -125 POSITION " 81-82" CENTERED.LABEL
8177 -125 POSITION " 83-84" CENTERED.LABEL
8908 -125 POSITION " 85-86" CENTERED.LABEL
7031 -150 POSITION " YEARS" CENTERED.LABEL
90 LABEL.DIR 90 CHAR.DIR
4000 25 POSITION " VOLUME (meters)" CENTERED.LABEL
0 LABEL.DIR 0 CHAR.DIR
3 COLOR
.14 IN. .235 IN. CHAR.SIZE 4850 117 POSITION " CHA-TB" LABEL
1 COLOR
\
NORMAL.COORDS
.45 .15 AXIS.SIZE
.5 .54 AXIS.ORIG
.5 .615 AXIS.POINT
```

```
6 2 AXIS.DIVISIONS
.06 IN. .12 IN. CHAR.SIZE
VERTICAL 0 1 LABEL.POINTS
HORIZONTAL NO.LABELS
VERTICAL -1.3 -.22 3 LABEL.FORMAT
0 .05 IN. TICK.SIZE
VERTICAL -4 4 WORLD.SET
XY.AXIS.PLOT
WORLD.COORDS
.07 IN. .13 IN. CHAR.SIZE
90 LABEL.DIR 90 CHAR.DIR
4000 .5 POSITION " FIRST" CENTERED.LABEL
0 LABEL.DIR 0 CHAR.DIR
2 COLOR XY.DATA.PLOT 1 COLOR
\
NORMAL.COORDS
.45 .15 AXIS.SIZE
.5 .38 AXIS.ORIG
.5 .455 AXIS.POINT
6 2 AXIS.DIVISIONS
.06 IN. .12 IN. CHAR.SIZE
VERTICAL -1.3 -.22 3 LABEL.FORMAT
VERTICAL -4 4 WORLD.SET
XY.AXIS.PLOT
WORLD.COORDS
.07 IN. .13 IN. CHAR.SIZE
90 LABEL.DIR 90 CHAR.DIR
4000 .5 POSITION " SECOND" CENTERED.LABEL
0 LABEL.DIR 0 CHAR.DIR
2 COLOR XY.DATA.PLOT 1 COLOR
\
NORMAL.COORDS
.45 .15 AXIS.SIZE
.5 .220 AXIS.ORIG
.5 .2950 AXIS.POINT
6 2 AXIS.DIVISIONS
.06 IN. .12 IN. CHAR.SIZE
VERTICAL -1.3 -.22 3 LABEL.FORMAT
VERTICAL -4 4 WORLD.SET
XY.AXIS.PLOT
WORLD.COORDS
.07 IN. .13 IN. CHAR.SIZE
90 LABEL.DIR 90 CHAR.DIR
4000 .5 POSITION " THIRD" CENTERED.LABEL
0 LABEL.DIR 0 CHAR.DIR
2 COLOR XY.DATA.PLOT 1 COLOR
\
NORMAL.COORDS
.45 .15 AXIS.SIZE
.5 .060 AXIS.ORIG
.5 .1350 AXIS.POINT
6 2 AXIS.DIVISIONS
.06 IN. .12 IN. CHAR.SIZE
VERTICAL -1.3 -.22 3 LABEL.FORMAT
```

```
VERTICAL -4 4 WORLD.SET
XY.AXIS.PLOT
WORLD.COORDS
.07 IN. .13 IN. CHAR.SIZE
90 LABEL.DIR 90 CHAR.DIR
4000 .5 POSITION " FOURTH" CENTERED.LABEL
0 LABEL.DIR 0 CHAR.DIR
2 COLOR XY.DATA.PLOT 1 COLOR
.08 IN. .14 IN. CHAR.SIZE
90 LABEL.DIR 90 CHAR.DIR
3200 15 POSITION " TEMPORAL EIGENFUNCTIONS" CENTERED.LABEL
AXIS.DEFAULTS ;
```

The following ASYST program was used to create figures 14-23.

```
:  SPLOT
\
\  WRITTEN BY JAMES C. GIBEAUT
\
\  PROGRAM DESCRIPTION
\
\  THIS PROGRAM PLOTS 5 SPECTAL PLOTS IN A COLUMN
\
\  PROGRAM REQUIREMENTS
\
\     5 PAIRS OF X AND Y ARRAYS MUST BE ON TOP OF THE STACK
WITH THE
\     TOP PAIR THE ONE TO BE PLOTTED AT THE TOP OF THE PAGE.
\     A SCALAR CALLED MAX MUST BE DEFINED.
\     POTTER MUST BE IN ROTATE AND HP7470 MODE.
\     PROPER LABELS MUST BE INSERTED BELOW.
3 PLOTTER.PENS
HORIZONTAL AXIS.FIT.OFF
VERTICAL AXIS.FIT.OFF
NORMAL.COORDS
0 0  DATA.ORIG
.45 .15 AXIS.SIZE
.5  .76 AXIS.ORIG
.5 .76 AXIS.POINT
HORIZONTAL GRID.ON VERTICAL GRID.ON
.05 IN. .0 IN. TICK.SIZE
1. 1. TICK.JUST
VERTICAL NO.LABELS
HORIZONTAL NO.LABELS
.07 IN. .13 IN. CHAR.SIZE
DUP  []MAX   MAX :=
0 MAX  VERTICAL WORLD.SET
10 1 AXIS.DIVISIONS
HORIZONTAL 0 5 WORLD.SET
XY.AXIS.PLOT
3 COLOR XY.DATA.PLOT 1 COLOR
WORLD.COORDS
\ THE 1ST # BELOW (X POSITION) AND THE CENTERED LABEL FOR
THE FOLLOWING
\ 5 LINES DEPEND ON THE X SCALE OF THE SPECTRAL PLOTS
.2 -.125 MAX * POSITION "  5"  CENTERED.LABEL
.5 -.125 MAX * POSITION "  2"  CENTERED.LABEL
1. -.125 MAX * POSITION "  1"  CENTERED.LABEL
2. -.125 MAX *  POSITION " .5" CENTERED.LABEL
4. -.125 MAX * POSITION  " .25" CENTERED.LABEL
.07 IN. .13 IN. CHAR.SIZE
2.5 -.24 MAX * POSITION "  PERIOD (YEARS)" CENTERED.LABEL
90 CHAR.DIR 90 LABEL.DIR
-.15 .5 MAX  * POSITION   "   RELATIVE ENERGY"
CENTERED.LABEL
0 CHAR.DIR 0 LABEL.DIR
0 0 POSITION
.14 IN. .235 IN. CHAR.SIZE
NORMAL.COORDS
```

```
2 COLOR
.51 .94 POSITION " EST-02 SPECTRAL PLOTS" LABEL
1 COLOR
.07 IN. .16 IN. CHAR.SIZE
.5 .917 POSITION "  PROFILE VOLUME" LABEL   BREAK
\
NORMAL.COORDS
0 0 DATA.ORIG
.45 .15 AXIS.SIZE
.5 .54 AXIS.ORIG
.5 .54 AXIS.POINT
0 0 TICK.SIZE
DUP []MAX  MAX :=
0 MAX VERTICAL WORLD.SET
0 5 HORIZONTAL WORLD.SET
XY.AXIS.PLOT
WORLD.COORDS
90 CHAR.DIR 90 LABEL.DIR -.6 .5 MAX * POSITION "  FIRST"
CENTERED.LABEL
3 COLOR XY.DATA.PLOT 1 COLOR
\
NORMAL.COORDS
0 0 DATA.ORIG
.45 .15 AXIS.SIZE
.5 .38 AXIS.ORIG
.5 .38 AXIS.POINT
0 0 TICK.SIZE
DUP []MAX MAX :=
0 MAX VERTICAL WORLD.SET
0 5 HORIZONTAL WORLD.SET
XY.AXIS.PLOT
WORLD.COORDS
-.6 .5 MAX * POSITION "  SECOND" CENTERED.LABEL
3 COLOR XY.DATA.PLOT 1 COLOR
\
NORMAL.COORDS
0 0 DATA.ORIG
.45 .15 AXIS.SIZE
.5 .22 AXIS.ORIG
.5 .22 AXIS.POINT
0 0 TICK.SIZE
DUP []MAX MAX :=
0 MAX VERTICAL WORLD.SET
0 5 HORIZONTAL WORLD.SET
XY.AXIS.PLOT
WORLD.COORDS
-.6 .5 MAX * POSITION "  THIRD" CENTERED.LABEL
3 COLOR XY.DATA.PLOT 1 COLOR
\
NORMAL.COORDS
0 0 DATA.ORIG
.45 .15 AXIS.SIZE
.5 .06 AXIS.ORIG
.5 .06 AXIS.POINT
```

```
0 0 TICK.SIZE
DUP []MAX MAX :=
0 MAX VERTICAL WORLD.SET
0 5 HORIZONTAL WORLD.SET
WORLD.COORDS
0 CHAR.DIR 0 LABEL.DIR
.07 IN. .13 IN. CHAR.SIZE
\ SEE NOTE ABOVE FOR NEXT 5 LINES
.2 -.125 MAX * POSITION "  5"  CENTERED.LABEL
.5 -.125 MAX * POSITION "  2"  CENTERED.LABEL
1. -.125 MAX * POSITION "  1"  CENTERED.LABEL
2. -.125 MAX *  POSITION " .5" CENTERED.LABEL
4. -.125 MAX * POSITION " .25" CENTERED.LABEL
.07 IN. .13 IN. CHAR.SIZE
2.5 -.24 MAX * POSITION "  PERIOD (YEARS)" CENTERED.LABEL
.05 IN. 0. IN. TICK.SIZE
XY.AXIS.PLOT
90 CHAR.DIR 90 LABEL.DIR
.07 IN. .16 IN. CHAR.SIZE
-.6 .5 MAX * POSITION "  FOURTH" CENTERED.LABEL
3 COLOR XY.DATA.PLOT 1 COLOR
NORMAL.COORDS
.08 IN. .18 IN. CHAR.SIZE
.3 .38  POSITION "     TEMPORAL EIGENFUNCTIONS"
CENTERED.LABEL
AXIS.DEFAULTS ;
```

The following ASYST program was used to create figures 25-34.

```
: EIGENPLOT
\
\  WRITTEN BY JAMES C. GIBEAUT
\
\  PROGRAM DISCRIPTION
\
\  THIS PROGRAM PLOTS THE MEAN BEACH PROFILE  AND 4 SPATIAL
EIGENFUNCTIONS
\  BELOW IT.
\
\  PROGRAM REQUIREMENTS
\
\  5 PAIRS OF X AND Y ARRAYS CALLED ANYTHING ON TOP OF THE
STACK
\  WITH THE MEAN PROFILE DATA ON TOP
\  PLOTTER MUST BE IN PLOT ROTATE AND HP7470 MODE
\  PROPER LABELS MUST BE PLACED IN THE PROGRAM
NORMAL.COORDS
0 0 DATA.ORIG
.6 .11  AXIS.SIZE
.3 .80   AXIS.ORIG
.3 .80    AXIS.POINT
.008 .008 TICK.SIZE
1 1 TICK.JUST
10 5 AXIS.DIVISIONS
VERTICAL -1.3  -.22 2 LABEL.FORMAT
HORIZONTAL  -.5 -1  4  LABEL.FORMAT
HORIZONTAL 0 100 WORLD.SET
VERTICAL 0 5 WORLD.SET
XY.AXIS.PLOT
2 COLOR  XY.DATA.PLOT 1 COLOR
WORLD.COORDS
50 -2.0 POSITION " METERS FROM DATUM STAKE" CENTERED.LABEL
2 COLOR
3.6 MM. 5.976 MM. CHAR.SIZE 0 5.5 POSITION " MAT-SP MEAN
PROFILE" LABEL
1 COLOR
2.8 MM. 3.724 MM. CHAR.SIZE
-9   -.25 POSITION " MLW" LABEL
90  LABEL.DIR 90 CHAR.DIR
-6 2.5 POSITION " M" CENTERED.LABEL
0 CHAR.DIR
0 LABEL.DIR
\
NORMAL.COORDS
.6 .11  AXIS.SIZE
.3 .58  AXIS.ORIG
.3 .635  AXIS.POINT
10 2  AXIS.DIVISIONS
VERTICAL 0 1 LABEL.POINTS
HORIZONTAL NO.LABELS
VERTICAL -1.3 -.22 3 LABEL.FORMAT
0 .010 TICK.SIZE
VERTICAL -.5 .5 WORLD.SET
```

```
XY.AXIS.PLOT
2 COLOR XY.DATA.PLOT 1 COLOR
WORLD.COORDS
3.3 MM. 5.0 MM. CHAR.SIZE
0 .58 POSITION " EIGENFUNCTION 1= 53.6% OF VARIANCE" LABEL
2.8 MM. 3.724 MM. CHAR.SIZE
\
NORMAL.COORDS
.6 .11  AXIS.SIZE
.3 .42  AXIS.ORIG
.3 .475  AXIS.POINT
VERTICAL -.5 .5 WORLD.SET
XY.AXIS.PLOT
2 COLOR XY.DATA.PLOT 1 COLOR
WORLD.COORDS
3.3 MM. 5.0 MM. CHAR.SIZE
0 .58 POSITION " EIGENFUNCTION 2= 21.3%" LABEL
2.8 MM. 3.724 MM. CHAR.SIZE
\
NORMAL.COORDS
.6 .11  AXIS.SIZE
.3 .26  AXIS.ORIG
.3 .315  AXIS.POINT
VERTICAL -.5 .5 WORLD.SET
XY.AXIS.PLOT
2 COLOR XY.DATA.PLOT 1 COLOR
WORLD.COORDS
3.3 MM. 5.0 MM. CHAR.SIZE
0. .58 POSITION " EIGENFUNCTION 3= 8.8%" LABEL
2.8 MM. 3.724 MM. CHAR.SIZE
\
NORMAL.COORDS
.6 .11  AXIS.SIZE
.3 .10  AXIS.ORIG
.3 .155  AXIS.POINT
VERTICAL -.5 .5 WORLD.SET
XY.AXIS.PLOT
2 COLOR XY.DATA.PLOT 1 COLOR
WORLD.COORDS
3.3 MM. 5.0 MM. CHAR.SIZE
0 .58 POSITION " EIGENFUNCTION 4= 5.1%" LABEL
2.8 MM. 3.724 MM. CHAR.SIZE
AXIS.DEFAULTS ;
```